

# Impact of Nano-Modified Epoxy on CFRP-Strengthened Concrete Bond in Aggressive Environments.

MPhil in Engineering

2024

Nirthiha Evanjely Maheswaran Fernando



Resilient Structures and  
Construction Materials (RESCOM)  
Research Group

---

Grŵp Ymchwil Strwythurau Gwydn  
a Deunyddiau Adeiladu  
(RESCOM)

## **Acknowledgement**

I would like to extend my sincere gratitude to my supervisor Dr Riccardo Maddalena for his invaluable guidance, support, and encouragement, and to Dr Nicholas Bill for his valuable insight and expertise. Their guidance has been instrumental in shaping the direction and quality of this work.

I am also deeply grateful for SIKA UK for their generous provision of the CFRP and epoxy adhesive, which were crucial to the success of this research.

Special thanks to my colleagues and fellow researchers Ibrahim and Zhebang for being so kind and helpful; and to lab technicians Carl, Richard, Ian, and Harvey for the immense support provided.

I am also grateful to Professor Kumari Gamage and Mr Vajira Attanayaka for inspiring me to work with CFRP.

Lastly, I am forever grateful to my uncle and aunt Mr and Mrs Johnson, my husband, my amamah, and my parents for their unwavering support and understanding throughout this journey; for my son Ehaan for being the source of strength and motivation.

## **Abstract**

The debonding of Carbon Fibre Reinforced Polymer (CFRP) from concrete; is one of the major issues in the civil retrofitting industry. Saline water and elevated temperature have been identified as couple of many reasons which could encourage debonding. This dissertation presents a research effort aimed at identifying the failure mechanisms within this polymer-concrete interface and establishing innovative strategies to enhance epoxy resin ( the polymer) performance using nanomaterials for the development of nanohybrid adhesives. The primary objective behind the addition of nanomaterial is to fortify the interfacial bond strength between CFRP and concrete, enhancing its durability in aggressive environmental conditions.

To achieve this goal, a comprehensive review of prior research on nanohybrid adhesives was conducted, to assess the influence of various nano particles on composite performance. Among the nanomaterials investigated graphene nano platelets (GNP) at concentrations of 0.25 wt.% and 0.5 wt.% and NS at concentrations of 0.25 wt.% and 0.5 wt.% exhibited significant potential for enhancing resin bonding capacity. Double shear test on externally retrofitted CFRP strips on concrete cubes using the proposed nanohybrid epoxy mixes were performed.

From the experiment it was observed that, 0.25 wt.% GNP mixed epoxy resin outperformed neat epoxy by 181% and it also showed better performance in stiffness as well.

## Contents

1. Introduction .....	1
1.1. Fiber Reinforced Polymer (FRP).....	1
1.2. Research Significance .....	4
1.3. Objectives of this study.....	6
2. Literature Review .....	1
2.1. Why Carbon Fibre Reinforced Polymer?.....	1
2.2. The substrate .....	4
2.3. The matrix .....	5
2.4. The composite.....	8
2.5. The causes of failure .....	10
2.6. Research significance.....	15
2.7. Nano-modified adhesives used with CFRPs.....	16
2.8. Design consideration.....	27
2.9. Interfacial bond performance .....	28
2.10. Research gap .....	28
3. Methodology.....	29
3.1. Test setup.....	29
3.2. Raw materials.....	31
3.3. Concrete samples produced for CFRP substrate.....	31
3.4. Mix design .....	34
3.5. Curing and accelerated ageing.....	36
3.6. Strength testing of cubes .....	36
3.7. Surface preparation .....	37
3.8. Adhesive preparation.....	39
3.9. CFRP application and test set up.....	43
3.10. Summary of the testing procedure .....	47
3.11. Testing.....	48
3.12. Double shear test .....	48
3.13. Scanned electron microscope analysis.....	49
4. Analysis and Discussion.....	50
4.1. Observation .....	50
4.2. Results .....	53
4.3. SEM images .....	58
4.4. Strain gauge analysis.....	61

4.5.	Summary of results.....	67
4.6.	Conclusion.....	68
4.7.	Future work .....	69
5.	Reference .....	70
6.	Appendix.....	76

## Figures and Tables

Figure 1	Types of fibres in the market. ....	2
Figure 2	CFRP composite structure. ....	1
Figure 3	Stages in the derivation of PAN precursors.....	1
Figure 4	Types of CFRP options available for retrofitting. ....	2
Figure 5	Application of CFRP forms in construction industry a) (Loud, 1996) b) (METHOD STATEMENT Substrate Preparation for Sika® Rigid Bonding and Structural Strengthening Systems, n.d.) c) and d) (Alkhrdaji, 2015) .....	3
Figure 6	Recommended surface preparation grade in concrete for CFRP application.....	4
Figure 7	Shear strain /strain relationship of different adhesives. (Worrall, n.d.) .....	7
Figure 8	Stress vs strain relationship between composite, fibre and matrix. (Gunaslan et al., 2014) .....	8
Figure 9	Externally bonded CFRP arrangement and Interface arrangement in a RCC element.....	9
Figure 10	Failure types in CFRP concrete composite.....	9
Figure 11	arrangement of atoms in graphite and graphene.....	17
Figure 12	SEM images of fracture surfaces. a neat epoxy. b Epoxy/GNP 0.1 wt%. c Epoxy/GNP 0.3 wt%. d Epoxy/GNP 0.5 wt%. e Epoxy/GNP 1.0 wt%, reproduced from [32](Fu et al., 2020).....	19
Figure 13	SEM of fracture surface of GNP (C-300 series) in epoxy at loadings of (a) fGNP = 1.0 wt %; (b) fGNP = 2.0 wt %; (c) fGNP = 10 wt %; (d) fGNP = 20.0 wt % (Ravindran et al., 2018) .....	20
Figure 14	SEM images of C300 nano-fillers failure mechanism: (a) crack pinning and bifurcation and (b) separation of graphene sheets and pull-out (Zafeiropoulou et al., 2020).21	
Figure 15	SEM images of C500 nano-fillers failure mechanism: (a, b) crack pinning and bifurcation and (c, d) separation of graphene sheets and pull-out (Zafeiropoulou et al., 2020) .....	21
Figure 16	SEM images of the tensile fractured surfaces at different % of nanocomposites (GO based) at liquid nitrogen temperature (Khalid et al., 2023).....	22
Figure 17	Scanning electron microscope (a) unmodified NS (b) NS modified (Gharehbash and Shakeri, 2015).....	23
Figure 18	Dispersion methods for nano particles in epoxy. ....	25
Figure 19	Test setup overview. ....	29
Figure 20	Naming method used on samples. ....	33
Figure 21	Casting concrete cubes in the laboratory a) applying form oil to the moulds b) and c) casted concrete cubes. ....	35
Figure 22	Concrete cubes in the 3 wt.% NaCl concentrated water. ....	36
Figure 23	The surface preparation used in the initial set of tests. ....	37
Figure 24	Surface preparation used in the experiment. ....	38

Figure 25 Surface humidity of the samples tested with FLIR humidity meter.....	39
Figure 26 Hand mixing of GNP in epoxy during the initial set of tests for calibration purposes. .....	41
Figure 27 Steps followed in the dispersion of nanoparticles in epoxy.....	42
Figure 28 Dispersion method used for the experiment using mechanical mixing methods such a rotator, ultrasonication to disperse nanoparticles in epoxy.....	42
Figure 29 Priming the prepared surface with the nanohybrid epoxy mix.....	43
Figure 30 CFRP application surface.....	44
Figure 31 Application of modified epoxy on CFRP sheet before installation on to the concrete surface.....	44
Figure 32 CFRP installed on the concrete surface. ....	45
Figure 33 Arrangement for strain gauge instalment on the CFRP surface.....	45
Figure 34 Illustration of strain gauge instalment on CFRP sheet. ....	46
Figure 35 Summary of experiment procedure .....	47
Figure 36 Test setup in the Cardiff University structural lab.....	49
Figure 37 Test setup. ....	50
Figure 38 Performance of GNP mixed epoxy in different exposure conditions. ....	55
Figure 39 Maximum load reached by each sample in different ageing conditions. ....	57
Figure 40 SEM image of nanohybrid epoxy /CFRP and concrete interface. ....	59
Figure 41(a) the agglomeration of GNP particles is denoted and (b) shows the bridging of cracks with the help of interpolmer links. ....	59
Figure 42 SEM image the composite in micro scale. (a) shows a trapped water bubble (b) shows trapped air pocket .....	60
Figure 43 SEM image of nanohybrid epoxy and concrete interface.....	60
Figure 44 SEM image of the composite in micro scale. ....	61
Figure 45 SEM image of dimple formation and agglomeration in nanohybrid epoxy under ageing condition C. ....	61
Figure 46 Stress vs strain graph of samples with neat epoxy and GNP mixed epoxy in Condition A .....	63
Figure 47 Stress vs strain graph of samples with neat epoxy and GNP mixed epoxy in Condition B .....	64
Figure 48 Stress vs strain graph of samples with neat epoxy and GNP mixed epoxy in Condition C .....	64
Figure 49 (a) Stress vs strain graph of samples with neat epoxy in condition A (b, c) Stress vs strain of samples with GNP and NS mixed epoxy in Condition A (d) Stress Vs Strain graph of 0.5 wt.% GNP mixed epoxy in Condition A.....	65
Figure 50 (a) Stress vs strain graph of samples with neat epoxy in condition B (b, c) Stress vs strain graph of samples with GNP and NS mixed epoxy in Condition B (d) Stress vs Strain graph of samples with 0.5 wt.% GNP mixed epoxy in Condition B .....	66
Figure 51(a) Stress vs strain graph of samples with neat epoxy in condition C (b, c) Stress vs strain graph of samples with GNP and NS mixed epoxy in Condition C (d) Stress vs Strain graph of samples with 0.5 wt.% GNP mixed epoxy in Condition C .....	67
 Table 1 Types of resins available in the market for CFRP installation and their properties (Abbood et al., 2021; Guidelines and Recommended Practices for Fiber-Reinforced-Polymer (FRP) Architectural Products, 2016; Resin Choice, 2024; RESINS IN FRP, n.d.; Qureshi, 2022; Stelios Antoniou, 2022) .....	6

Table 2 Research papers on nanomodified adhesives .....	24
Table 3 Properties of CFRP and epoxy used in the experiment from the manufactures technical data sheet. ....	31
Table 4 Summary of test samples .....	33
Table 5 Type of environmental conditions used in this experiment.....	36
Table 6 Mix ratio of GNP in epoxy.....	40
Table 7 Mix ratio of GNP and NS in epoxy. ....	40
Table 8 Type of failure modes observed in the experiment. ....	51
Table 9 Summary of experimental results .....	53
Table 10 Overview of performance comparison of samples based on ultimate loading. ....	56

## 1. Introduction

The discipline of civil engineering is crucial to changing the planet we currently inhabit. In the future, the infrastructure created by the construction industry will leave its mark upon the urban landscape of every country across the globe. Given the adverse impact that many human activities are having on the natural environment, particularly those related to CO<sub>2</sub> emissions and climate change, engineers need to develop solutions that are sustainable. Strategies based on Reduce, Reuse, and Recycle are the primary means of improvement; yet sustainability remains a major challenge in the field of civil engineering. Since the structures have already been constructed, the focus of this study is on finding methods to maintain them and extend their lifespan.

Most of the structures used in civil engineering are constructed using concrete, steel, timber, or masonry. Each of them uses resources on Earth throughout production, shipping, use, and recycling. Nevertheless, after some use, the performance of these core materials for construction degrades. Strengthening them is one of the many ways to improve such elements once their service life is up. However, how will we reinforce them with less of the same material this time? or will we try innovative and sustainable ideas to do the same?

Reinforcement made of carbon fibre have been assisting these dilapidated buildings function better in a more creative and long-lasting manner since recent times. The lightweight design has been found to fairly address potential aesthetic concerns and significantly lower the carbon footprint.

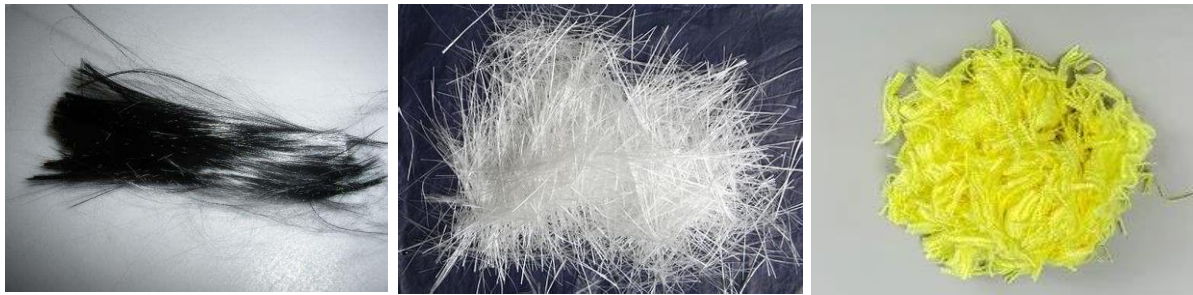
### 1.1. Fiber Reinforced Polymer (FRP)

Fibre-reinforced polymers (FRP) are known to have significant capabilities for reinforcing concrete, steel, and wood under compressive, bending and shear loadings. Compared to other fibre-reinforced polymers, carbon fibre reinforced polymers have the highest resilience in all three aspects mentioned above. The material is widely used in aerospace, automobile, construction, sporting goods, etc.



As illustrated in Figure 1, there are mainly three types of Fibre Reinforced Polymers (FRP) in the construction market.

1. Carbon fibre reinforced polymer- used in strengthening of structure.
2. Glass fibre reinforcement - helps to strengthen and to increase durability of the structures.
3. Aramid fibres - good at impact resistance.



a) Carbon Fibers

b) Glass Fibers

c) Aramid Fibers

*Figure 1 Types of fibres in the market.*

In addition to this, there are also other types of fibres, such as basalt fibres, natural fibres, steel fibres, and hybrid-fibre reinforced polymers, which are used in different construction applications. However, their application is not widespread, owing to a relatively lack of applicable standards and codes of practice, limited awareness and familiarity with the material, and the material's limited availability and consequent expense to the general construction industry.

Of all the FRP systems available, carbon fibre reinforced polymers (CFRP) are the most used in the construction industry. Typically, available in the form of fabric, plates or rebars, they are bonded externally or internally to structural members via an adhesive (normally an epoxy resin), thus forming a composite section that possess a higher load-bearing capacity than the original (Figure 4). CFRP can be installed on to new and existing structures, however their successful application depends on multiple factors such as the concrete grade at the time of retrofitting, environmental conditions, and the existing reinforcement details etc.

In the construction industry, Falahi et al (Falahi et al., 2017) noted that CFRP is ideally suited as it possesses the following characteristics,

- Reasonable fatigue life and durability
- High strength to weight ratio.
- Versatile application possibility
- Corrosion and weather resistance
- Light weight
- Cheaper to manufacture.
- Less damage to the core structure and noise pollution.

The load bearing capacity of structures reduces when deterioration of their material is brought on by exposure to different environmental factors, external forces, and operational circumstances. However, these structures can be repaired or renovated, thus extending their service life. While there are many alternative retrofit solutions available in the market, including shotcrete, steel jacketing, concrete jacketing, techniques involving the use of post-installed fibre reinforced systems are considered highly effective because of their significant properties.

Although CFRP possess exemplary mechanical properties and chemical resistance in general, RC structures strengthened with CFRP have been known to fail under loading due to the occurrence of debonding whereby the CFRP detaches from the underlying concrete surface rather than the fracture of CFRP itself. Hence the adhesive or resin plays a vital role in keeping the CFRP attached to the substrate and acts as a medium to transfer loads among the fibres assisting them to act homogeneously.

Even though the carbon fibre composite has an average tensile strength of about 4300 N/mm<sup>2</sup> (Table 3), it fails long before this value is reached due to debonding (Jiang et al., 2022). There are reasons why debonding could occur including the improper installation, improper mixing of resin, failing to adhere to manufactures environmental conditions during installation and recommended curing conditions or improper design of the composite. Even in cases where all the aforesaid criteria are met, the environment where CFRP strengthened structural elements resides during its lifetime can weaken the adhesive layer. Consequently, CFRP are known to perform not as well in aggressive environments (Y. L. Wang et al., 2020).

CFRPs have been tested in the past for their behaviour in aggressive environments when applied externally, pre-installed internally or near surface bonded in the material. From these studies, it has been demonstrated that moisture, alkalinity, thermal effects, creep, fatigue, ultraviolet radiation, and fire are but a few aggressive environments that could affect the performance of CFRP through processes such as plasticisation, hydrolysis, saponification, etc in the interface layer resulting in cracking, oxidation, chemical degradation and delamination (Al-Tamimi et al., 2015). Therefore, several types of coatings have been proposed to improve the composite effect of the structures strengthened with CFRP.

For instance, the installation of CFRP on weathered and ion-concentrated concrete poses an even greater challenge, as the performance of such situations still need to be properly analysed and solutions derived. The penetration of moisture and other contaminants into the concrete matrix of a substructure such as walls, columns or beams can present a challenge for CFRP installers. Even though it is required that the humidity of the substructures must be less than 4% before FRP application, usually the location and environmental conditions the structure is present can lead to unfavourable conditions such as providing a higher substrate moisture (METHOD STATEMENT Substrate Preparation for Sika® Rigid Bonding and Structural Strengthening Systems, n.d.).

## 1.2. Research Significance

The literature review provides a thorough insight into the status of the problem; CFRP debonding in aggressive environment and the gap that required further investigation to find a possible answer to the questions:

1. How could CFRP be installed on a reinforced concrete, which has been exposed to aggressive environment for an extended period (about three months) behave?
2. How will the long-term effects of an aggressive environment such as salt and elevated temperature, affect the performance of the CFRP/concrete composite?
3. What could be the possible solution to extend the lifespan of the composite?

When considering real world applications, the following structures are kept on mind while working on this research.

- Piers of bridges in water
- Wastewater recycling tanks
- Basement structural elements exposed to poor waterproofing.
- Structural elements in chemical factories
- Concrete tunnels and drainage systems

Moreover, to improve the composite the following improvement criteria were considered:

- A simple method
- A cost-effective solution
- Less toxic to the environment

To reach the above conditions, the possible improvement areas in a composite were analysed,

1. Improving the concrete.

- That is to remove impurities or remove moisture so that there will not be any medium for ions to travel from within the concrete to the resin. But as we are installing them on existing structures, this option is not always practical.
- Yet improving the surface area of the concrete can assist in creating a stronger bond between the resin and the substrate.

2. Improving the condition in the interfacial regions.

- that is, providing a layer of primer of any improved kind, to act as a barrier for impurities and ions to sabotage the crosslinks of the resin polymer. But this method was not encouraged as this could have effects on the bonding.

3. Improving the resin.

- That it does not plasticise and create stronger locking mechanism with the concrete substrate and create a stronger crosslink within the polymer.

From all the above criteria, it was decided to improve the characteristic features of the resin based up on several studies done in automotive, and polymer industries.

### 1.3. Objectives of this study

1. Investigate the impact of water with deleterious ions and the external stress factors on the performance of CFRP-reinforced concrete specimens.
2. Evaluate the effectiveness of various methods for reducing the impact of such situations and improving the bond between the CFRP and concrete. (Further explained in Section 3.7)
3. Develop recommendations for optimising the use of CFRP reinforcement in concrete structures in the presence of water with deleterious ions and the external stress factors. (The issues in concrete surface retrofitted with CFRP is explained in Section 3.2)

## 2. Literature Review

To assess potential causes and remedies, the literature study attempts to go over every aspect of the composite environment. The fundamental components of the composite are covered in detail first (Figure 2), then potential influences that could affect the composite's ongoing performance and failure modes. The review ends with potential ways to improve the composite structure's ability to withstand harsh environmental conditions.



Figure 2 CFRP composite structure.

### 2.1. Why Carbon Fibre Reinforced Polymer?

Among the different type of fibre-reinforced polymers available; carbon fibre has proven to perform particularly well when exposed to aggressive environments such as moisture, acidity, and alkalinity (Falahi et al., 2017; Jack Weitsman, 1995a; Karbhari and Ghosh, 2009; Yang et al., 2022).

Although it was originally introduced by Sir Joseph Wilson Swan in the form of cellulose-based carbon fibre filaments for incandescent light bulbs in 1879, it was not until 1970 that the material was considered by Dr Akio Shindo, who made a huge leap in development and was commercialised worldwide as carbon fibre composites (Keyte et al., 2019a; Lu, 2021).

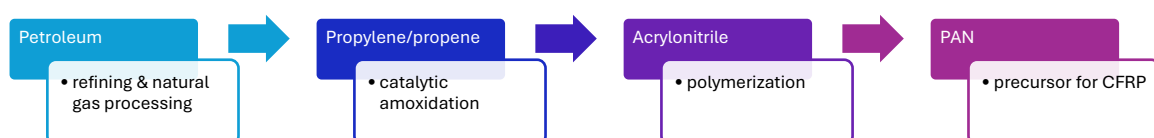
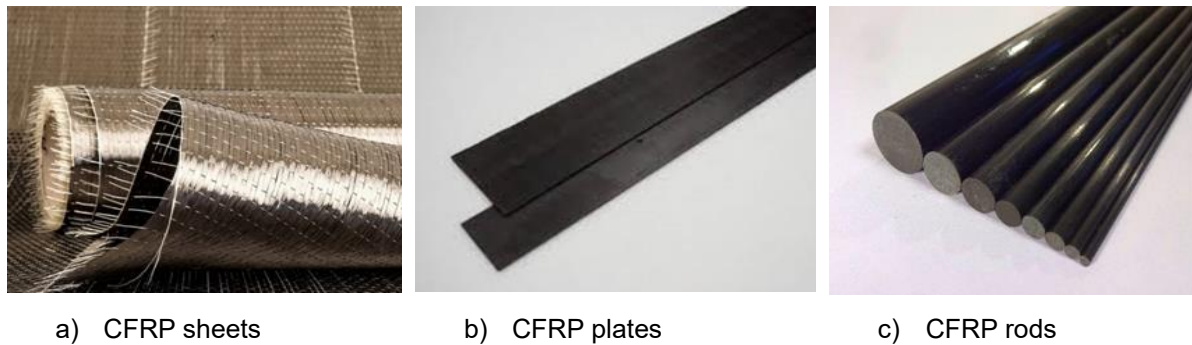


Figure 3 Stages in the derivation of PAN precursors.

The carbon fibre reinforced polymers used in the construction industry (Figure 3) are derived from polyacrylonitrile fibres (PAN) precursors, synthetic precursor materials for carbon fibres. PAN has high carbon content and is characterized by high tensile

strength, good thermal stability, and excellent chemical resistance. They are produced in various forms, such as woven fabric, the pultruded plates/laminates, and as rebars/tendons (Figure 4) (Lu, 2021). CFRP plates and sheets are anisotropic. (*Guide-to-Composites-1*, n.d.).



*Figure 4 Types of CFRP options available for retrofitting.*

The mechanical properties of FRP are determined through the matrix in which it is incorporated, the orientation in which the fibres are woven or placed in the matrix, and the way FRP is processed and fabricated (Falahi et al., 2017).

Numerous investigations have explored the mechanical properties of CFRP sheets, plates, and bars independently. Out of these, CFRP sheets have exhibited a certain degree of vulnerability such as debonding in comparison to other CFRP options. Nevertheless, CFRP sheets are extensively employed for strengthening concrete structures against shear and flexure. Consequently, this research emerged as an imperative endeavour, aimed at enhancing the overall performance of CFRP sheets.

CFRP is available in unidirectional and bidirectional variations in the form of sheets and plates. Unidirectional CFRP is preferred when the loadings are known, due to its exceptional tensile strength and modulus. This is why unidirectional CFRP is highly renowned in the construction industry (Figure 5). On the other hand, bidirectional FRP is woven or pultruded in directions at different angles between  $0^\circ$  to  $90^\circ$  angles, providing enhanced strength and stiffness in both the longitudinal and transverse directions. It is widely utilised in aerospace and automotive applications where components may experience different loading scenarios and necessitate strength in multiple directions.



a) CFRP rods used in the construction of retaining wall



b) CFRP plates installed under a beam to gain flexural strength



c) CFRP sheets installed around beams for shear stress



d) CFRP sheets installed around columns to increase compression capacity

*Figure 5 Application of CFRP forms in construction industry a) (Loud, 1996) b) (METHOD STATEMENT Substrate Preparation for Sika® Rigid Bonding and Structural Strengthening Systems, n.d.) c) and d) (Alkhrdaji, 2015)*

CFRP sheets are used to enhance shear strength, flexural strength, and confinement pressure in structural elements. They are applied on to the substrate by the following methods:

- Wet layup method

This technique involves manually impregnating the CFRP fabric or prepreg with epoxy resin before applying it to the substrate. It is known for its fast-curing capability, making it a quick process. However, it is important to supervise the handling, storing, and application method to prevent the resin from hardening too quickly and to account for the resin's sensitivity to temperature. Wet layup method is used in this research.

- Dry layup method

One method involves applying CFRP to the substrate followed by the application of resin. Alternatively, resin may be applied to the substrate prior to installation to saturate it and ensure a strong bond. The need for this step depends on factors such as the number of sheets being installed and the condition of the substrate.



## 2.2. The substrate

The substrate preparation can be divided into two categories: 1) contact critical application, which is when a bond is provided to facilitate installation even though it is not mandatory for certain situations, such as when columns are confined, and 2) the bond critical application, which calls for proper bonding with the substrate and FRP to accommodate loading such as flexure and shear (American Concrete Institute. and ACI Committee 440., 2017).

Adhesive bonding with the substrate is one of the key elements influencing the CFRP-concrete composite performance. It is advised that the concrete surface be prepared in accordance with International Concrete Repair Institution Guideline No 310.2R.2013, considering the surface roughness of Concrete Surface Profile (CSP) 2,3, and 4 (Figure 6) for bond critical applications which will be tested in this study (Dolan et al., n.d.; Al-Tamimi et al., 2015).



*Figure 6 Recommended surface preparation grade in concrete for CFRP application.*

(Method Statement Substrate Preparation for Sika® Rigid Bonding and Structural Strengthening Systems, n.d.)

The surface temperature, humidity, and surface moisture are but a few parameters which need to be assessed before the CFRP installation process. Usually, it is expected that the surface temperature must be at room temperature or below the glass transition temperature ( $T_g$ ) of the resin, which is around 40 °C to 50 °C, and the substrate must be at least 3 °C above dew point, as per the manufacturer's technical data sheet (METHOD STATEMENT Substrate Preparation for Sika® Rigid Bonding and Structural Strengthening Systems, n.d.; Ruíz de Azúa et al., 2023)

### 2.3. The matrix

In terms of FRP composites, a matrix is a homogenous monolithic material where FRP will be embedded, and through which load transfer occurs. Meanwhile to do this job a resin, a high viscous polymeric substance, will be used and will act as the matrix. The resin also helps to adhere the FRP material on/into the substrate thereby acting as an adhesive.

In summary, the matrix in a composite

1. binds the fibres together and to create a cohesive surrounding to maintain the orientation of the fibres.
2. helps in load transfer within fibres and in-between fibres and concrete/substrate.
3. protects the fibres from external damages by laminating them.
4. creates the composite and helps concrete and fibre to act as one, influencing the overall behaviour of the concrete/FRP composite.

For CFRP applications, epoxy, polyester, or vinyl ester are commonly used as matrices and adhesives. The selection of the binding material depends on the precursor utilized in the manufacturing process of the fibre reinforced polymer. Epoxy is often paired with CFRP for its excellent compatibility (Blackman and Teo, 2009; Huang et al., 2021).

The effectiveness of CFRP attachment is crucial in increasing the material's capacity by facilitating the transfer of loads from the substrate to the externally bonded FRP system through the matrix. The thickness of the adhesive line is a critical factor that should be considered, as it can significantly impact the composite's performance. This

thickness is referred to as the Bond Line Thickness (BLT). Typically, BLT for epoxies ranges from 0.05 mm to 0.1 mm. To achieve optimal peak strength and expedite the curing process, it is advisable to maintain a BLT of 0.1 mm (Worrall, n.d.). But this could be hard to maintain in a wet layup.

It becomes imperative to conduct an initial analysis of the resins currently offered in the market to determine their suitability for CFRP applications. Resins used for CFRP applications are mostly thermosetting resins. Table 1 lists several different types of epoxy resins that are currently used in the market. Figure 7 explains the shear strain and strain behaviour of different types of adhesives which in turn helps to identify the best possible epoxy. It shows that epoxy has a very small change in length relative to slippage, as opposed to polyurethane.

*Table 1 Types of resins available in the market for CFRP installation and their properties (Abbood et al., 2021; Guidelines and Recommended Practices for Fiber-Reinforced-Polymer (FRP) Architectural Products, 2016; Resin Choice, 2024; RESINS IN FRP, n.d.; Qureshi, 2022; Stelios Antoniou, 2022)*

Resin	Epoxy (araldite)	Polyester	Vinyl ester	Phenolic	Polyurethane
<b>Type</b>	Thermosetting	Thermosetting	Thermosetting	Thermosetting	Thermoplastic
<b>Tensile Strength (MPa)</b>	High 55-130	Moderate 34.5- 104	Moderate 73-81	Moderate to high 40	Moderate to high 71
<b>Young's Modulus (GPa)</b>	High 2.75-4.10	Moderate 2.1-3.45	Moderate 3.0-3.5	High 2.5	High 2.9
<b>Adhesion</b>	Excellent	Moderate	Moderate	Moderate	Moderate
<b>Chemical Resistance</b>	Good	Good	Enhanced	Good	Good
<b>Dimensional Stability/Poisson's ratio</b>	Good 0.38-0.40	Good 0.35-0.39	Good 0.36-0.39	Good	Good
<b>Processing methods</b>	Versatile	Relatively easy	Versatile	Complex	Versatile
<b>Cost effectiveness</b>	N/A	Yes	N/A	N/A	N/A
<b>Coefficient of thermal expansion (10<sup>-6</sup>/ °C)</b>	45-65	55-100	50-75	Good	Good
<b>T<sub>g</sub> / °C</b>	40-50	70-120	102-150	260	135-140
<b>Flexibility</b>	N/A	High	N/A	Low	High
<b>Impact Resistance</b>	N/A	Moderate	N/A	N/A	Excellent
<b>Vibration damping</b>	N/A	N/A	N/A	N/A	excellent

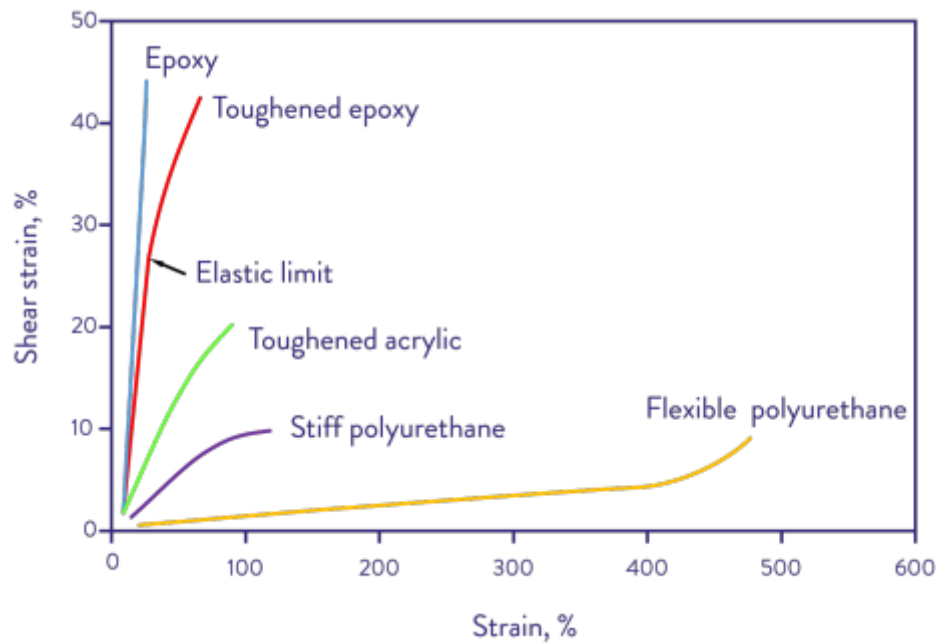


Figure 7 Shear strain /strain relationship of different adhesives. (Worrall, n.d.)

For the experimental study initially the thermosetting resin from the above list and as per manufactures preference, epoxy has been chosen. It is also because it shows good resistance to acidic and sulphate reactions (Hadigheh et al., 2017).

### 2.3.1. Epoxy resin.

Epoxy resins are widely used thermosetting polymers known for their exceptional mechanical properties, adhesion, and chemical resistance. They are formed by the reaction between epoxide groups (glycidyl groups) and curing agents such as aliphatic/aromatic amines or carboxylic anhydrides. This chemical reaction leads to the cross linking of the epoxy molecules, creating a three-dimensional network structure that transforms the liquid resin into a rigid and durable material.

The curing reaction is exothermic thus could be initiated at room or elevated temperatures or in the presence of appropriate catalyst in room temperature.(Hood, n.d.)

Although epoxy resin has been the manufacturers recommended solution, in another interesting study instead of the idea of employing resins to embed CFRP in concrete, research on CFRP grids bonded to the surface with polymer cement mortar has produced encouraging pull-out test results (Dai et al., 2021) .The study only specifically mentions tensile stress loading, even though this solution could effectively

address the majority of problems caused by unfavourable environmental conditions. Additionally, the maximum loads this solution could withstand would be significantly lower than those of CFRP sheets due to the lower number of carbon fibres per unit area.

#### 2.4. The composite

Combination of the carbon fibres and matrix with the substrate creates a CFRP retrofitting. The composite (Dry fibres and polymer/matrix) will behave as one and will have different physical and mechanical characteristics when compared to the individual components. Figure 8 depicts the performance of a composite under stress with comparative to dry fibres and matrix. Even though fibres as an individual or in bundle exhibits high tensile strength, when mixed with a matrix could achieve higher mechanical properties by the matrix spreading the stress between the fibres and preventing the fibres from abrasion or impact. The design of these composites has been found in ACI 440-2R, TR 55 and 57, Fib bulletin 14 and 15 and now recently in Eurocode 2023.

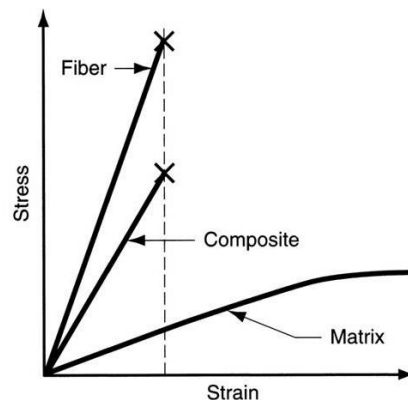


Figure 8 Stress vs strain relationship between composite, fibre and matrix. (Gunaslan et al., 2014)

There are three interfaces which comes into action during a failure in composite. They are the fibre reinforced polymer, the primer/the matrix, and the primer/substrate interaction layer (Figure 9) (Cui et al., 2021).

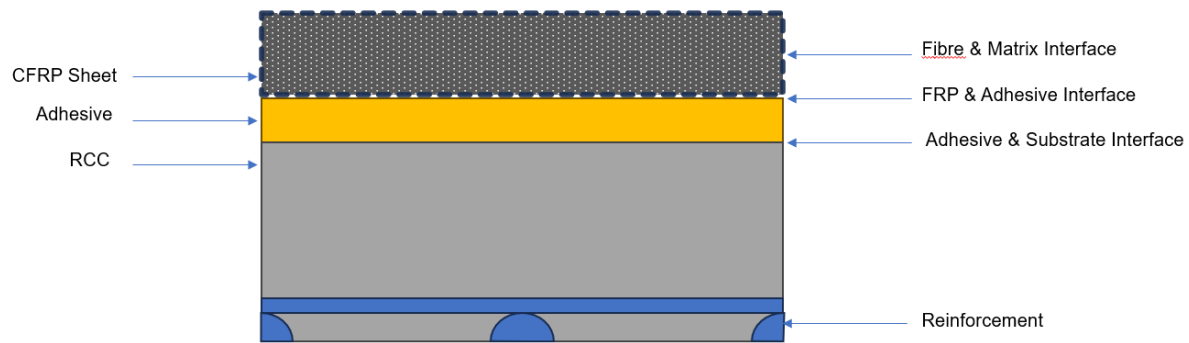


Figure 9 Externally bonded CFRP arrangement and Interface arrangement in a RCC element.

Numerous studies have revealed that the kind of CFRP (plate or sheet) and resin (epoxy) employed have a negative, varied impact due to extreme environmental conditions (Al-Khafaji et al., 2022; Alnuaimi et al., 2021; Choi et al., 2012; Falahi et al., 2017; Hattori et al., 2000; K et al., 2015; Rifai et al., 2020; Wei et al., 2019; Yin et al., 2023). Given the critical function that the CFRP/Concrete interface plays, more attention is being paid to interface studies under different environmental conditions and with various types of resin in order to evaluate the circumstances and enhance the performance of the composite system. Mainly the adhesive failure due to debonding has been considered in this study (Figure 10).

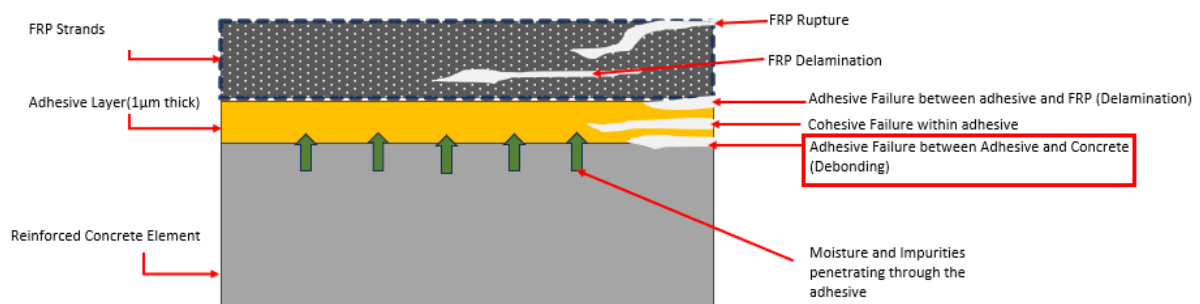


Figure 10 Failure types in CFRP concrete composite.

Meanwhile, a number of studies have supported the idea that an epoxy adhesive may fail for a variety of reasons, including inadequate surface preparation, incorrect hardener and base mixing, inappropriate adhesive selection for the receiving element, harsh environmental conditions, and inadequate adhesive design for the applicable CFRP. A study made on bars revealed that these factors can lead to a shear loss through matrix osmotic cracking, interfacial debonding, and delamination in the FRP

matrix interface. The contact, which is 1  $\mu\text{m}$  thick, is highly susceptible to degradation (Benmokrane et al., 2017).

The primary reference for the influence of aggressive environments on the composite in this study was the research conducted by Böer et al. (2013). In addition to this the combined effect of moisture and temperature has also been one of the concerns to this study. As per the research it has been proved, that for every 1% increase in polymer weight in water, lowers the  $T_g$  of the polymer by 10  $^{\circ}\text{C}$  explaining the non-Fickian diffusion in polymer matrix when exposed to water and temperature together. The accelerated concentration variation due to rapid mobility of polymers due to the above process is called plasticization (Jack Weitsman, 1995b). The investigation further suggests that behaviour in a combined solution must be observed. It is yet unclear whether a chemical reaction in the medium would manifest itself in a unique way when it diffuses to the matrix. Given that this can cause the polymeric matrix to either grow or lose weight (plasticization or hydrolysis) (Jack Weitsman, 1995b).

When it comes to loading the structure exposed to aggressive environment, it must also be noted that, at lower load levels chemical reactions govern the crack propagation, whereas at higher load levels the diffusion of corrosive substances governs the same.

## 2.5. The causes of failure

The reasons for delamination or failure are several and each one has been analysed individually in previous research sources, as outlined below.

### 2.5.1. Moisture

According to Cui et al. (2021), the epoxy could be easily plasticized due to the presence of moisture which eventually reduces the mechanical properties of the system by creating cracks and wrinkles with time. This adversely reduces the interfacial performances. To monitor this issue, it has been suggested that a time dependant bond slip method will be appropriate (Cui et al., 2021).

Moisture can penetrate the concrete; through cracks and general sorption and to the matrix; through the voids and delaminated areas present. Mechanical methods for

desorption, have been found to only increase absorption rate in concrete. Frequent drying and wetting also increases the rate of absorption and thereby has produced interfacial fibre matrix cracks.(Jack Weitsman, 1995b).

Meanwhile it has also been proven through experimental studies that the surface preparation plays a vital role in the moisture absorption. A single lap shear test conducted by Shrestha et al on concrete specimens immersed in water for a period of 18 and 24 months, concludes that the grade of concrete and surface roughness are key to bond strength durability(Shrestha et al., 2015). A two-year experimental study conducted by Dai et al. (2021) on the initial and long-term bond behaviour in concrete prisms which were tested for flexure and pull off strength, suggested that the use of primer could eliminate the moisture between the interface (Dai et al., 2021; Al-Tamimi et al., 2015).

A study on moisture penetration into composites under external stresses carried out by Marom and Broutman (n.d.) explains how external loads affect the moisture intake into the composites. The study shows that the diffusion coefficient increases along with the load and the angle of the load applied. However, it was also found that the loading angle is independent of the diffusion coefficient keeping the ratio constant.

### 2.5.2. Acidity

When concrete is exposed to acidic environment, acid reacts with its constituents, such as calcium hydroxide and cementitious minerals, resulting in acid dissolution and leaching of cementitious material. It also reacts with calcium-based compounds, including calcium silicates and calcium aluminate hydrates, leading to their breakdown and loss. Since concrete is an alkaline material, acid will react with it to reach an acid-base neutralized state. This forms free water and salts inside the concrete. It must be noted that the leaching and loss of other material increases the porosity of the concrete. But with time the process may retard as the salt formation can block the cracks and pores in the concrete, preventing further penetration of acid within the structure (Hadigheh et al., 2017). During surface preparation for CFRP application this protective layer has the possibility to get damaged.



Sulphate attack has been identified as one of the most harmful acids to concrete, which leads to ettringite formation causing coarse aggregates to dislodge. Within a short period of exposure time. It has also been found that the cement content had a direct impact on this, thus increasing the ettringite formation when the cement content is high. It was also advised FRP application in acidic concentration above 80% is not advisable (Hadigheh et al., 2017).

Further to this, a novel study on the effect of sewage environmental conditions on CFRP strengthened concrete has proved that the maximum bond strength in externally bonded reinforcement specimens reduced by 19.7% with the increase in exposure duration. Meanwhile the study also confirmed that when CFRP was externally bonded in grooves and when exposed to the same sewage environment it performed better under stress (Mohammadi and Mostofinejad, 2021).

### 2.5.3. Alkalinity

The alkaline solutions can affect the performance of resins by degrading them if they are not properly cured which results in plasticization and swelling of the resin (Hattori et al., 2000; Karbhari et al., 2003). Further to reinforce this statement, a study on bond strength of GFRP-RC beams in alkaline accelerated solution for 8 years, has proved, alkaline environment degrades the bond stiffness of the structure (Wu et al., 2022).

### 2.5.4. Salts

Saline solutions encourage the failure of adhesives due to the formation of microcavities and inhibiting micro cracking. This thereby increases the moisture ingression, which swells the adhesive, hence promoting a residual stress. The higher the salt concentration the higher moisture ingression is (Fry-Taylor et al., 2023).

### 2.5.5. Thermal effects

Alnuaimi et al. (2021) found that CFRP exposed to elevated temperature showed varying performance with time. The CFRP reinforced structures exposed to elevated temperatures (close to  $T_g$  of the resin) and saline environments showed lower performances after 180 days but escalated its mechanical behaviours after 360 and 730 days; proving that the  $C_E$  (Environmental reduction factor) provided in the ACI 440 code is within the limits of the reduction factor found through the research. But the

study also requested to further investigate on this for a much longer period to assess the true nature of performance.

In aerospace industry CFRP has reached its performance efficiency through its high temperature-controlled curing of resin systems, whereas the room temperature curing in construction industry does not cater well with the long-term durability of the bonding.(Karbhari and Ghosh, 2009). Elevated temperature curing can affect the interface which will result in debonding if not properly maintained and executed.

Every resin will have its own glass transition temperature where a resin turns into its plastic form from elastic form. Usually for Epoxy this lies between 50 °C to 80 °C. Any temperature above it could result in a failed bond (Lee et al., 2021). Through their experiments with CFRP strengthened concrete prisms, Gamage et al. (2005) could identify that temperature exceeding 60 °C or the  $T_g$  of the epoxy resin brought down the loading capacity of the element rapidly.

The most critical situation is noticed when concrete is immersed in heated water. The moisture ingress into the matrix damages the cross links of the polymer thereby breaking the interfacial bond between the CFRP and the concrete. (Alnuaimi et al., 2021).

#### 2.5.6. Freezing and thawing

Freeze and thaw situation has been observed to be of contradicting when compared to other factors affecting the FRP bonding by so many other researchers giving different ideas on the conditions (Jiang et al., 2022; Al-Tamimi et al., 2015). A very recent study has been completed in 2022 on freeze and thaw cycles-based changes in the flexural performances of beams. After 300 freeze-thaw cycles, the specimens demonstrated a 22% reduction in ultimate load capacity accompanied by a 26.7% increase in deflection at midspan and a 50% increase in maximum strain of the CFRP. (Jiang et al., 2022).

### 2.5.7. Fire

An experimental study conducted by Falahi et al. (2017) on carbon and glass FRP laminates at elevated temperature demonstrated three different types of failure modes when tested for elastic modulus and tensile strength, as follows:

1. Brittle fibre rupture at 100 °C to 150 °C
2. Softened of epoxy adhesive at 200 °C to 250 °C
3. Burned of adhesive and specimen fail at 300 °C.

The study also noted that the hybrid CFRP and GFRP laminates showed better performances. It also showed lower and higher temperature has an adverse effect on the mechanical properties of the tested composite (Falahi et al., 2017)

### 2.5.8. UV radiation

Al-Tamimi et al. (2015) noticed an increase in strength when CFRP wrapped concrete specimens were exposed to UV. This is due to the great polymer crosslinking in the polymer matrix. Their experiment was carried out over a period of 150 days (3600 h) in a harsh marine environment. Similarly, Lee et al. (2021) also assessed FRP-concrete (reinforced with CFRP and GFRP) subjected to both external environments over a period of 13 years. They observed a clear reduction in debonding onset strain in the CFRP beams which were outdoor.

### 2.5.9. The modes of failure at the adhesive-concrete interface

Many studies have been conducted on the failures on FRP adhesive and concrete interface. Many tests conducted under hygrothermal effects has shown that adhesive cohesive failure dominating other failures such as FRP-concrete bond failure, or failure due to shear or flexural stresses regardless of the method of testing. In addition to hygrothermal effects, cyclic loading also creates an immense impact on the FRP bond failure and contributes to reduced fatigue life cycle. Wet and dry cyclic loading under hygrothermal situations has shown reduced interface bond strengths. Even though it could be concluded under hygrothermal conditions the dominating failure will be FRP concrete interface bond failure, it was also found through several studies that the specimen size played a significant role in the failure mode.

Mukhtar and Arowojolu (2020) concluded in their study on what govern the FRP-bonding interface failure, that the failure is mostly governed by the specimen size that's

been tested in the laboratory, exposure conditions, surface conditions of the FRP concrete interface, method of conditioning, exposure duration and methods of testing. They also denoted that bond slip method and accelerated ageing test are insufficient to gain the full picture of FRP-concrete bond failure. While discussing the possible implemented approaches for FRP-concrete bond performance they suggested that a nano-modified epoxy could be a solution for FRP-concrete bonding. They also call for more research requirement on numerical models that consider all possible failure modes including,

- FRP-concrete,
- FRP-FRP,
- Adhesive-FRP

## 2.6. Research significance

It has been proven through research work from several authors, that FRP-Concrete bond interface deteriorates in aggressive environmental conditions and tend to fail before the fatigue failure occurs in a reinforced concrete structure. The testing done on these factors are difficult to rely on as different sample sizes gave varying results for similar conditions.

Even though several studies have been made on the interfacial bond performances, yet a standard testing method has not been proposed so far. It was also said that one testing criteria alone could not evaluate the performance of the bond and requested further study on this matter (Mukhtar and Arowojolu, 2020).

Going forward it was also found there had been few studies on different types of improvement methods which mainly focused on the interfacial bond. Initially the following possibilities of improvement were taken into consideration and justified despite their drawbacks, as follows:

### Improving the concrete conditions

1. Removing moisture through rapid heat may allow more moisture to be absorbed.

### Improving FRP

2. There had been failures within FRP such as delamination and fibre pullouts, but this is very low.

### Improving adhesive

3. This could be an alternative as most of the failures have been found within the adhesive region, even in the wet layup systems.

Above all the suggested methods, there have been several studies on improving the adhesive as it plays a vital role in keeping the composite together. It also significantly affects the bond created with the concrete surface thus reducing the potential of debonding.

Many studies investigated the effects of aggressive environment on CFRP strengthened concrete. Several steps have been undertaken to improve the epoxy with cementitious products to analyse the effects of the new proposed system in aggressive environments. The relevant studies have been done by Alwash et al., 2021, Dai et al., 2021 and F. Wang et al., 201.

A modified adhesive can act as a barrier to moisture, ions and temperature. Likewise, several methods of improving the status of adhesive had been studied in polymer composite, mechanical and material engineering fields. From all the methods applied, nanomodified adhesives have shown promising outcomes (Al-Zu'bi et al., 2024)

#### 2.7. Nano-modified adhesives used with CFRPs.

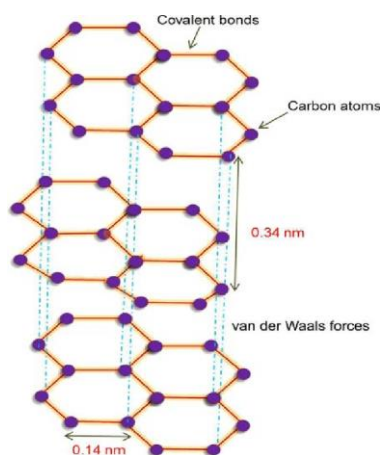
Nanomaterials have been the subject of discussion for several decades instigating new paths for scientific and engineering technologies. The application of nanomaterials is emerging into research and development of macro, molecular and atomic scale of material and living organisms. This innovation is creating innovative technologies, material and even organisms (Khan et al., 2016).

Several nanomodified epoxies have been found in the past with Kevlar fibres, nanotubes, polymer cement mortar (PCM), and graphene oxide (GO). Yet the studies on graphene nanoplatelets (GNP) have demonstrated their better mechanical performances.

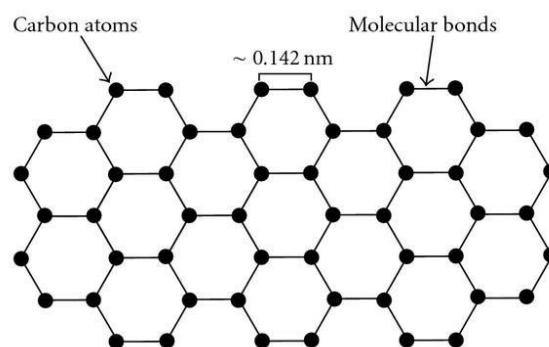
### 2.7.1. Graphene based nanomaterial.

One of the most popular materials being researched by the building, automotive, and electric industries is graphene. Numerous honours, including the Nobel Prize and the Kavli Award, have been given to the research on this. The carbon atoms in graphene function drastically differently due to their sp<sup>2</sup> bonded atomic structure, displaying a range of mechanical and chemical properties which leads graphene to be used in variety of applications (Figure 11) (Lalwani et al., 2016).

Graphene is considered as the basic building block of carbon allotropes. It is a two-dimensional sheet of carbon atoms arranged in a honeycomb structure. Graphite being one of the naturally occurring element is composed of several sheets of graphene. Even though isolating graphene sheets have been a challenge for a very long time, when it became possible in 2004 by Novoselov and Geim, graphene became one of the widely used and experimented material (Clemons et al., 2010; Lalwani et al., 2016).



a) Arrangement of carbon atoms in graphite (Khan et al., 2016)



b) Arrangement of carbon atoms in graphene (Clemons et al., 2010)

*Figure 11 arrangement of atoms in graphite and graphene.*

Many research papers have proved the mechanical properties of the graphene, yet the testing on chemical properties or the response of graphene base epoxies in aggressive environments are limited. The study of using graphene induced adhesives on CFRP and Concrete has very limited studies in the past. (de Sousa et al., 2015; Gao and Mäder, 2015; Keyte et al., 2019; Minea, 2020; Neto et al., n.d., 2013)

Carbon-based nanofillers are popular in the automotive and construction industry when it comes to retrofitting. Carbon nanofibers, carbon nano tubes (CNT), graphene nano species (GNSs), GNP are some of the carbon forms which are going through intensive testing to reinforce the matrix used in CFRP composites.

When it comes to graphene-based nanomaterial it has been found that lower concentration of graphene within the epoxy exhibit promising results compared to other carbon nanofiller concentrations. Likely 1% to 2% graphene in weight to epoxy adhesive have shown an increase in failure load by a factor of approximately 1.3 and at 1 wt.% showed a decrease in corrosion of the metal substrate when tests were made with CFRP and metal (Fry-Taylor et al., 2023).

It has been found that GNPs have performed well among multiwalled carbon nanotubes, carbon nanotubes, single wall carbon nano horn in ageing studies. Through past research it is assumed that a wt.% of GNP less than 0.3% has the possibility of giving better mechanical performance. Agglomeration is possible when GNP content is increased in the composite (Fry-Taylor et al., 2023; Jojibabu et al., 2017; Keshavarz et al., 2020) . Another study on the GNP induced epoxy when tested for dynamic mode II fracture toughness has shown promising results until 0.75 wt.% (Jia et al., 2018).

Graphene is insoluble in water in their pristine form. Pristine graphene which is single layer graphene or few layer graphene has a strong tendency to agglomerate due to strong Vander Waals forces between the individual sheets. As a result, it forms large insoluble aggregates that are difficult to disperse in water.

Yet there had been developments to make this possible through functionalising the graphene surface with different chemical groups such as oxygen containing functional groups (-OH, -COOH, etc) which can improve its compatibility with water molecules. These functionalised graphene materials are often referred to as GO or reduced Graphene Oxide (rGO). At the time of this study, both the material has expressed high cost. Therefore, the use of GO has been considered not cost effective.

Sonication is a common method used to disperse GNPs in epoxy resin, in which high frequency sound waves are used to break apart nanoparticles. As this method is not viable in large-scale manufacturing, the method has been not much used in the industry. Another method to improve the dispersibility of pristine graphene in water or other solvents is to use surfactants or other stabilising agents that help prevent agglomeration and promote dispersion of the solvent. Dispersion methods are a necessity for graphene to incorporate with any liquid. Several dispersion methods have been suggested in the past studies which will be further discussed in Section 3.8.4 of this dissertation.

Since SEM analysis will be undertaken to understand the presence of GNP in the epoxy, few past studies were considered relevant to this study.

Fu et al. (2020), (Figure 12) studied the difference in epoxy nature when GNP is mixed in different ratios. Following are images of SEM analysis on epoxy mixed with GNP from Fu et al. study. It could be observed that the flaky nature of the epoxy kept increasing with the increase of GNP particles, proving the intermolecular crosslinks formed within the resin (Fu et al., 2020).

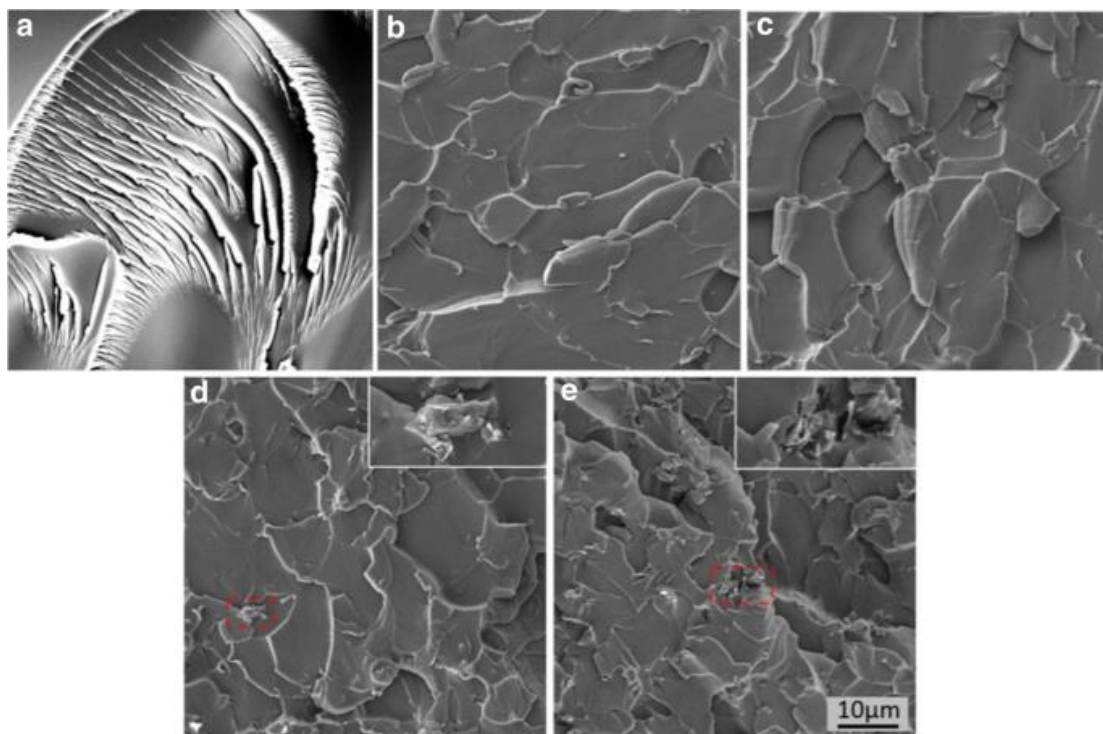


Figure 12 SEM images of fracture surfaces. a neat epoxy. b Epoxy/GNP 0.1 wt%. c Epoxy/GNP 0.3 wt%. d Epoxy/GNP 0.5 wt%. e Epoxy/GNP 1.0 wt%, reproduced from [32](Fu et al., 2020)



Another experiment conducted by Ravindran et al. (2018) showed how the fracture of epoxy brings GNP out from the polymer. Also note that the fracture surface gets rougher with the increase in GNP % (Figure 13).

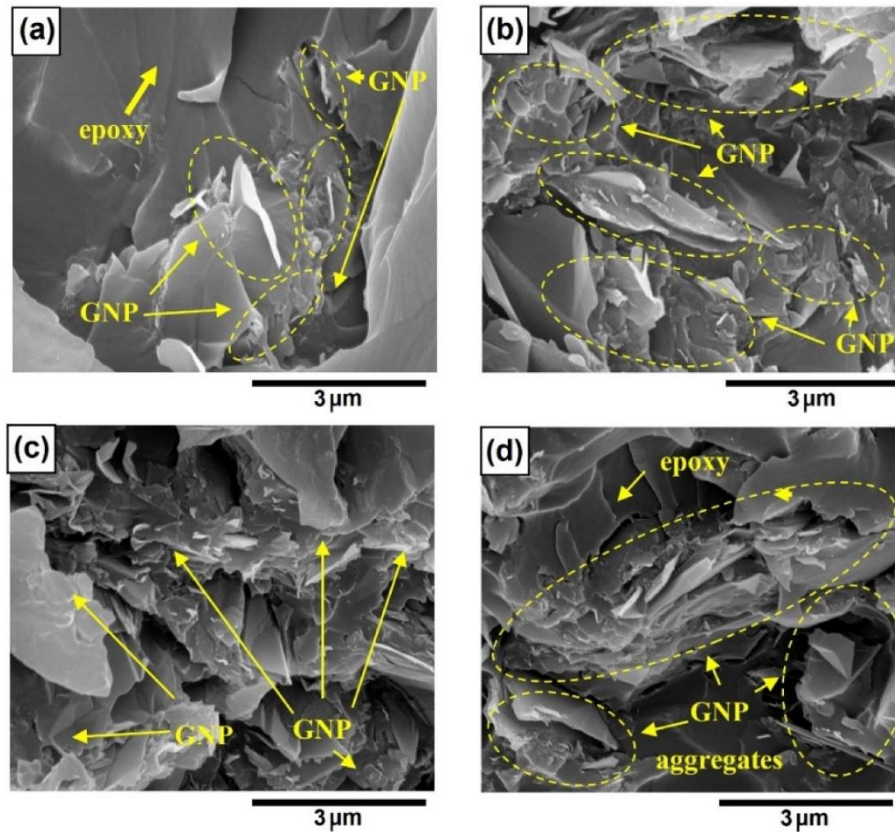


Figure 13 SEM of fracture surface of GNP (C-300 series) in epoxy at loadings of (a)  $f_{\text{GNP}} = 1.0 \text{ wt } \%$ ; (b)  $f_{\text{GNP}} = 2.0 \text{ wt } \%$ ; (c)  $f_{\text{GNP}} = 10 \text{ wt } \%$ ; (d)  $f_{\text{GNP}} = 20.0 \text{ wt } \%$  (Ravindran et al., 2018)

A study conducted on the interlaminar fracture in GNP infused epoxy and CFRP composite by Zafeiropoulou et al. (2020), depicts the behaviour of GNP under stress (Figure 14,15). The study categorises the failure modes of GNP reinforced epoxy into three categories,

1. Crack pinning which is done by the nano filler.
2. Separation within the layers of graphite.
3. Crack bridging.
4. Shear failure within the resin due to the different in heights of fracture surface.

As per the study the crack generated are pinned by GNP and then bifurcated into new crack paths which is later pinned again by GNP. The individual cracks may or may not

connect with other cracks in different heights in the fracture plane. When the crack comes across the surface of the GNP, there is a pullout of GNP sheets, this relates to the second type of failure mode discussed above. The Vander Waals forces between the graphene sheets makes it much easier for the force to pull the individual sheets of the system. The studies concludes that higher specific surface area of GNP leads to better load transferring within the adhesive, preventing cracks formed within the epoxy or by diverting them (Khalid et al., 2023; Zafeiropoulou et al., 2020).

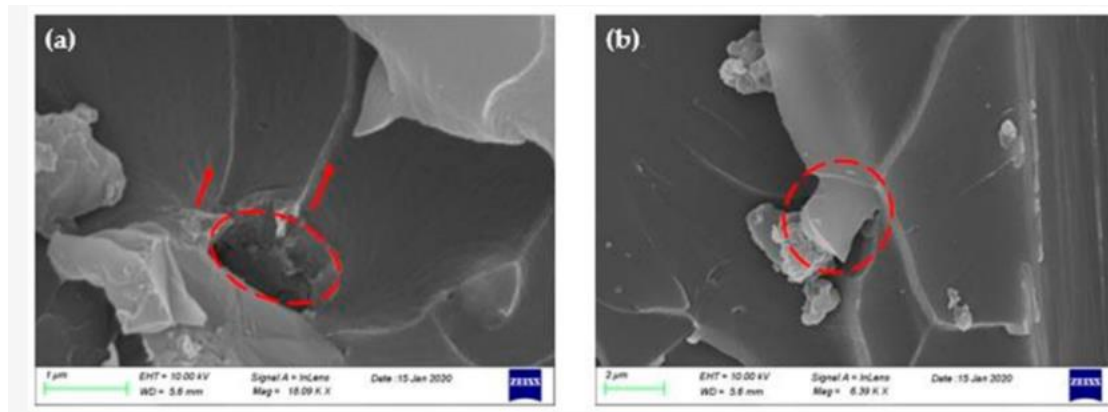


Figure 14 SEM images of C300 nano-fillers failure mechanism: (a) crack pinning and bifurcation and (b) separation of graphene sheets and pull-out (Zafeiropoulou et al., 2020).

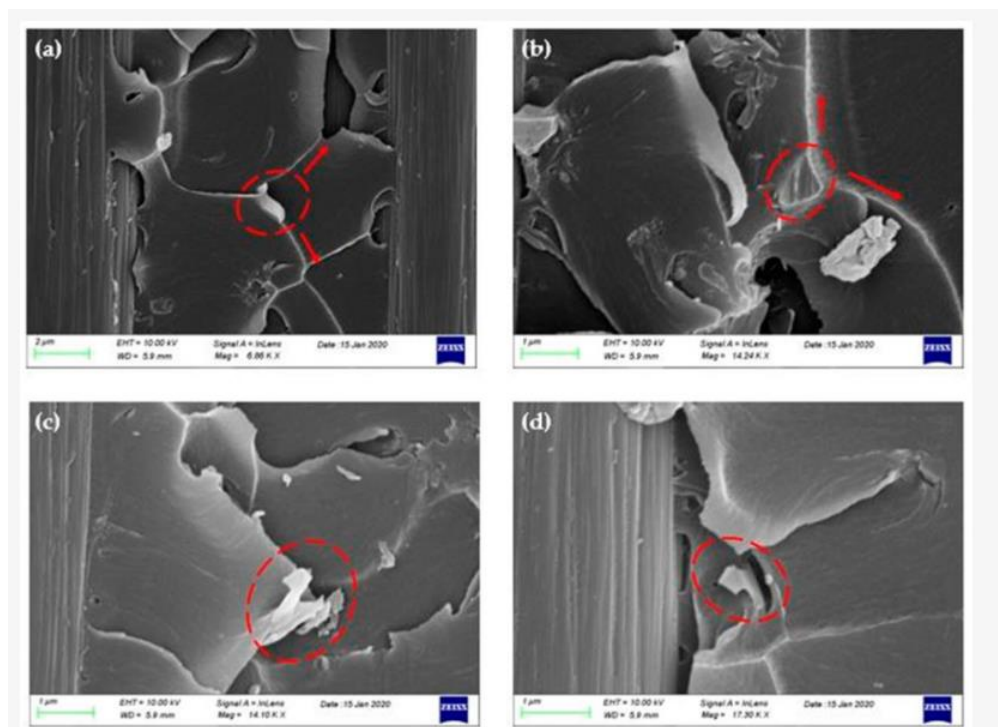


Figure 15 SEM images of C500 nano-fillers failure mechanism: (a, b) crack pinning and bifurcation and (c, d) separation of graphene sheets and pull-out (Zafeiropoulou et al., 2020)

A review study on the toughness of graphene and epoxy by Khalid et al. (2023), gave a further knowledge on the type of failure mechanism and the involvement of graphene in them. Figure 16 shows the SEM images derived.

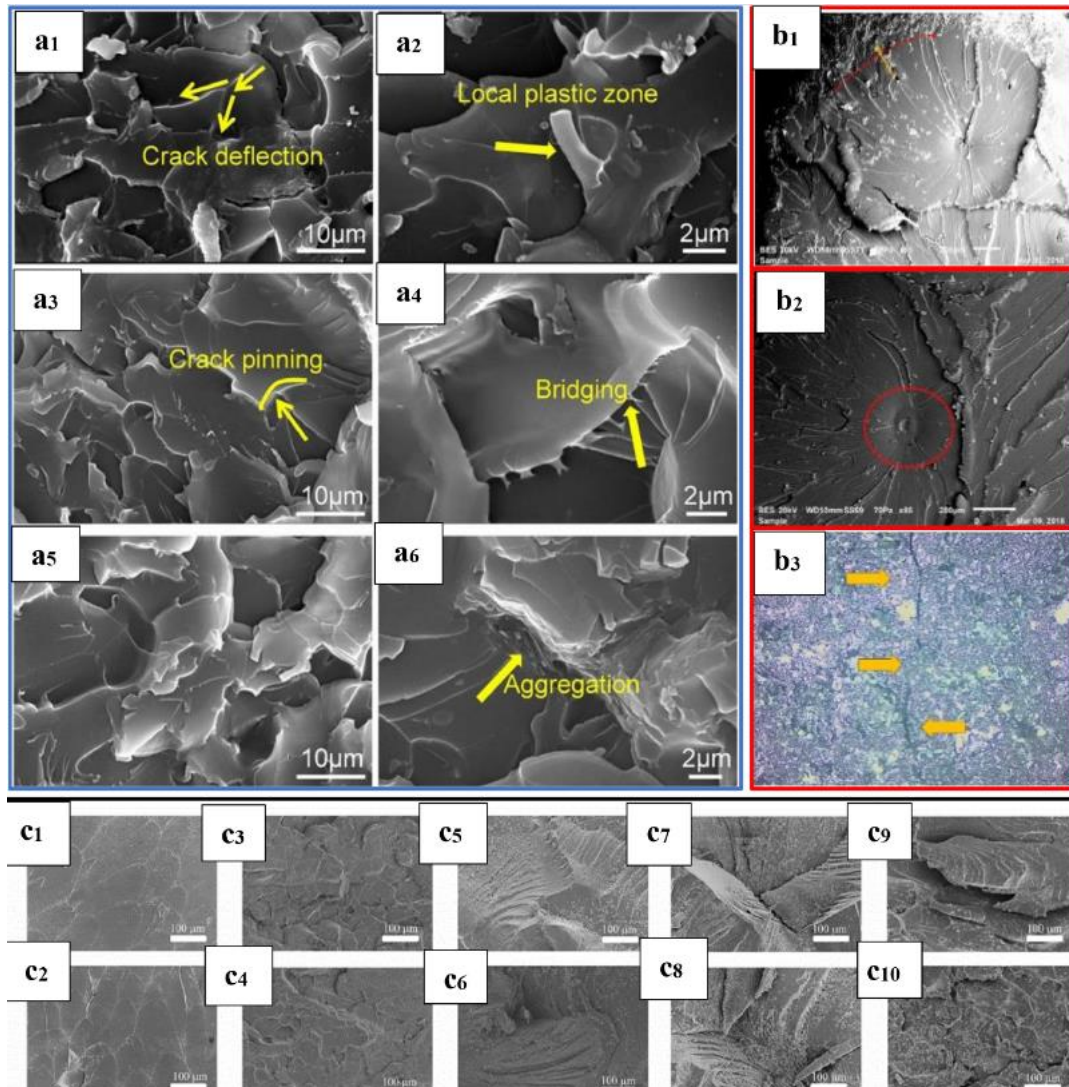


Figure 16 SEM images of the tensile fractured surfaces at different % of nanocomposites (GO based) at liquid nitrogen temperature (Khalid et al., 2023)

### 2.7.2. Silicone based nanomaterial.

One of the most abundant elements on Earth is silicon dioxide, or silica. It can be acquired naturally in a variety of settings, in both crystalline and non-crystalline (amorphous) forms. Amorphous silica can either be artificially produced or formed through natural biogenic processes. Similarly crystalline silica is also found naturally created by crystallisation and compression of cooling magma or it can be produced artificially by vitreous, pyrogenic, or colloidal processes. When combined, these silica

types are important for both natural processes and human uses (Liu and Sayes, 2022). Figure 17 shows an SEM image of the modified and unmodified NS. Silica can be used to remove agglomeration in GNP.

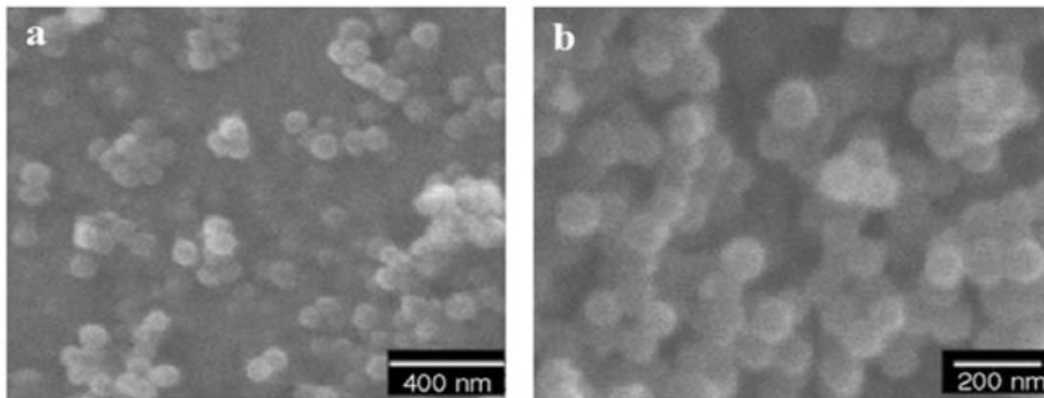


Figure 17 Scanning electron microscope (a) unmodified NS (b) NS modified (Gharehbash and Shakeri, 2015)

### 2.7.3. Hybrid nanofluids

Hybrid nanofluids are formed when combining different types of nanoparticles or additives within the nanofluid to create synergistic effects and enhance stability. Surface modified NS is considered as one of the options for the hybrid nano fluid for its compatibility and previous attempted trials with concrete (Minea, 2020).

Table 2 Research papers on nanomodified adhesives

Research Article	Reference	Purpose	Significant Material	Environment	Duration	Findings
Marine environmental effects on a graphene reinforced epoxy adhered single lap joint between metals and CFRP.	(Fry-Taylor et al., 2023)	Effects on the bonding strength	GNP -1wt%	Marine – 3.5% NaCl at 50 °C	1,2,3 weeks	Dry Condition- Average 15.5% increase in lap shear strength Immersed- did not show any improved performances and for instant it even magnified the manufacturing defects
Nano-modified Adhesive by Graphene: The Single Lap-Joint Case	(Neto et al., n.d.)(Neto et al., n.d.)	Performance study on FRP and metal	Nano modified adhesives by graphene	Room temperature		57% increase in joint strength. All failures were cohesive failures
Effect of GNP on water absorption and impact resistance of fibre-metal laminates under varying environmental conditions	(S. Wang et al., 2022)	Water absorption and impact resistance of fibre reinforced metals	GNP in epoxy with glass fibre metal laminates	Hygrothermal and salt spray		Addition of 0.3% of GNP reduced water absorption in FML by 57.6% and increased impact resistance by 150%
The effect of GNP on the flexural properties of fibre metal laminates under marine environmental conditions	(Keshavarz et al., 2020)	Flexural properties of FML with GNP added epoxy under marine env	GNP in epoxy with glass fibre metal laminates	Marine exposure	7, 14, 28 days	With 0.25% of GNP flexural strength and modulus increased by 128% and 63% and strain values by 1.85 times with 0.5% GNP the water absorptions were 31% lower than the systems without GNP
Single lap joints bonded with structural adhesives reinforced with a mixture of silica nanoparticles and multi walled carbon nanotubes.	(Razavi et al., 2018)	Shear strength and elongation at failure of adhesively bonded single lap joint	MWCNT and SNP (Silica nano particles) (1:1)	Room temperature		28% improvement in shear and 36% in elongation at failure with 0.8% wt. nano particles

#### 2.7.4. Dispersion of nano materials in the resin

Several mixing methods pertaining to the dispersion of nanoparticles in epoxy have been examined in previous studies (Figure 18). Al-Zu'bi et al. (2024), combined the nanoparticles in a few drops of acetone and hand-mixed for three minutes before adding the base to the mix; in a recent study on mixing nanoparticles with epoxy to test nanohybrid epoxies on near surface mounted FRP in concrete. The solution was manually mixed for two minutes before being placed in the ultrasonication bath for five minutes. Before installation, the hardener was later added to the mixture and manually stirred for an additional two minutes.

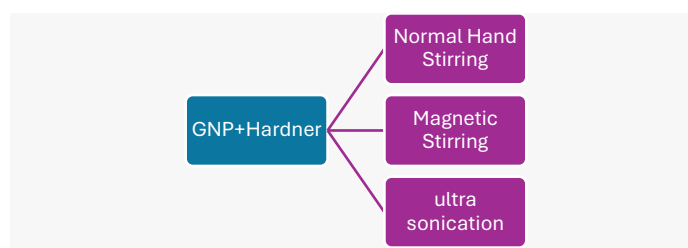


Figure 18 Dispersion methods for nano particles in epoxy.

Razavi et al. (2018) employed mechanical techniques to scatter nanoparticles in epoxy in a further attempt to combine silica nanoparticles and multiwalled carbon nanotubes in order to test for shear and elongation at failure in metal. According to Razavi et al. (2018), the resin's viscosity can affect how well the nanoparticles disperse. In order to do this, they first mixed the base with the nanoparticles and stirred the mixture mechanically for 15 minutes at 100 rpm. The mixes were then subjected to 45 to 60 minutes for nanoparticle concentration of 0.25 wt.% and 0.4 wt.% in a Bandelin SONOPLUS HD 3200 sonicator, which had a power of 70W and a pulse rate of 1:1. The mixture was then mechanically stirred once more for 25 and 30 minutes at 1500 rpm before the combination was run through the sonicator once more for thirty minutes at the same pulse rate. The mixture was subjected to 5 more minutes of mechanical stirring at 100 rpm before the base was gradually added. Finally, the combination must degas for a further 20 minutes to eliminate the trapped air. The entire procedure had been carried out in an ice bath to prevent overheating as sonication can be exothermic (Razavi et al., 2018).

In a separate investigation, Zamani et al. (2021) employed acetone in the base material initially and manually stirred the mixture with a spoon for five minutes to examine the impact of GNP and NS mixed in epoxy on the fatigue life and fracture start phase in Al-GFRP composite. After that, the mixture was magnetically stirred for 10 minutes at 180 rpm. Subsequently, the necessary quantity of nanoparticles was added to the base and acetone mixture and mixed for a further half hour at 180 revolutions per minute using a magnetic stirrer. Additionally, the third step of this dispersion approach has been substituted in the study with an 80W ultrasonic probe that pulses at a 1:1 ratio to mix the nanoparticles. The mixture was degassed for one hour at 0.65 bar pressure to eliminate the air bubble, and it was then baked for three hours at 70 °C to evaporate the acetone (Zamani et al., 2021).

Similar to this, Hashim et al. (2021) employed mechanical stirring at 400 rpm for 15 minutes to distribute nanoparticles dissolved in ethanol within epoxy. This was followed by three roll milling at 2000 rpm at 70 °C, and lastly, five minutes of vacuum oven degassing (Hashim et al., 2021; Zafeiropoulou et al., 2020).

In a study by Jia et al. (2018) GNP combined with acetone was mechanically stirred with epoxy using a magnetic stirrer set at 2000 rpm for three hours. After the mixture's temperature dropped, it was heated to 100 °C to evaporate the acetone. After that, they mixed the hardener for three minutes at 2000 rpm using a planetary mixing (ZYMC-180V). They have applied this technique to GNP levels of 0.5 wt.% and 0.75 wt.% (Jia et al., 2018).

After gathering most data from earlier research, it was first thought that combining acetone with nanoparticles may pose a risk, as it is believed that acetone will evaporate during application. However, this may not always be the case. The epoxy polymers might also be harmed by heating the epoxy mixture to between 70 °C and 100 °C. Therefore, when conducting experiment in this study, a combination of mechanical stirring and an ultrasonication bath was used. The experimental approach mostly adopted the dispersion method of Razavi et al. (2018) since it appeared more feasible and required less equipment.

#### 2.7.5. Other effects to consider.

One of the major concerns aroused during the study of this nanohybrid mixture is how could this commercially viable. Since CFRP is an internationally used material and since some countries does not have the manufacturing facilities, these need to be transported via sea. But the question is whether these dispersion methods sustain the days of voyage or whether the nanoparticles in these nanohybrid resin would sediment with time while transportation and storage. This requirement needs further research on long term behaviour of these nanohybrid resins.

Apart from this, other matters that needs to be considered is the toxicology of these nano particles when used in the application. This is analysed to provide a safe environment for production and for safe discarding of waste.

#### Toxicology of graphene

When assessed for the cytotoxicity of graphene, GNP have shown promising applications in stem cell imaging/ therapy and in anticancer therapy through research conducted with several derivatives of graphene. Yet Lalwani et al noted in their study that a toxicity of graphene nano particle is based on several physical aspect of the material and if it must be applied in medical application it has to be coated with several biocompatible moieties to mitigate cytotoxicity effects (Lalwani et al., 2016).

#### Toxicology of NS

The morphological and physiochemical factors determine the cytotoxicity of Silica nano particles. Surface modification of the SiO<sub>2</sub> nano particles, have been found to reduce cytotoxicity up to certain level but not completely. As the size of the nano particles decrease it may absorb into the bloodstream and cause damage to the organs (Liu and Sayes, 2022).

#### 2.8. Design consideration.

Bond length plays a very crucial role in a CFRP composite. Usually, the recommended bond length as per ACI and fib bulletin code is around 150 mm to 200 mm. In future work, the chosen nanohybrid mix with bond lengths more than 100 mm and less than 100 mm must be tested to identify whether the adhesive mix could reduce the required bond length to achieve the expected load capacity. This will contribute to a significant reduction in CFRP installation costs.



Even though the cost of the resin could go up due to the addition of nano particles, if the proposed nano hybrid mix could succeed in the market, it could sure save more important structures in the future.

### 2.9. Interfacial bond performance

Interfacial bond performance in FRP-concrete composites refers to the quality and strength of the bond between the FRP material and the concrete substrate. This is mainly governed by three phases in the composite that is the FRP/ adhesive in the matrix, FRP and adhesive, and Adhesive and substrate (Section 2.4). Usually, the quality of the interfacial bond is determined by a pull off shear test and many models have been designed through several studies. It had been found that the interfacial bond performance is determined by the FRP sheet stiffness, FRP bond length, the CFRP to concrete width ratio, concrete mechanical properties, properties of adhesive (such as type and thickness), environmental conditions, and loading types. The investigations have been conducted in cyclic and quasistatic loading patterns which gives clear idea on how the interfacial bond behaves including mechanical experiments, analytical analysis and numerical analysis to reinforce the findings (Li et al., 2018; Yuan, 2020).

From the literature review it was found the main governing criteria to quantify the interfacial bond performance is through the bond shear stress and its corresponding local slip and the interfacial fracture energy. Interfacial bond energy is a criterion which resembles the energy required to propagate a crack along the interface which in terms quantifies the resistance of the bond to crack propagation and thereby provides insight into the bond's strength and durability.

### 2.10. Research gap

Based on the literature review and the initial question in Section 1.2, the following gaps in the research were identified to be further analysed for the CFRP-concrete composite

1. How would GNP and NS mixed epoxy perform on a concrete substrate, qualitatively?
2. What proportion of GNP and NS could be much suitable for a better performance?
3. How would the GNP and NS mixed epoxy perform in an aggressive environmental condition such as salty water and elevated temperature?

### 3. Methodology

#### 3.1. Test setup

The test procedure presented in Figure 19 was created to determine the effect of nanomodified epoxy resin on CFRP-reinforced concrete in aggressive environments. The main objective of the test is to monitor the interface behaviour between substrate and fibre when the adhesive is modified with nanomaterials, by assessing the bond strength between substrate (concrete) and CFRP.

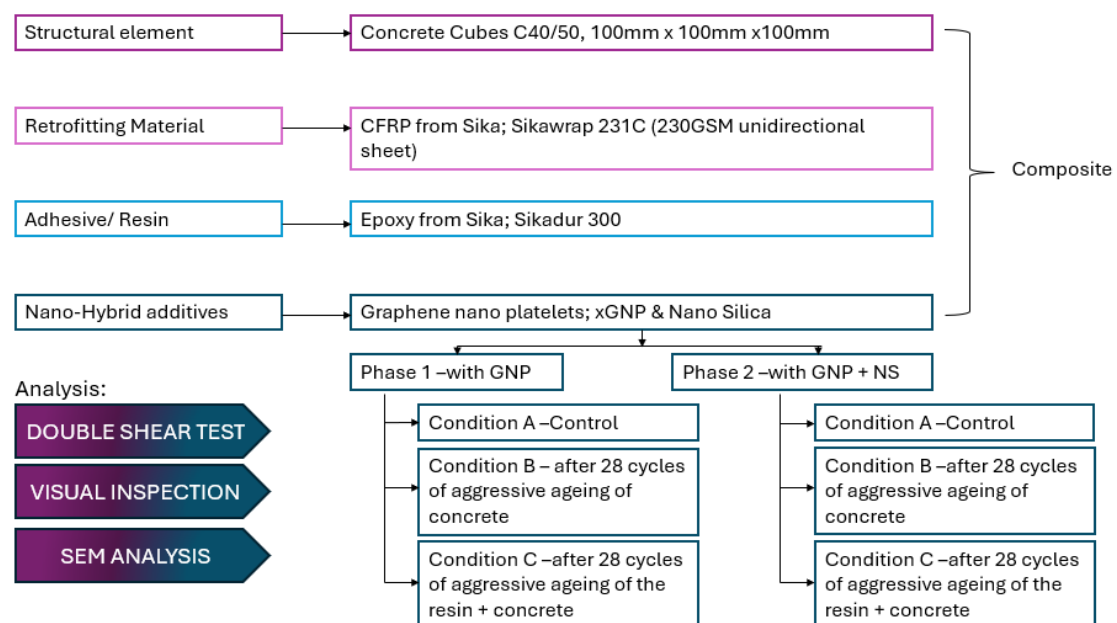


Figure 19 Test setup overview.

Since the adhesive has the potential to be improved to increase the efficiency of the composite, two proposals have been put forward to improve the adhesion of the epoxy resin in aggressive environments.

1. Input and adjustment of GNP into the epoxy resin composition.
2. Input and adjustment of NS in the GNP modified epoxy resin composition.

This study is based on the information gathered through research to improve the performance of epoxy adhesives in the automotive, polymer and mechanics industry. The use of GNP and NS to enhance the performance of the epoxy adhesive has been tested several times with different percentages of the nanoparticles, with metal or

aluminium being as the substrate element. The two most successful percentages 0.25 wt.% and 0.5 wt.% identified in previous studies (Jia et al., 2018; Keshavarz et al., 2020; S. Wang et al., 2022; Zafeiropoulou et al., 2020) were therefore considered in this research study to understand the effect on concrete substrate. The application of nanoparticles with epoxy adhesive on concrete substrate is a novel attempt to date.

Considering the sort of real-world applications such as bridge piers, wastewater tanks etc. where concrete structural elements are typically exposed to excessive aggressive environmental conditions, the use of concrete grade of C40/50 as the substrate choice was regarded as for this experiment. The main objective of this test is to identify the best percentage of nanomaterial/s used in the adhesive to improve the adhesive strength of the epoxy resin when used on concrete substrate, therefore two best percentage of nanomaterials were used.

The test involves two different phases, phase 1 and phase 2. In phase 1, concrete cubes are strengthened with CFRP, and epoxy resin made from 0 wt.%, 0.25 wt.% and 0.5 wt.% of GNP by weight, respectively. A total of 36 cubes were cast. The cubes were first cured in water for 28 days. 12 cubes were tested after standard curing time (28 days) to assess the impact of GNP under controlled conditions. Further 12 cubes were exposed to accelerated ageing by subjecting the 28-day old specimens to 28 cycles of wet and dry conditions and evaluate the effect of the GNP under harsh environmental conditions. The remaining 12 cubes were tested for an additional 28 wet and dry cycles to assess the impact after CFRP ageing process. In phase 2, the series of experiments was repeated with the addition of NS along with GNP in a weight ratio 1:1.

The samples were then tested to measure the debonding load and identify the maximum load capacity each condition could withstand, and the corresponding slip the bond could undergo. This allowed to further characterise the shear resistance the adhesive could impose on the composite.

### 3.2. Raw materials

The Portland Cement used was procured from Tarmac Blue Circle General Purpose Portland Limestone Cement with a density of 3,950 kg/m<sup>3</sup> (CEM II, 32.5MPa). Coarse aggregate used with density of 2,650 kg/m<sup>3</sup> and fine aggregate with density of 2,550 kg/m<sup>3</sup> were used.

*Table 3 Properties of CFRP and epoxy used in the experiment from the manufactures technical data sheet.*

	<b>Tensile Strength N/mm<sup>2</sup></b>	<b>Modulus of Elasticity N/mm<sup>2</sup></b>	<b>Elongation at break</b>	<b>Thickness mm</b>	<b>Density</b>
Sikawrap 231C (Dry Fiber)	4,900	230,000	1.7%	0.129	1.8 g/cm <sup>3</sup>
Sikadur 300	45	3,500	1.5%		1,160 g/l
Laminate	4,300	225,000	1.91%	0.129	

Unidirectional CFRP sheets with 0° fibre orientation, Sikawrap 231c with a 235 gsm, the two component Sikadur 300 epoxy adhesive were provided by SIKA UK. Further details are presented in Table 3. The nano material chosen for the nanohybrid resin was GNP of surface area 500 m<sup>2</sup>/g purchased and NS of 99.8% purity, both commercially available at Sigma Aldrich.

### 3.3. Concrete samples produced for CFRP substrate.

Approximately 78, 100 mm cubes were cast for the experiment in accordance with BS EN 12390-4:2019. Specimens were cured underwater for standard 28 days. 9 cubes were used for compressive strength tests, 15 were used to calibrate the shear tests setup and 54 were used for the shear test (Section 4.3.2).

#### 3.3.1. Control samples for compression test.

The compressive strength was determined using 9 numbers of standard 100 mm cubes and following the BS EN 12390-3:2019. The compressive strength was measured to verify that concrete had reached the target strength. Specimens were subjected to 28 cycles of wet-dry ageing in simulated aggressive environmental conditions (NaCl 3 wt.% water) curing strength testing and 28 days of standard curing strength testing (Section 4.3.3).

### 3.3.2. For calibration

For calibration, 15 cubes were first tested with 0 wt.%, 0.25 wt.%, and 0.5 wt.% GNP content in the epoxy resin. The following flaws were found in this sample test and fixed for the subsequent round of testing.

1. Surface preparation technique.
2. Techniques for preparing adhesives.
3. CFRP must be installed on the substrate, and the strip must remain perpendicular to the surface.
4. The process for calculating strain values.

### 3.3.3. For testing, from the remaining 54 cubes

#### Phase 1

After standard curing for 28 days, 12 cubes were installed with CFRP using GNP mixed epoxy resin with 0 wt.%, 0.25 wt.%, and 0.5 wt.% of GNP in the mix. After being aged for 28 cycles in an oven and salt water, another 12 cubes were installed with CFRP using GNP-mixed epoxy resin at various GNP percentages. After 28 cycles of ageing, 12 more cubes were installed with CFRP using GNP-mixed epoxy resin at various GNP percentages, and they were left to age for an additional 28 cycles making the concrete expose to aggressive environment for 56 cycles and the resin 28 cycles.

#### Phase 2

Once the cubes had undergone a standard 28-day curing period, 6 of them were installed with CFRP using a GNP and NS mixed epoxy resin that contained 0.5 wt.% of GNP and varying percentages of NS. Additionally, six cubes were aged in salt water and an oven for 28 cycles before being installed with CFRP using the resin. After being aged for 28 cycles, six cubes were installed using a mixed epoxy resin consisting of GNP and NS, and they were then aged for an additional 28 cycles.

Figure 20 illustrates the acronyms used for the samples, the first two digits represents the GNP % used, the second two digits represents the NS % used. The letter following the digits "F," represents that the cubes has not been aged but installed with CFRP. The letters following the digits "AF," represents that the cubes have gone through 28 cycles of aggressive wet-dry cycles and then CFRP has been installed. The letters following the digits "AFA," represents that the cubes initially went through a 28 wet-dry

cycle and then CFRP was installed and later again the cubes went through and additional 28 wet-dry cycles. The Table 4 summarises the conditions used for the tests.

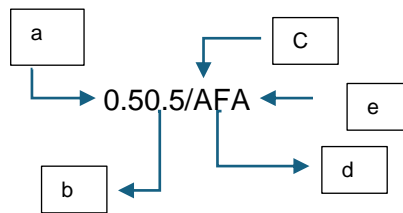


Figure 20 Naming method used on samples.

- a = the GNP % added to the resin
- b = the NS % added to the resin
- c = cubes which were aged before CFRP was installed
- d = cubes which were installed with CFRP
- e = cubes which were aged after CFRP was installed

Table 4 Summary of test samples

Description		GNP % in adhesive mix		NS % in adhesive mix		28 days curing	CFRP	28 cycles of ageing without CFRP	CFRP	28 days ageing with CFRP	No of samples
		0.25%	0.5%	0.25%	0.5%						
Control	C1					x					3
	C2					x		x			3
	C3					x		x		x	3
Calibration Test	0.0/F					x	x				4
	0.25/F	x				x	x				7
	0.50/F		x			x	x				4
Tested for Shear	0.0/F					x	x				4
	0.25/F	x				x	x				4
	0.50/F		x			x	x				4
	0.0/AF					x		x	x		4
	0.25/AF	x				x		x	x		4
	0.50/AF		x			x		x	x		4
	0.0/AFA					x		x	x	x	4
	0.25/AFA	x				x		x	x	x	4
	0.50/AFA		x			x		x	x	x	4
	0.50.25F		x	x		x	x				3
	0.50.5F		x		x	x	x				3
	0.50.25AF		x	x		x		x	x		3
	0.50.5AF		x		x	x		x	x		3
	0.50.25AFA		x	x		x		x	x	x	3
	0.50.5AFA		x		x	x		x	x	x	3

### 3.4. Mix design

The mix design procedures utilized to create the C40/50 concrete are displayed in the following calculation. Considering 78 cubes with dimensions of 100 mm × 100 mm × 100 mm and accounting for 10% waste, the total volume of the cubes to be cast is roughly 0.086 m<sup>3</sup>.

*Type of Cement = OPC*

Density of fine aggregate = 2550 kg/m<sup>3</sup>

Density of coarse aggregate = 2650 kg/m<sup>3</sup>

Density of cement = 3150 kg/m<sup>3</sup>

$$\frac{W}{C} \text{ ratio} = 0.46$$

Total volume of concrete

$$= 0.086 \text{ m}^3 \text{ (for laboratory testing of } 100 \times 100 \times 100 \text{ mm cubes)}$$

#### Cement Content

Even though the water to cement (W/C) ratio proposed is 0.40, 0.46 was assumed for laboratory purposes. This is to adjust the overall fresh properties and workability.

The minimum cement content for C40/50 concrete would be 360 kg/m<sup>3</sup>.

*Water Content = cement content × water/cement ratio*

$$\text{Water Content} = 360 \times 0.46 = 165.6 \text{ Kg/m}^3$$

#### Absolute Volume of Cement

$$\text{Absolute Volume of Cement } (V_{cem}) = \frac{\text{Cement Content}}{\text{Density of Cement}} = \frac{360}{3150} = 0.114 \text{ m}^3$$

#### Absolute Volume of Coarse Aggregate

Assuming 50% of the concrete volume is coarse aggregate

$$\text{Absolute Volume of Coarse Aggregate } (V_{coarse}) = 0.5 \times 1 = 0.5 \text{ m}^3$$

#### Absolute Volume of Fine Aggregates

$$V_{fine} = \text{Total Volume of the concrete} - (V_{cem} + V_{coarse})$$

$$V_{fine} = 1 - (0.114 + 0.5) = 0.386 \text{ m}^3$$

### Weight of Coarse Aggregate

$$W_{Coarse} = V_{Coarse} \times \text{Density of coarse aggregate}$$

$$W_{Coarse} = 0.5 \times 2650 = 1038 \text{ kg}$$

### Weight of Fine Aggregate

$$W_{fine} = V_{fine} \times \text{Density of fine aggregate}$$

$$W_{fine} = 0.386 \times 2550 = 837 \text{ kg}$$

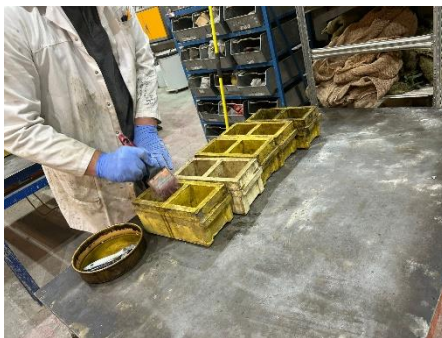
Hence after finding the right mix for 1m<sup>3</sup> of concrete, weight required to make 0.086m<sup>3</sup> of concrete. Figure 21 shows the concrete samples casted in the laboratory.

$$W_{cement} = 30.96 \text{ kg}$$

$$W_{Coarse} = 89.44 \text{ kg}$$

$$W_{fine} = 72.06 \text{ kg}$$

$$W_{water} = 14.24 \text{ kg}$$



a)



b)



c)

Figure 21 Casting concrete cubes in the laboratory a) applying form oil to the moulds b) and c) casted concrete cubes.



### 3.5. Curing and accelerated ageing.

For the first 28 days, 78 cubes were cured in tap water. The cubes were taken out of the water for accelerated ageing, after being cast. The specimens selected for accelerated ageing were subjected to 28 cycles of wet/dry curing, with 21 hours submerged in NaCl 3 wt.% water (Figure 22), followed by oven drying at 60 °C for 3 hours, following the methodology reported in (Marangu et al., 2024).



Figure 22 Concrete cubes in the 3 wt.% NaCl concentrated water.

The cubes were kept in water until the following cycle when it was not feasible to continue the cycle (e.g. laboratory closure during weekends and holidays).

Table 5 Type of environmental conditions used in this experiment.

Ageing Condition	Representing Symbol	Average Compressive Strength (MPa)	St. Dev. (MPa)
28 cycles of standard 28 days curing before CFRP installation	A	53.29	0.34
28 cycles of accelerated curing before CFRP application	B	45.46	1.48
28 cycles of accelerated curing after CFRP application	C	45.62	0.63

Symbols A, B and C (Table 5) will represent the corresponding ageing condition herein forth. Symbols B and C represents the aggressive environmental conditions the cubes were exposed to.

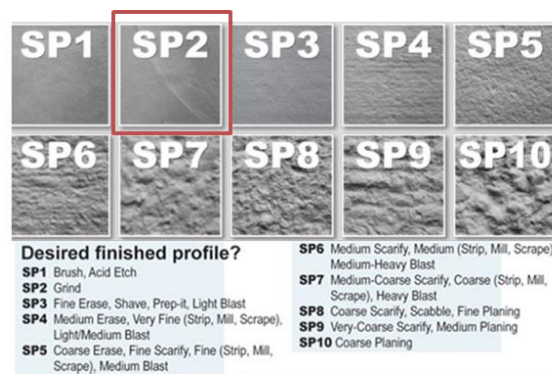
### 3.6. Strength testing of cubes

Of the nine cubes, 3 yielded an average compressive strength of 53.29 MPa. After being aged for an additional 28 cycles in an oven and salt water, the remaining 3 cubes demonstrated a further decrease in strength, yielding a compressive strength of 45.46 MPa. The cubes did not show a significant difference in compressive strength

after undergoing an additional accelerated ageing for another 28 days, yielding a compressive strength of 45.62 MPa in average of testing 3 cubes (Table 5).

### 3.7. Surface preparation

The surface of the cured samples was ground to the SP2 standard in the sample test mentioned in Section 4.3.2 to make them ready to accept the adhesive (Figure 23). However, it was then discovered that the calibration experiment's unsatisfactory results might have been caused by the grinding technique employed. To meet the SP4 criteria, sandblasting was therefore employed in the actual test (Figure 24). Hodge Clemco Limited's standard expandable abrasive of 1.4–2.5 mm in size (as per the supplier), was utilized for this purpose.



a) Type of surface preparation reference used in the initial set of tests

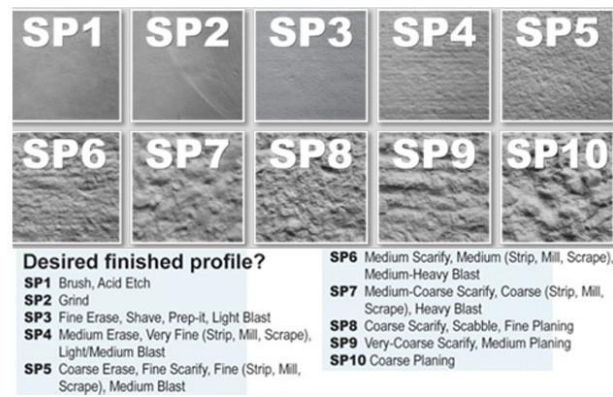


b) Hand grinding was used to achieve the SP2 grade



c) The surface preparation achieved from hand grinding the concrete

Figure 23 The surface preparation used in the initial set of tests.



a) Type of surface preparation reference used for the experiment



b) Sand blasting machine in the concrete lab



c) SP4 Level of surface preparation achieved

*Figure 24 Surface preparation used in the experiment.*

Concrete surface humidity was another aspect which was required to be below 4% as per the manufacturer's specification. Even though the samples were aged in salty water, during the application of CFRP the surface moisture was recorded and was found to be within the range of 1% to 2% for class 10 classification for concrete in the FLIR humidity meter (Figure 25).

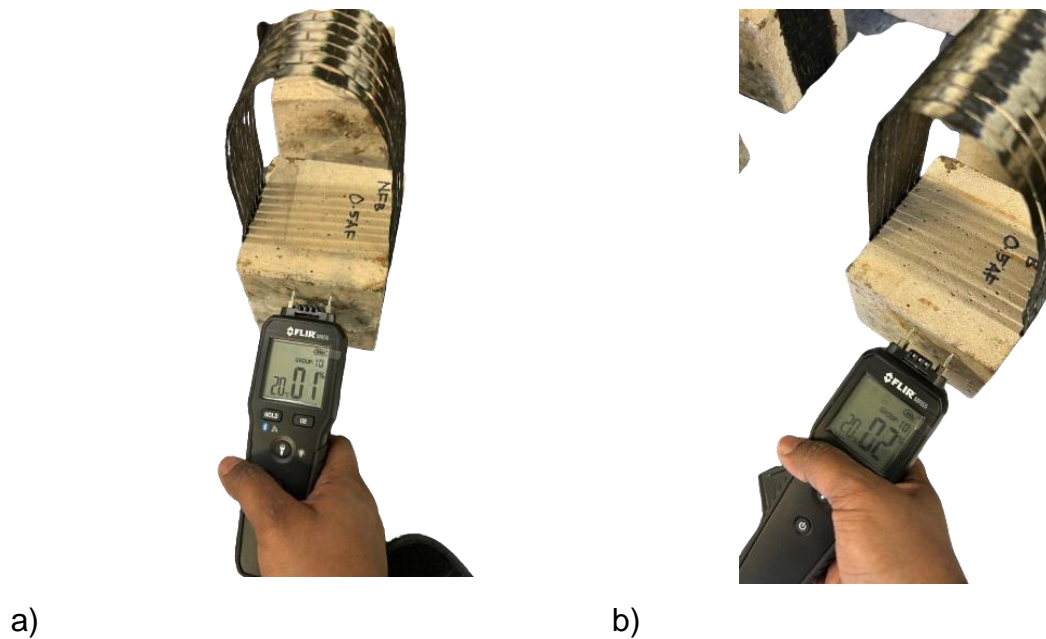


Figure 25 Surface humidity of the samples tested with FLIR humidity meter.

### 3.8. Adhesive preparation

Comprising two components, Sikadur 300 is an adhesive that has two main chemicals: component B contains polyoxypropylenediamine (polymer) with a concentration range of  $\geq 5\%$  and  $\leq 10\%$  and component A, which has the main chemical bisphenol-A-(epichlorhydrin) epoxy resin with a concentration range of  $\geq 50\%$  and  $\leq 100\%$ . The technical data sheet states that the components for the epoxy resin mixture should be combined in a weight ratio of 100:34.5.

#### 3.8.1. Epoxy resin for 0% GNP mix.

The yield of Sikadur 300 for wet application as per TDS is 1.0-1.3 kg/m<sup>2</sup>. The CFRP strip size is 50 mm x 500 mm in which only 200 mm will be prepared with the adhesive. Therefore, about 156 g of adhesive was prepared for each set of 12 number of cubes in the ratio of Part A: Part B = 100: 34.5 by weight.

#### 3.8.2. GNP + Adhesive

To investigate the impacts, two potential contents of the GNP were initially examined using the data from earlier studies. Twelve cubes containing 0.39 g and 0.78 g of GNP each were evaluated for each scenario. The initial set of adhesive mixing tests was limited to epoxy resin and GNP to better understand how the GNP-epoxy, nano-hybrid combination behaved.

Mixed resin density = 1.16kg/l

Table 6 represents the total volume of the mix used,

*Table 6 Mix ratio of GNP in epoxy.*

Combination	Base (g)	Hardner (g)	GNP (g)
0.25% of GNP	115.99	40.01	0.39
0.5% of GNP	115.99	40.01	0.78

### 3.8.3. GNP + NS+ Adhesive

Following testing on samples from the nanohybrid resin mix in Section 4.8.2, it was determined that 0.5 wt.% of the epoxy mix's weight had the best graphene blend. Through research, it was discovered that adding NS or using improved dispersion techniques could increase the interpolymer crosslinks. Therefore, in the following series of studies, both techniques were used. Consequently, 0.25 wt.% and 0.5 wt.% of NS, which is mostly employed to disperse GNP in epoxy, was added to the resin mix to study its effects (Table 7).

*Table 7 Mix ratio of GNP and NS in epoxy.*

Combination	Base/g	Hardner/g	GNP/g	NS/g
0.5 wt.% of GNP and 0.25 wt.% of NS	115.99	40.01	0.78	0.39
0.5 wt.% of GNP and 0.5 wt.% of NS	115.99	40.01	0.78	0.78

### 3.8.4. Dispersion methods

Two distinct dispersion procedures were investigated to determine the best dispersion for the nanoparticles in the epoxy mixture. Both manual mixing and mechanical mixing are used. To stop the resin from hardening too soon, nanoparticles were first mixed with the base in both techniques. In this case, it was mixed with component A. Component B, often known as the hardener, was added to the resin mixture after the nanoparticles were mixed.

#### Method 1 – Hand mixing (adhesive for samples intended for calibration).

The first effort was done with a regular hand stirrer (Figure 26). To test this approach, a combination of just GNP and resin was utilised. Initially, the GNP was added to the epoxy resin, and then manually stirred for approximately five minutes. After adding the hardener, the mixture was hand-stirred for an additional five minutes. This strategy

was originally attempted since it is a straightforward mixing procedure that might work depending on the site conditions.

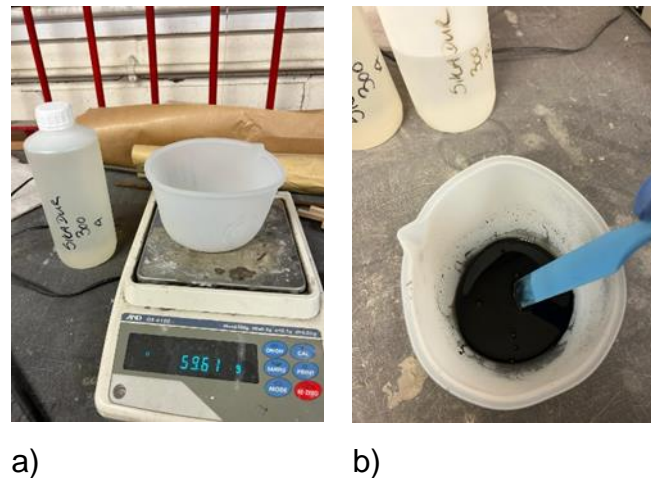


Figure 26 Hand mixing of GNP in epoxy during the initial set of tests for calibration purposes.

The test results obtained using this method was insufficient. One possibility was that the ineffective dispersion of the nanoparticles was the cause of this. When combined with epoxy, GNP is extremely prone to agglomeration. To maximise its performance, effective dispersion techniques must be used. A means of improving the dispersion is to use sophisticated mechanical mixing techniques.

#### Method 2- Mechanical dispersion (used for the main tests)

The concept of mechanical dispersion of nanoparticles were derived from techniques presented by Zamani et al. (2021) and modified as per the apparatus available in the laboratory (Figure 27).

The base and the nanoparticles were first weighed and combined for 5 minutes at a speed of 80 to 100 rpm in a mechanical stirrer. This range of rpm was maintained to prevent the dispersion of nanoparticles into the atmosphere. After that, the mixture was left in the 340 W ultrasonic bath (Fisher FB 15053) for 45 minutes in an ice bath. A mechanical stirrer was thereafter used to re-mix the mixture for a further 25 minutes at a speed of 1000–1100 rpm. Once more, with ice in the water, the mixture is kept in the ultrasonic bath for approximately 25 minutes. Weighing the hardener, then add it to the base-nanoparticle mixture and run it through the motorised stirrer one more time

for 5 minutes at 80 to 100 rpm. Finally, the mixture was placed in the ultrasonic bath for degassing for about 20 minutes. Figure 28 shows the procedure used.

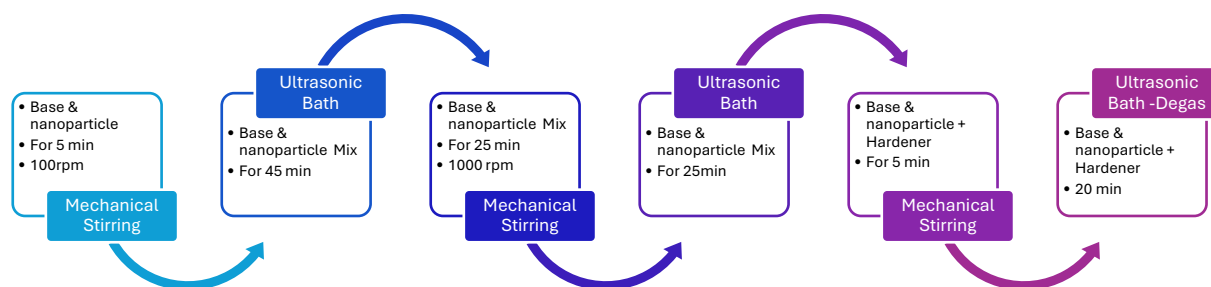


Figure 27 Steps followed in the dispersion of nanoparticles in epoxy.



a) Measuring the weight of GNP



b) Slow mixing of GNP and hardener



c) Ultrasonication of adhesive components



d) Ultrasonic bath used in this test



e) Mechanical stirrer used in this experiment

Figure 28 Dispersion method used for the experiment using mechanical mixing methods such a rotator, ultrasonication to disperse nanoparticles in epoxy.

### 3.8.5. Priming/ resin pre-coating

The samples were then primed with the same adhesive mixer prepared for the testing (Figure 29). The manufacturer's recommended primer was not used in this case to understand the efficiency of the nanohybrid epoxy on priming surfaces. In future, if a cost analysis could prove that nanohybrid epoxy are cost effective, then it would be useful to use the same.

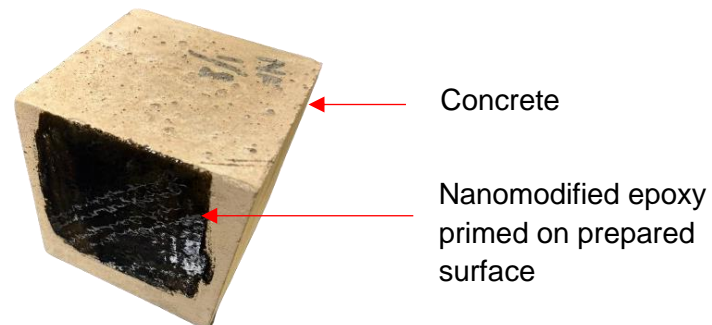


*Figure 29 Priming the prepared surface with the nanohybrid epoxy mix.*

There are numerous techniques currently in use to strengthen the bond in the CFRP concrete interface regions. These techniques include drilling grooves and installing CFRP into them, a process known as near surface mounting (NSM) or externally bonded reinforcement on grooves (EBROG), as well as screwing the ends of the CFRP plates together using a mechanical fastening technique. However, it was noted that improving concrete surface standards and regulations before bonding is essential as it contributes to microdefects repair in concrete (Yang et al., 2022).

Through penetration, resin pre-coating can fill in these gaps. However, since the adhesive resin will have a high viscosity, Han et al. (2019) found that efficiently penetrating the material's surface was made possible by adding acetone to the resin's hardener to increase its viscosity. Due to the closure of pores and microcracks on the surface, acetone is now totally evaporating. RPC improves the cohesiveness of the interfacial area, boosting the bond strength's efficacy.

### 3.9. CFRP application and test set up.

A total of 60 cubes were selected for CFRP application from different age categories.



### 3.9.1. CFRP application

CFRP strips were cut in the direction of the fibres, 50 mm broad and 500 mm long. Subsequently, they were fastened to the 50 mm wide marker positioned in the middle of the concrete surface, on either side of the cube (Figure 30).

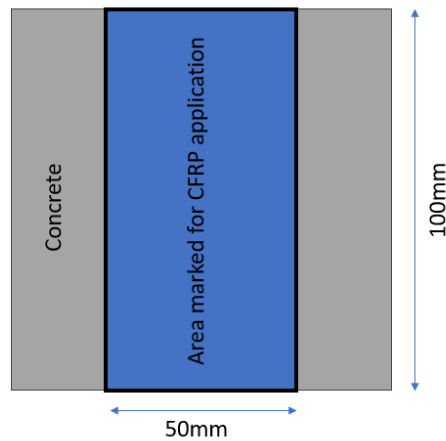


Figure 30 CFRP application surface.

Once the marked surface is primed with the relevant adhesive for WFT of 1  $\mu\text{m}$ , the strip was impregnated with the resin for up to length of 100 mm on both ends using a brush (Figure 31). The bonded length was initially assumed as the minimum length possible for an experiment of this sort and since the initial aim of this experiment is to understand the efficiency of the proposed nanohybrid epoxy.



Figure 31 Application of modified epoxy on CFRP sheet before installation on to the concrete surface.

After that, the strip is fastened to the sample cube in the form of a half loop. Each end of the strip was secured for up to 100 mm along the concrete surface, leaving enough room for the loop to be fastened along the tensile machine (Figure 32). The CFRP installed cubes were left in room temperature for 7 days prior to testing.

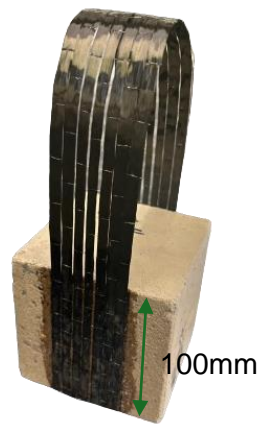


Figure 32 CFRP installed on the concrete surface.

The video strain gauge device was then used to record the strains in each strand (the 231 Sika wrap had fibres apart due to the 50 mm wide pieces cut from the 50 m roll). For the video strain gauge device to identify the virtual strain gauges white dots were used on the CFRP and black dots were used on the concrete. Each strand has two strain gauges, each marked by three white dots. Four additional strain gauges, two on each side, were fastened to the concrete surface. With one datum on the CFRP sheet, two LVDT were fastened to the bottom of the cube (Figure 33,34).

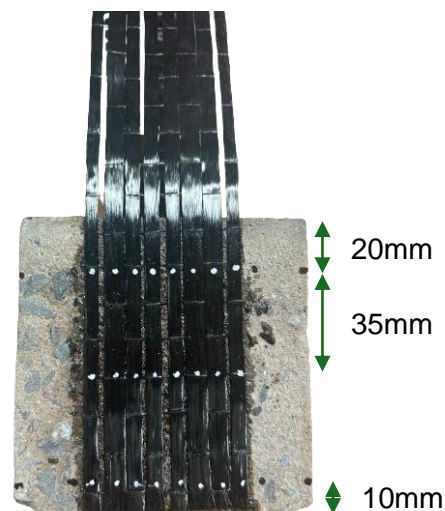


Figure 33 Arrangement for strain gauge instalment on the CFRP surface.

Although the sheets were trimmed to a 50 mm width, some strips featured eight fibre bundles while others had just seven. Nonetheless, a few strain gauges were used to identify each bundle to interpret its behaviour. Thus far, most comparable tests have been conducted using CFRP plates or sheets with a greater gsm, meaning that they

are typically packed closely together. However, it is clear from CFRP sheets that the fibres do not behave as a bundle when put through testing. Later in the test, it was noticed that, although not entirely de-bonded, the bundles emerged one after the other or in multiples. Furthermore, it was noted that the load capacity continued to increase even after a single or few bundle de-bonded. Even though the setup was designed not to give any resultant forces, it is possible to have varying loads exerted on each fibre due to the bonding quality.

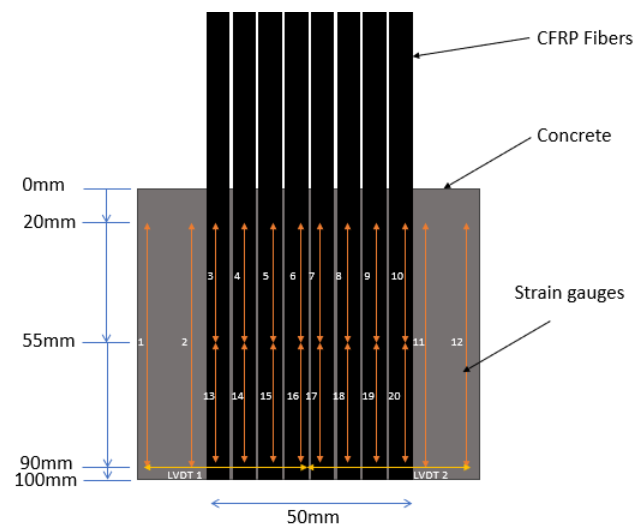
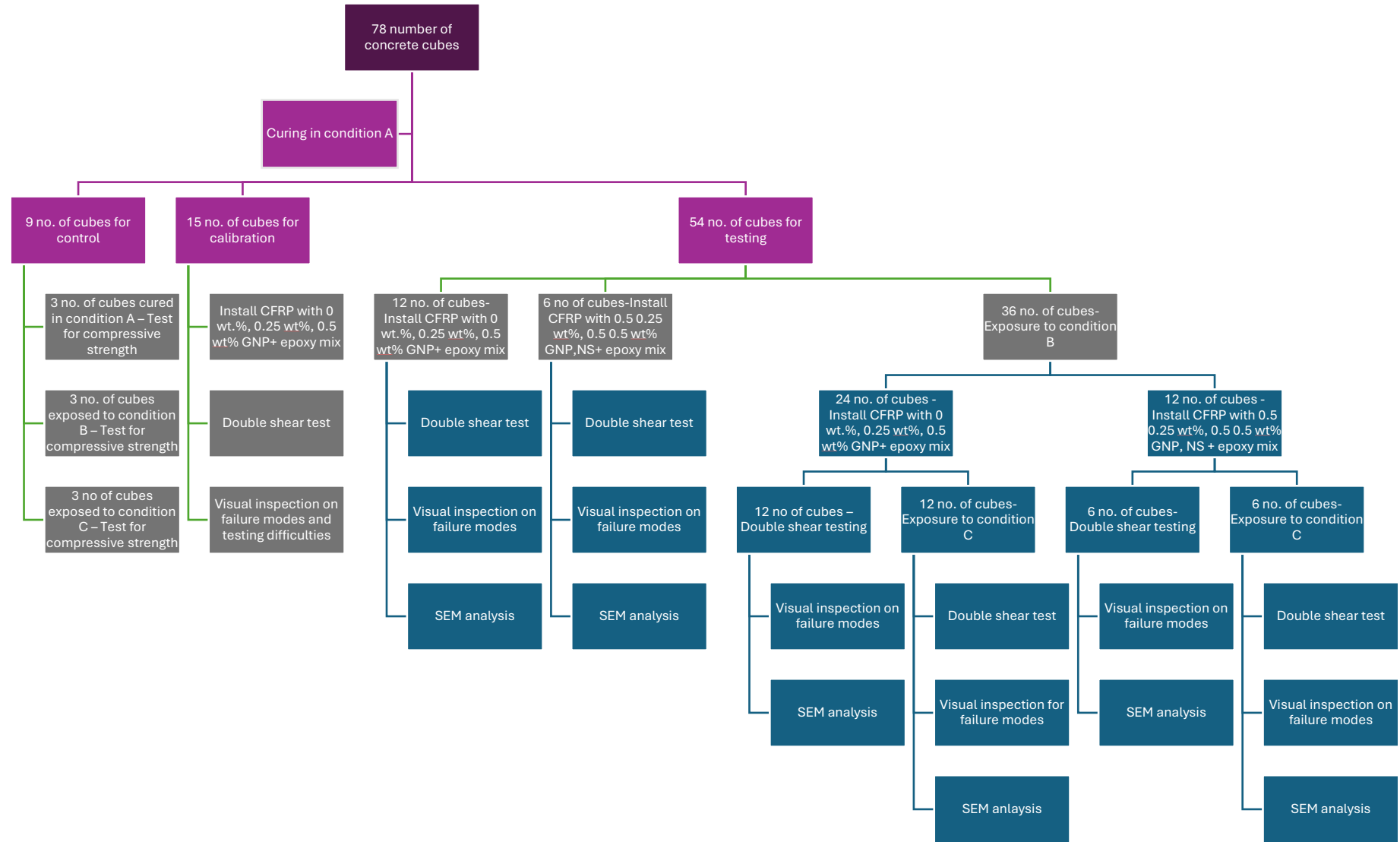


Figure 34 Illustration of strain gauge instalment on CFRP sheet.

3.10. Summary of the testing procedure



### 3.11. Testing.

The double shear test set up was used for the testing procedure which was also used in several other studies (Al-Khafaji et al., 2022; Al-Rousan and Abu-Elhija, 2020; Li et al., 2018). Also, the testing refers to ASTM D7522/D7522M-21 (*Standard Test Method for Pull-Off Strength of Coatings on Concrete Using Portable Pull-Off Adhesion Testers 1*, n.d.)

As per ACI 440 2R the recommended bond length of the CFRP on the substrate must be 150mm. a lesser bond length was used since this initial set of experiments were only to prove the efficiency of the adhesive and not to analyse the behaviour in the failure which will be considered important to improve the adhesive and to analyse the failure modes in the future.

### 3.12. Double shear test

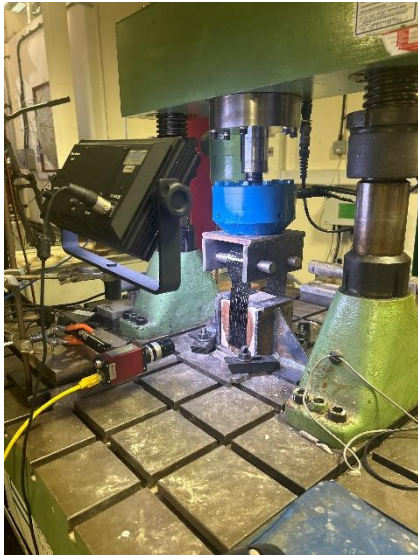
The testing was done using Servocon universal hydraulic test machine (compression and tension) and iMETRUM imaging software – (video strain gauge and 2D Strain mapping) at Cardiff University Civil and Structural Laboratory.



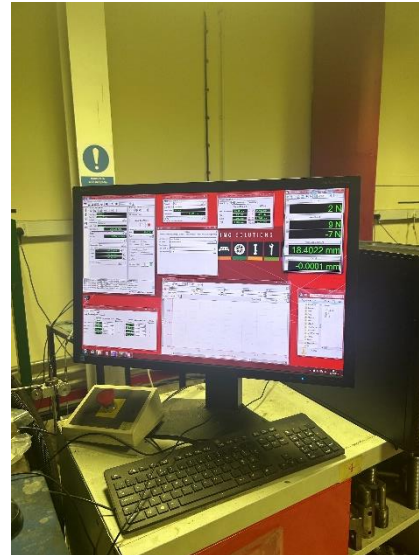
a) steel cage used to place sample and the universal hydraulic test machine



b) CFRP installed sample



c) iMETRUM Video Gauge setup



d) Example of Data acquisition system

*Figure 36 Test setup in the Cardiff University structural lab.*

iMETRUM Video Gauge™ was used to analyse the CFRP surface that was affixed to the concrete. The Video Gauge was positioned approximately 1.5 m away from the specimen, and the test area was illuminated by an integrated light. The cost can be decreased since the instrument can measure stresses and displacements throughout the CFRP's bonded region without the need for actual strain gauges that are fastened to the specimen. White dots were used to indicate the locations of the strain gauge on the surface.

A steel encasement was used to secure the specimens on the Servocon universal hydraulic test equipment, preventing them from flipping, rotating or being raised during the test. The first two cubes were tested for calibration. Through this it was decided that a static load would be applied at a speed of 2 mm/sec. This rate had also been used in previous research studies for similar type of experiments (Mohammadi Ghahsareh and Mostofinejad, 2021; Mohammadi and Mostofinejad, 2021; Salimian and Mostofinejad, 2019).

### 3.13. Scanned electron microscope analysis

A 2 mm long and a 1 mm width samples were collected from the tested sample. They were placed on a stub using a carbon disc.

#### 4. Analysis and Discussion

By neglecting any frictional forces generated between the CFRP strip and the apparatus, it was assumed that the tension force generated in the CFRP strip (beyond the anchorage) was uniform along its length. Therefore, the ultimate force recorded during the experiment was divided by two to determine the applied shear load at the failure of the CFRP strip (Figure 37). In addition to recording the load, displacement, time, and two LVDT points placed at the bottom of the strip, the iMETRUM video strain gauges recorded the strains in twenty strain gauges that were virtually fixed on one surface of the CFRP put on one face of the cube. The total number of samples examined in each category was used to calculate the average ultimate load for debonding for each type of sample. Based on the load and the fixed area of contact (100 × 50 mm) with the concrete, the shear stress was computed.

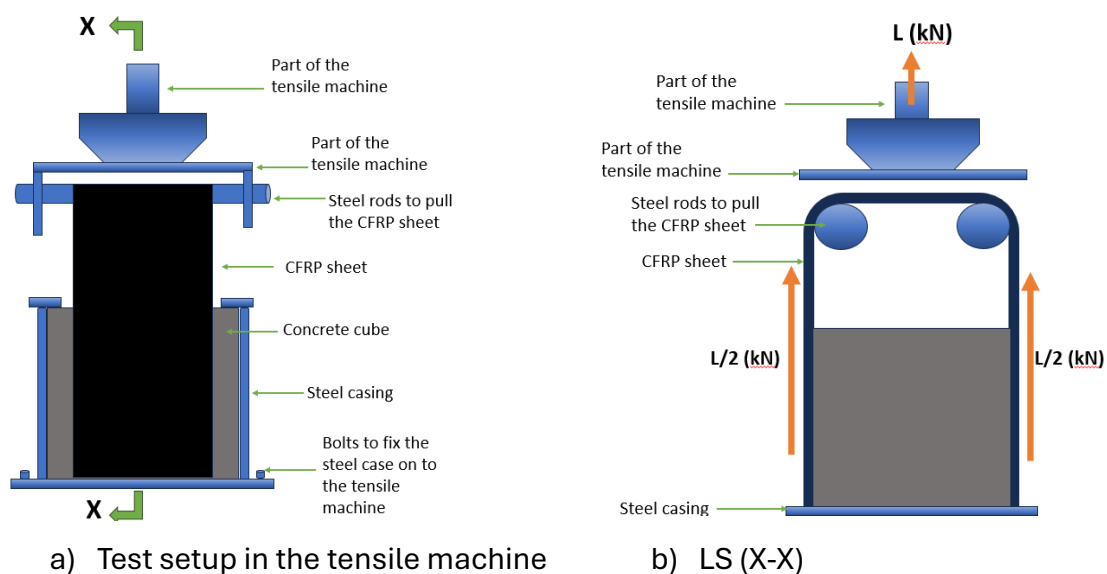


Figure 37 Test setup.


##### 4.1. Observation

Majority of the time, the side facing the camera was the one which de-bonded when the load was applied. During the initial stages of the test, mild cracking sounds were heard. This was assumed to be, the CFRP sheets—which may have shrunk as a result of the hardened epoxy during application—are being stretched and relaxed.




Furthermore, as time went on, a very distinct rupture sound was heard, which served as a warning to indicate debonding. However, the loading persisted and increased until a portion of the fibres broke. It is not always necessary for all 7 CFRP strands to reach the maximum capacity because occasionally, even when some fibres fell out, the load increased while a small number of other strands remained attached to the concrete substrate. Although the initial crack noise was recorded, it was difficult to determine if it was the result of debonding or the stretching of hardened CFRP caused by epoxy adhesive.

After every test, the mode of failure of each cube was categorised into four classes of failure, as summarised in Table 8.

*Table 8 Type of failure modes observed in the experiment.*

Reference Image	Type	Description
	Concrete Shear Failure	A failure mode where the concrete shears along the bonded interface



 A photograph showing a concrete specimen wrapped in black CFRP strips. The specimen has failed under tension, with the concrete substrate ruptured and broken into several pieces. The CFRP strips remain attached to the remaining concrete fragments.	Concrete Rupture	The concrete substrate fails when in tension, indicating that the bond between the CFRP and concrete is stronger than the concrete itself.
 A photograph showing a concrete specimen wrapped in black CFRP strips. The specimen has failed under tension, with the CFRP strips peeling away from the concrete surface. The strips are broken into several pieces, and the concrete surface is exposed.	Cohesive Debonding	Failure within the adhesive layer itself, often due to insufficient strength or improper curing.
 A photograph showing a concrete specimen wrapped in black CFRP strips. The specimen has failed under tension, with the CFRP strips peeling away from the concrete surface. The strips are broken into several pieces, and the concrete surface is exposed.	Interfacial Debonding	Failure at the bond interface between the CFRP and concrete, indicating a lack of adhesion. This occurs when more than 40% of the concrete surface detach with adhesive debonding.

## 4.2. Results

As was previously indicated in Section 5.1, it was challenging to obtain the initial debonding load of a fibre sheet, and more research is required to address this issue. This is due to snapping without pre warning and being unable to track the exact loading at which samples failed.

It is necessary to indicate the debonding load to determine the actual or maximum load needed to cause the initial failure. This might be regarded as the minimum load necessary for the initial debonding and designed accordingly, even if it might be less than the greatest load the composite could sustain under those specific environmental conditions.

*Table 9 Summary of experimental results*

<b>Sample</b>	<b>Average ultimate load kN</b>	<b>Standard deviation kN</b>	<b>GNP %</b>	<b>NS%</b>	<b>Ageing Condition</b>	<b>Failure Mode</b>
0F	7.33	1.39	0	0	A	Concrete Shear failure
0.25F	8.50	0.42	0.25	0	A	Concrete Rupture
0.5F	8.50	0.08	0.5	0	A	Concrete Shear Failure
0AF	3.46	0.99	0	0	B	Cohesive Debonding
0.25AF	6.38	0.63	0.25	0	B	Interfacial Debonding
0.5AF	7.49	0.30	0.5	0	B	Cohesive Debonding
0AFA	1.98	0.48	0	0	C	Interfacial debonding
0.25AFA	5.57	0.53	0.25	0	C	Cohesive Debonding
0.5AFA	3.62	0.4	0.5	0	C	Cohesive Debonding
0.50.25F	8.89	0.57	0.5	0.25	A	Concrete Rupture
0.50.5F	8.23	1.62	0.5	0.5	A	Concrete Shear Failure
0.50.25AF	7.32	0.51	0.5	0.25	B	Cohesive Debonding
0.50.5AF	6.23	0.05	0.5	0.5	B	Cohesive Debonding
0.50.25AFA	4.24	0.36	0.5	0.25	C	Cohesive Debonding
0.50.5AFA	5.40	0.45	0.5	0.5	C	Cohesive Debonding

Table 9 represents the results obtained from adding GNP and NS in the epoxy mix to strengthen concrete cubes with CFRP. To calculate the average, four samples from condition with GNP only mix and three samples from GNP and NS mix were analysed.

#### 4.2.1. Results with addition of GNP alone in the epoxy mix

In the first batch of tests, CFRP was mounted on cubes that had been cured under standard curing conditions using a standard epoxy mix and epoxy mix consisting of 0.25 wt.% and 0.5 wt.% GNP. The cubes with GNP performed 16% better than the cubes with regular epoxy among these cubes (Figure 38). It was also observed that concrete rupture was the mode of failure for 0.25 wt.% of the GNP in epoxy.

The next twelve sets of cubes were used to study the behaviour of composites when CFRP was meant to be put in aged cubes (ageing condition B). Each set of four sets was tested again using pure epoxy, epoxy with 0.25 wt.% of GNP, and epoxy with 0.5 wt.% of GNP. It was observed that the failure mechanism changed from concrete shear failure and concrete rupture, which focused on the quality of the concrete substrate to cohesive and interfacial debonding, which in turn concentrated on the quality of adhesive. This is because water was absorbed into the epoxy, plasticizing it. Additionally, it was noted that the neat epoxy's strength decreased by 53% because of an expedited ageing process. However, 0.25 wt.% GNP in epoxy showed a loss in loading capacity of 25%, but 0.5 wt.% GNP mixed epoxy showed a drop of just 12%. The condition that may have resulted from neat epoxy under condition A circumstances was saved by 117% because to the inclusion of 0.5 wt.% GNP in the epoxy.

In ageing Condition C, where the previously aged samples were aged again after the installation of CFRP, testing showed interesting results with neat epoxy showing interfacial debonding and epoxy with GNP mixed showing cohesive debonding. But in this type of ageing the 0.25 wt.% GNP mixed epoxy exhibited the highest debonding load which was only 13% lower than of Condition B ageing with the same GNP + epoxy mix. Yet the 0.5 wt.% GNP mixed epoxy showed a significant decline of 53% when the adhesive was further aged. Although the reduction in loading capacity was considerable with GNP mixed epoxy in Condition C ageing, as expected the neat epoxy showed a further 43% decline in loading capacity when compared to ageing B.

The crucial point to note here is that Condition C ageing could be the most likely state of exposure for a composite, if exposed to aggressive environment. In case of strengthening bridges and wastewater tanks built in aggressive environmental conditions, it is obvious that the concrete structure will be pre and post exposed to aggressive environments. In such cases the modified epoxy should be able to bear the moisture and other ion attacks efficiently. Moisture being the main cause of failure, there comes a necessity to further strengthen the interpolymer crosslinks with modifications in the nanomodified epoxy. Therefore, the epoxy mix was mixed with NS. The NS was expected to disperse GNP preventing agglomeration creating more crosslinks.

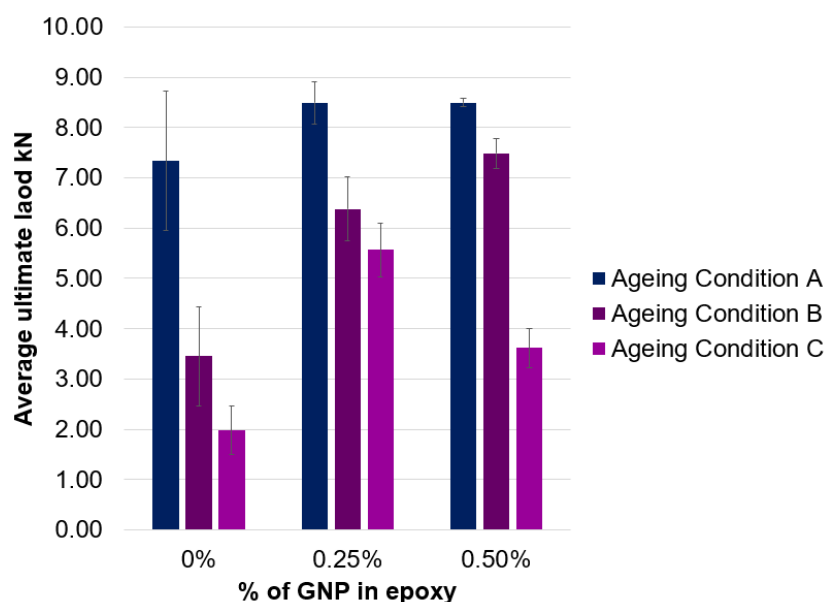


Figure 38 Performance of GNP mixed epoxy in different exposure conditions.

#### 4.2.2. Results with the addition of GNP and NS in the epoxy mix

It was not feasible to wait for the Condition C experiment findings to be gathered to comprehend the behaviour of GNP during the further ageing process due to time constraints. Thus, 0.5 wt.% GNP in epoxy mix was thought to perform better since it demonstrated 17% better outcomes than 0.25 wt.% GNP mixed epoxy, based on the Condition B ageing data from the first set of studies (Figure 38).

Considering the above, tests were performed on samples containing 0.5 wt.% GNP combined with 0.25 wt.% and 0.5 wt.% NS. Under typical ageing settings, both NS

percentages demonstrated the same capacity. Furthermore, the outcomes were mostly consistent with those obtained with epoxies and GNP alone. As anticipated, the load capacity of the aged concrete (ageing condition B) decreased by 18% when the nanohybrid mix was applied, compared to the original loading capability prior to ageing condition A. However, the nanohybrid epoxy content in ageing condition B was kept below the 0.5 wt.% GNP blended epoxy's load capability (Table 10 and further explained in Section 5.5). The load capacity attained by the 0.5 wt.% GNP mixed epoxy was nearly identical to that of the 0.5 wt.% GNP and 0.25 wt.% NS mixed epoxy. Moreover, the epoxy with 0.5 wt.% GNP and 0.5 wt.% NS added was 17% less bearing than the epoxy with 0.5 wt.% GNP alone.

When the nanohybrid epoxy was further aged for 28 days under aggressive environment, a 42% load capacity drop was noted in epoxy mixed with 0.5 wt.% GNP and 0.25 wt.% NS with relative to Condition B of the same mix and only a 13% reduction was observed in epoxy with 0.5 wt.% GNP and 0.5 wt.% NS. Yet when compared to the neat epoxy mix which went through aggressive environmental Condition C, 0.5 wt.% GNP and 0.25 wt.% NS mixed epoxy showed a performance of 114% and 0.5 wt.% GNP and 0.5 wt.% NS mixed epoxy showed a performance of 173% better than that of the neat epoxy.

Table 10 Overview of performance comparison of samples based on ultimate loading.

Reduction in performance	Increase in performance	
<b>0F to 0AF</b>	<b>0F to 0.25F</b>	<b>0F to 0.50.25F</b>
53%	16%	21%
<b>0F to 0AFA</b>	<b>0F to 0.5F</b>	<b>0F to 0.50.5F</b>
73%	16%	12%
<b>0.25F to 0.25AF</b>	<b>0AF to 0.25AF</b>	<b>0AF to 0.50.25AF</b>
25%	85%	112%
<b>0.25F to 0.25AFA</b>	<b>0AF to 0.5AF</b>	<b>0AF to 0.50.5AF</b>
34%	117%	80%
<b>0.5F to 0.5AF</b>	<b>0AFA to 0.25AFA</b>	<b>0AFA to 0.50.25AFA</b>
12%	181%	114%
<b>0.5F to 0.5AFA</b>	<b>0AFA to 0.5AFA</b>	<b>0AFA to 0.50.5AFA</b>
57%	83%	173%

From Table 10 and Figure 39 the following could be concluded :

- In condition A, the nanohybrid epoxy with 0.5 wt.% GNP and 0.25 wt.% NS has performed well.
- In condition B, the 0.5 wt.% GNP mixed epoxy and the nanohybrid epoxy where 0.5 wt.% GNP and 0.25 wt.% NS has performed almost similarly.
- In condition C, the 0.25 wt.% GNP mixed epoxy and the nanohybrid epoxy with 0.5 wt.% GNP and 0.5 wt.% NS has performed almost similarly.

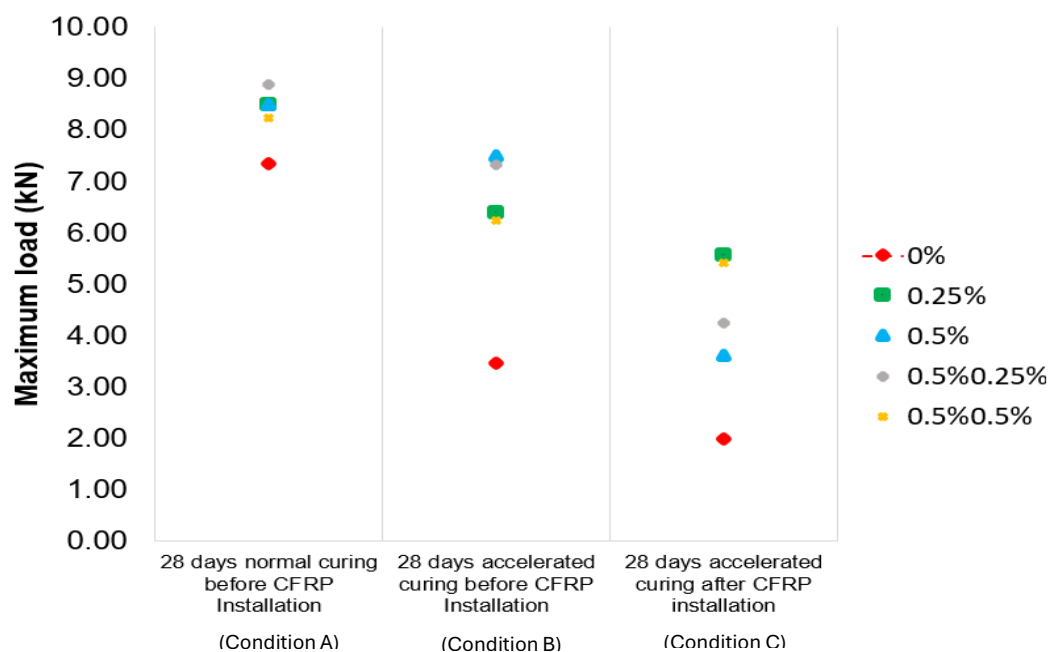


Figure 39 Maximum load reached by each sample in different ageing conditions.

However, it must be acknowledged that every design is carried out assuming the worst-case scenario. If we were to select one mix that worked well under all three ageing conditions, it would be the nanohybrid epoxy mix containing 0.5 wt.% GNP and 0.25 wt.% NS, as presented in Table 10.

Additionally, it was noted that when the resin was exposed to moisture, cohesive debonding accounted for most of the failure mechanism. This was very likely caused by the water molecules weakening the intermolecular crosslinks and penetrating the adhesive. SEM photos were used for the following samples to delve deeper into the subject.

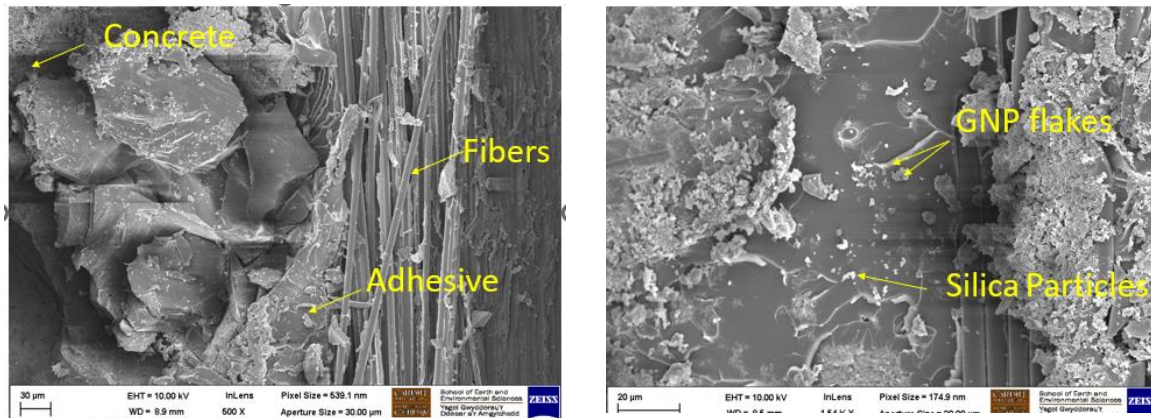
Nevertheless, the material's price remains a significant factor. When using neat epoxy, in condition A most cases demonstrate sufficient load capacity to meet current design requirements. However, neat epoxy fails to reach the desired loading in aggressive environmental conditions (B and C). However, test results indicate that adding 0.25 wt.% GNP will increase performance by 16%. Furthermore, the study also shows that 0.25 wt.% GNP mixed with epoxy achieved around 181% performance increment when compared to a neat epoxy that went through condition C, making it more cost-effective to use just GNP in a mix rather than GNP and NS.

One of the challenges encountered in the use of NS is material handling. When the dust-like particles were put into beakers for measurement, they became difficult to control and began to disperse into the air. Additionally, because part of the NS was lodged in the beaker, it was challenging to determine the quantity (maybe because of the insignificant amounts).

#### 4.3. SEM images

6 samples were selected for the SEM examination. The samples in all three environmental conditions (A, B, and C) with 0.5 wt.% GNP mixed epoxy, 0.5 wt.% GNP, and 0.25 wt.% NS were selected. 4 cubes were evaluated for every batch of samples. For the SEM analysis, the sample whose load was closest to the average of all four cubes was chosen.

Understanding the presence of GNP flakes and NS particles in the samples is the goal of the first series of SEM pictures from condition A. The interface between the concrete and adhesive, as well as the GNP flakes and NS particles, is seen in Figure. 40a. Additionally, Figure 40b displays the crack formation and GNP flakes peel off. NS particles are primarily utilised to help with greater particle dispersion by spreading the GNP throughout the adhesive.

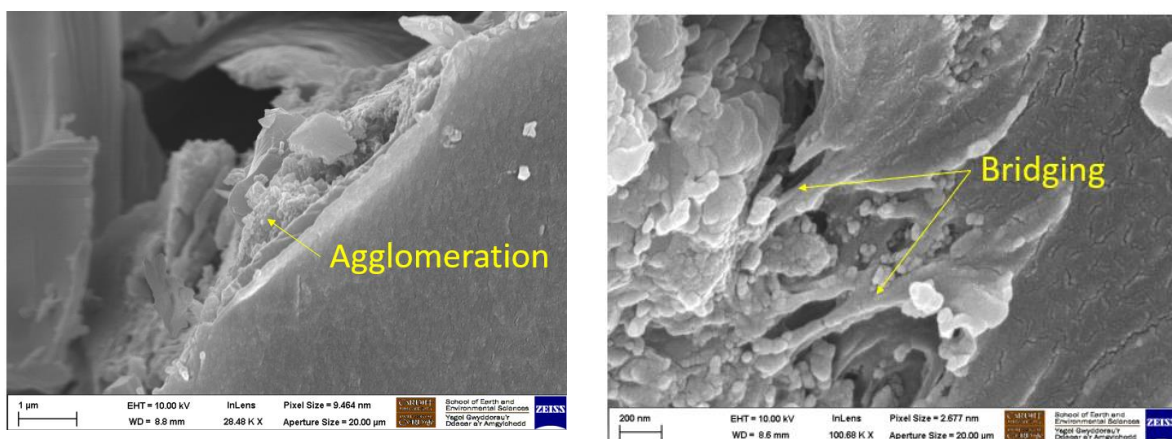


a) Interface 0.5F4

b) Interface 0.50.25F1

Figure 40 SEM image of nanohybrid epoxy /CFRP and concrete interface.

The testing sample used in Figure 41a was installed with GNP only mixed epoxy. Agglomeration of particles is clearly visible in this sample. Whereas the sample with the addition of NS has created more bridging in the polymer, and this is clearly visible in Figure 41b.



a) Interface 0.5F4

b) Interface 0.50.25F1

Figure 41(a) the agglomeration of GNP particles is denoted and (b) shows the bridging of cracks with the help of interpolymer links.

The samples which went through Condition B were examined under the scanned electron microscope (SEM). It was observed from Figure 42a that the moisture in the concrete has been entrapped in the adhesive during the curing process of the adhesive. In Figure 42b the circular hole in the interface is assumed to be an air trapped during the installation process.



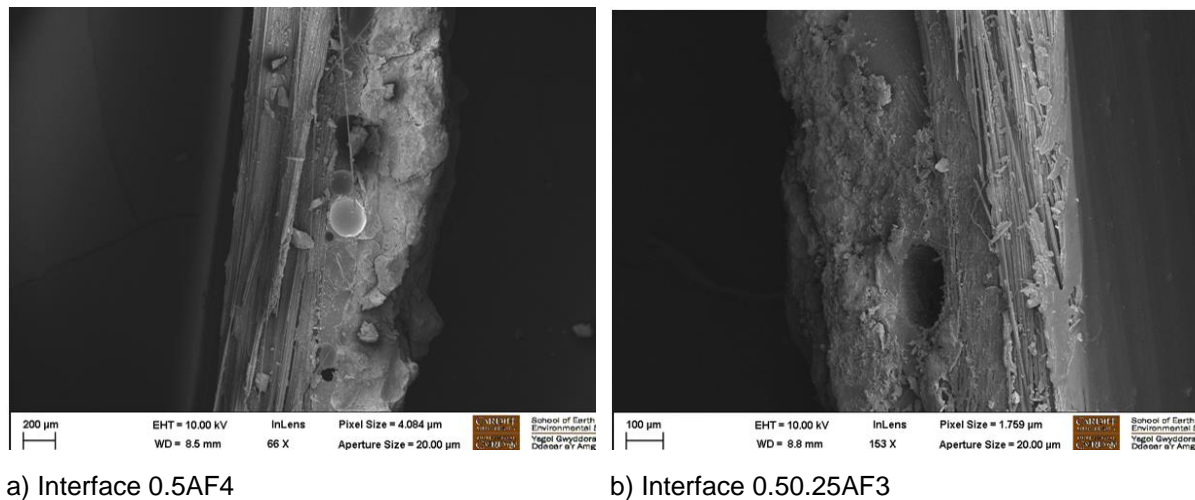


Figure 42 SEM image the composite in micro scale. (a) shows a trapped water bubble (b) shows trapped air pocket

Figure 43a shows an insight into the delamination of adhesive from the concrete. Even though 0.5AF samples exhibited a cohesive debonding, there were areas of complete adhesive pull out from the concrete surface. From Figure 43a the GNP flakes being isolated from the crack path due to shear failure can be seen clearly. Also, the crack generation and pinning can be observed from Figure 43a and 43b.

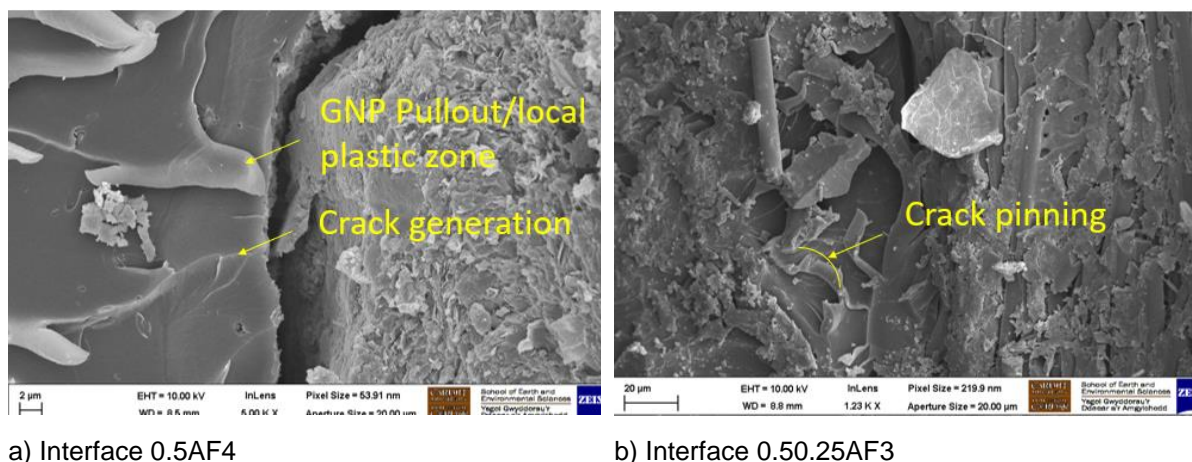


Figure 43 SEM image of nanohybrid epoxy and concrete interface.

It was observed that entrapped water bubbles were found in samples from GNP only epoxy mixes in condition B and condition C. Figure 44a depicts a water bubble entrapped in its adhesive region where as Figure 44b does not show any signs of entrapped water bubble.

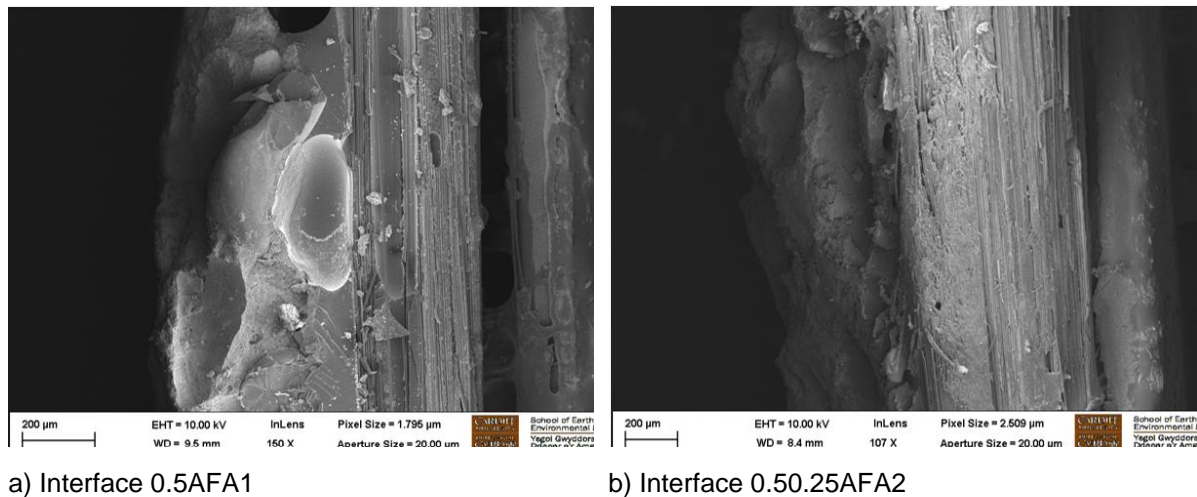


Figure 44 SEM image of the composite in micro scale.

Furthermore, figure 45a depicts the dimple formation and bifurcation by which means cracks are redirected. Agglomeration of particles were observed in Figure 45b, and it is assumed to be NS.

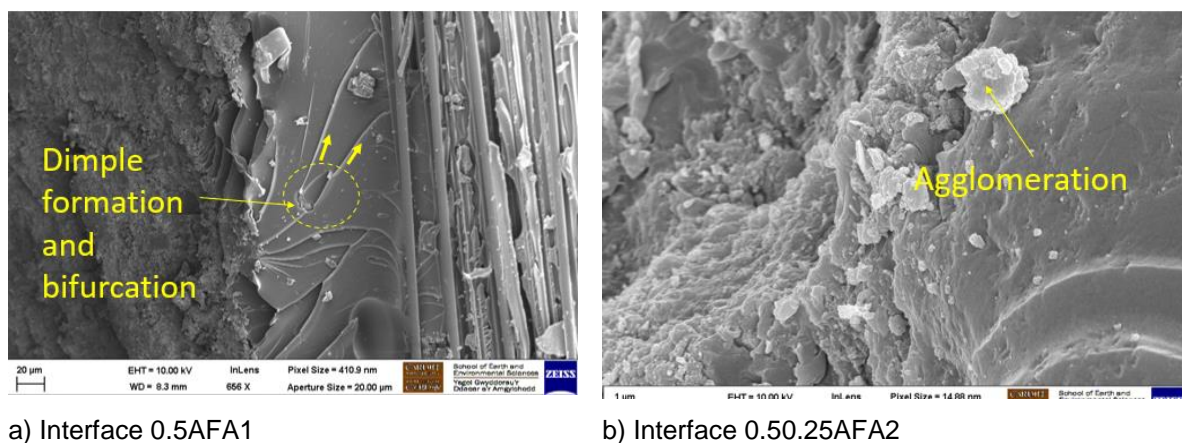


Figure 45 SEM image of dimple formation and agglomeration in nanohybrid epoxy under ageing condition C.

#### 4.4. Strain gauge analysis.

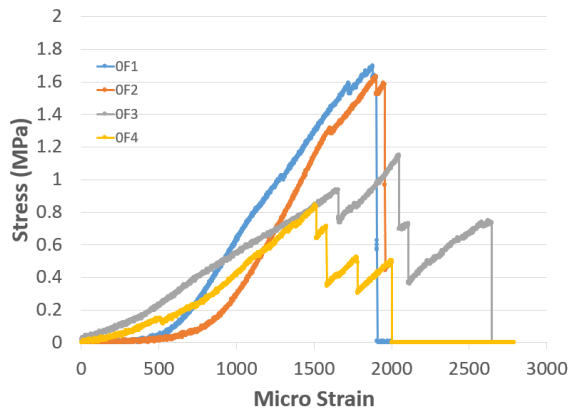
For the strain gauge results, the value of strains on the middle FRP strand out of the 7 strands was recorded for analysis. The stress throughout the loading was calculated using the load exerted per area of contact (i.e. the area of contact of FRP with concrete using the adhesive). The plotted results of stress vs strain for three different exposure conditions with different nanohybrid adhesives, was used to visually analyse the young modulus of the composite.

When composites are utilised in the construction sector, it is best for them to have somewhat higher Young's moduli because of the stiffness required under stress. The key is to maintain the stiffness of the composite (CFRP and Nanohybrid epoxy) before failure.

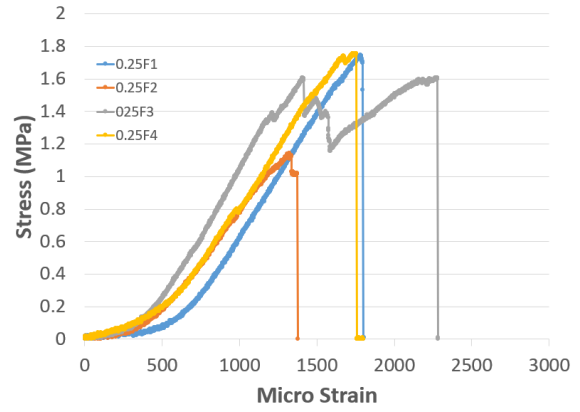
The overall gradient of the 0.5 wt.% GNP epoxy was found to be larger than that of the neat epoxy and the blended epoxy with 0.25 wt.% GNP (Figure 46). This is because the presence of GNP strengthens the polymer crosslinks in the adhesive decreasing the composite's elastic region. However, it further states that, in comparison, the 0.5 wt.% GNP blended epoxy has produced larger loadings. According to the results shown in condition A for solely GNP mixed epoxies (Figure 46), at least one of the samples eventually tended to reach the same debonding load regardless of the GNP level.

However, as can be shown in Figure 47, where the samples with GNP solely mix were tested in condition B, the samples with 0.5 wt.% GNP mixed epoxy (Figure 47c) were able to withstand a higher load than the other two samples (Figure 47a and 47b). Because the adhesive is passing through a plastic zone as a result of absorbing moisture, the graphs' slopes have remained quite consistent in this scenario. However, the GNP mixed epoxy exhibits a higher modulus than the pure epoxy.

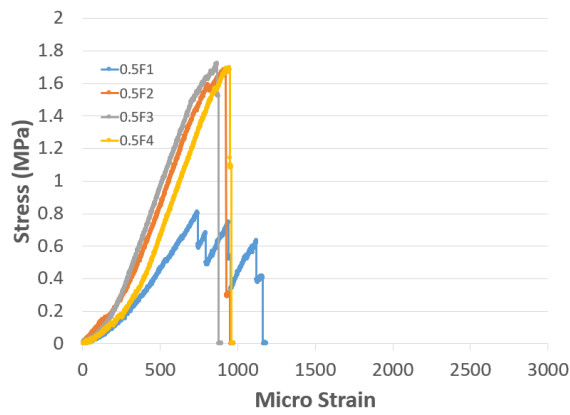
Figure 48 clearly shows how the adhesive undergoes a higher deformation for even a smaller increase in load since the adhesive has been further plasticized due to the aggressive environmental ageing process. Yet it is also important to notice that epoxy with 0.25 wt.% GNP has achieved an overall higher loading (Figure 48b) than the other two epoxies (Figure 48 a and c) proving that 0.25 wt.% GNP content in epoxy could take load under aggressive environmental conditions.



a)

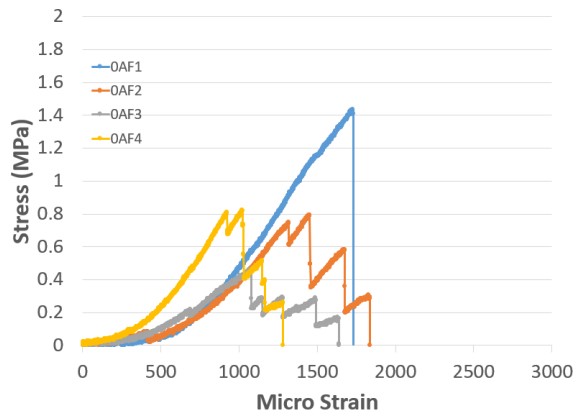


b)

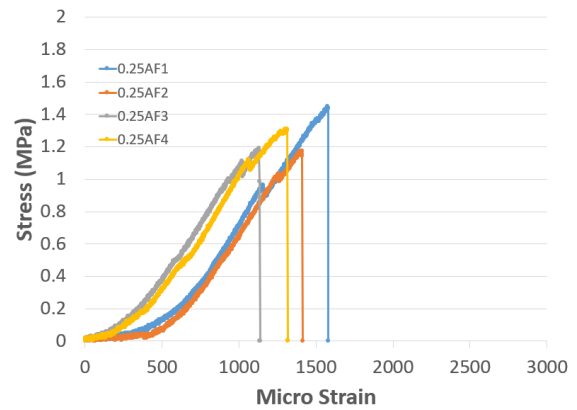


c)

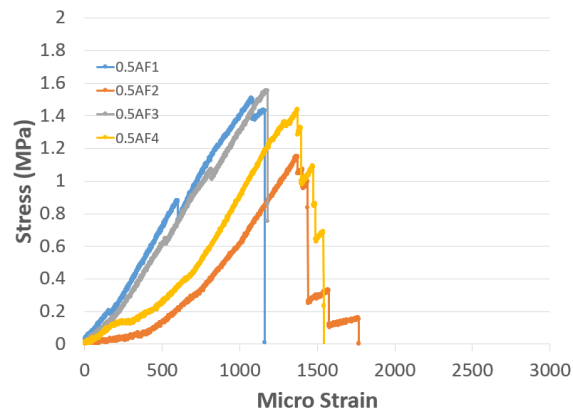
Figure 46 Stress vs strain graph of samples with neat epoxy and GNP mixed epoxy in Condition A



a)

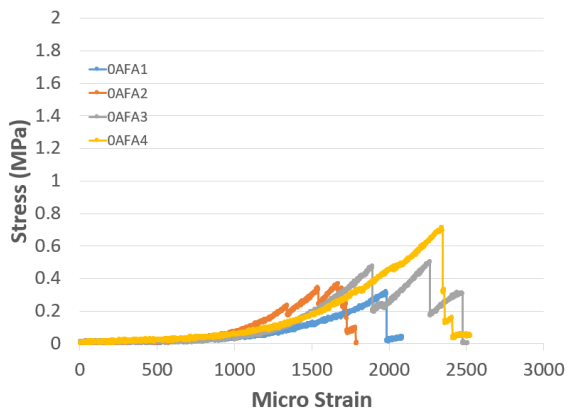


b)

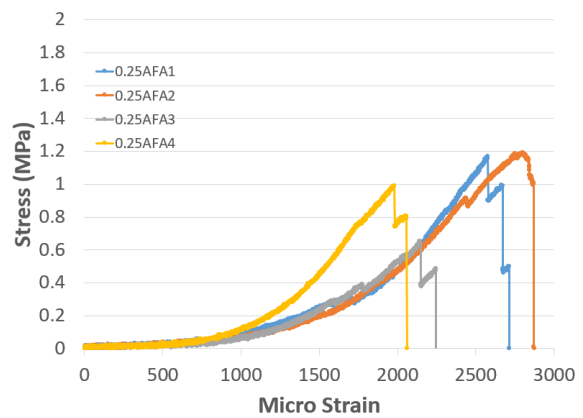


c)

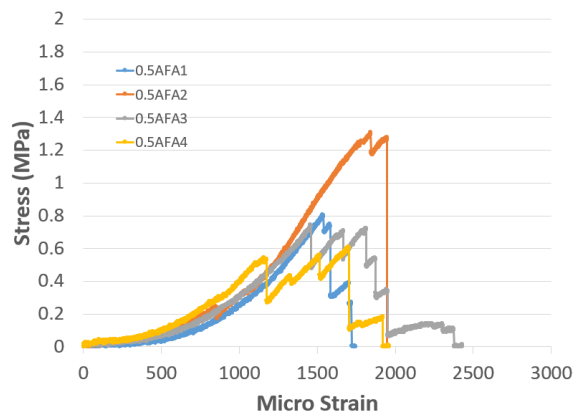
Figure 47 Stress vs strain graph of samples with neat epoxy and GNP mixed epoxy in Condition B



a)



b)



c)

Figure 48 Stress vs strain graph of samples with neat epoxy and GNP mixed epoxy in Condition C

The presence of NS in the GNP infused epoxy mix has improved the stiffness of the nanohybrid mix as per Figure 49. As per the Figure 49a and 49c, as the percentage of NS increased more dispersion has occurred and more crosslinks have been formed

between the epoxy and GNP creating more chances of bonding with the concrete. It also must be noted that this is still less than the stiffness achieved by 0.5 wt.% GNP only epoxy mix (Figure 49d).

The nanohybrid adhesive which went through the condition B showed minimal difference in stiffness when compared to condition A. The adhesive mix with 0.5 wt.% of NS (Figure 50c) showed a young's modulus greater than that of 0.25 wt.% NS in condition B (Figure 50b). This proves that the effect of moisture in these adhesive mixtures have been less when compared to the other situations.

When the nanohybrid resin was aggressively aged as per condition C, the behaviour of the adhesive had a significant shift from higher stiffness to much greater elastic region. The nanohybrid mix with 0.25 wt.% NS (Figure 51c) behaved much better with comparatively higher load and acceptable young modulus.

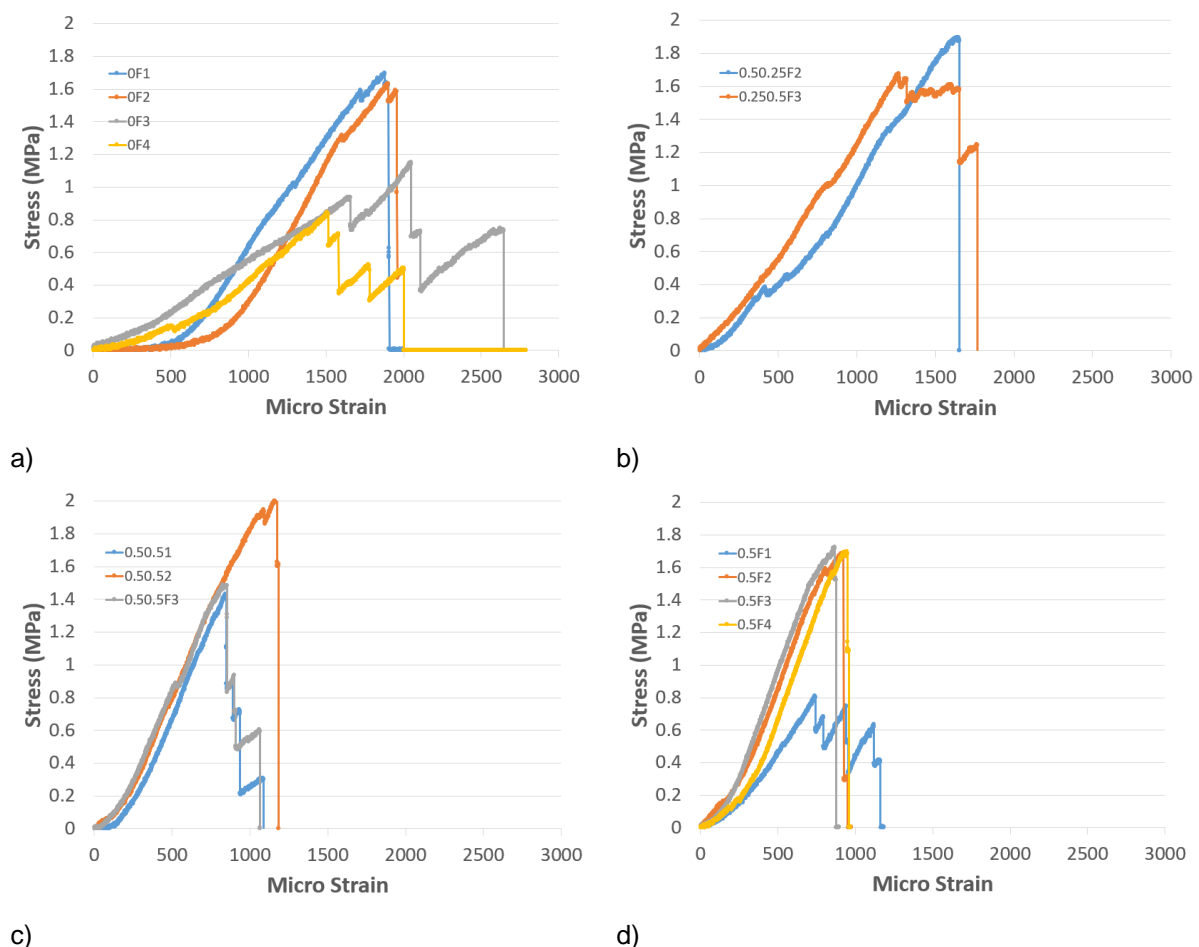
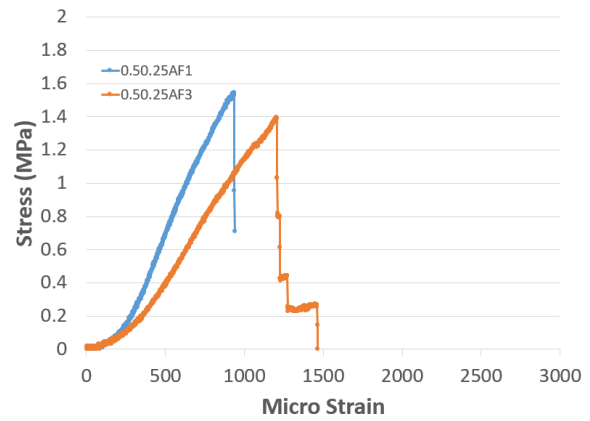
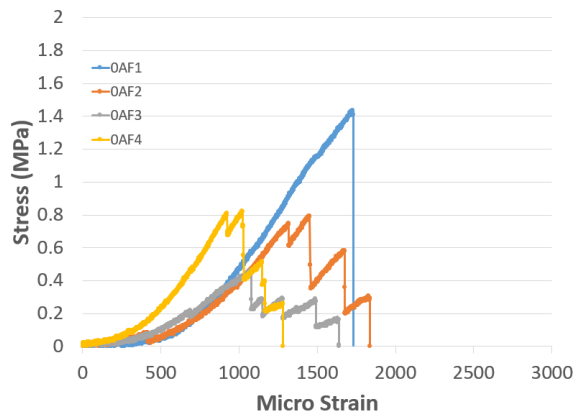
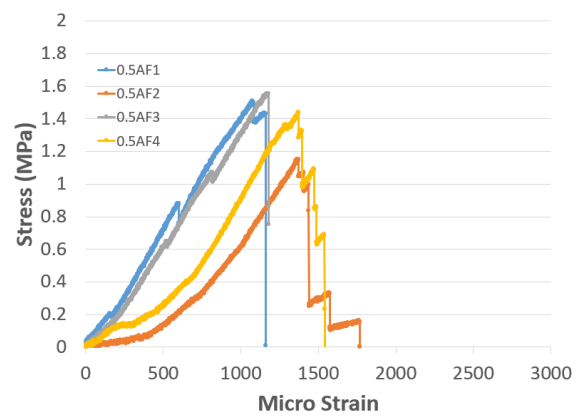
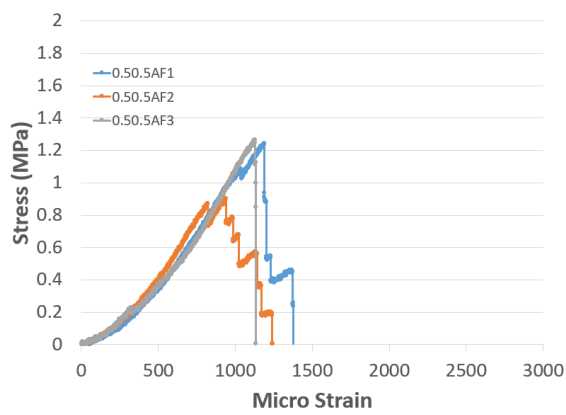


Figure 49 (a) Stress vs strain graph of samples with neat epoxy in condition A (b, c) Stress vs strain of samples with GNP and NS mixed epoxy in Condition A (d) Stress Vs Strain graph of 0.5 wt.% GNP mixed epoxy in Condition A



a)

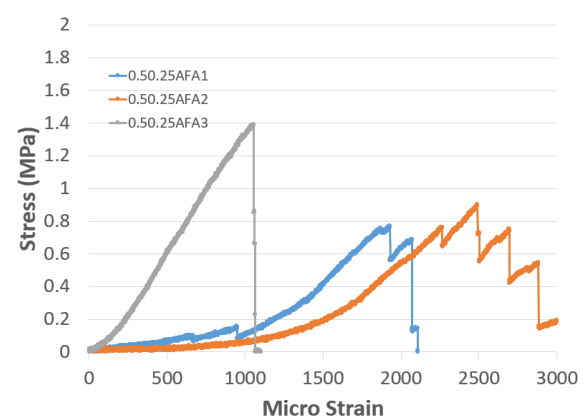
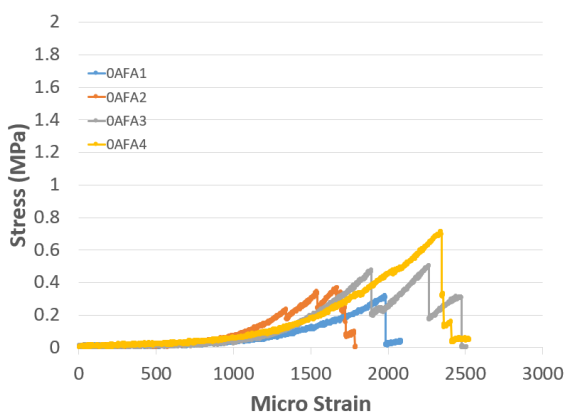
b)



c)

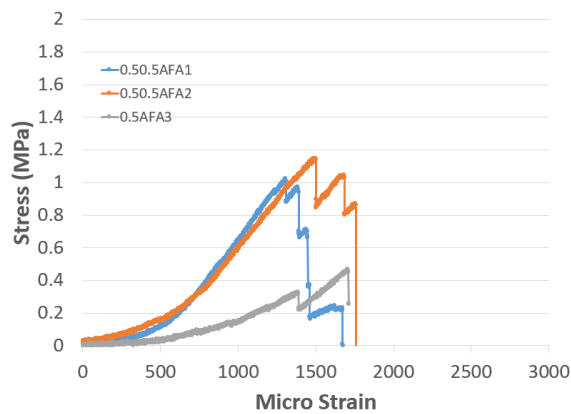
d)

Figure 50 (a) Stress vs strain graph of samples with neat epoxy in condition B (b, c) Stress vs strain graph of samples with GNP and NS mixed epoxy in Condition B (d) Stress vs Strain graph of samples with 0.5 wt.% GNP mixed epoxy in Condition B

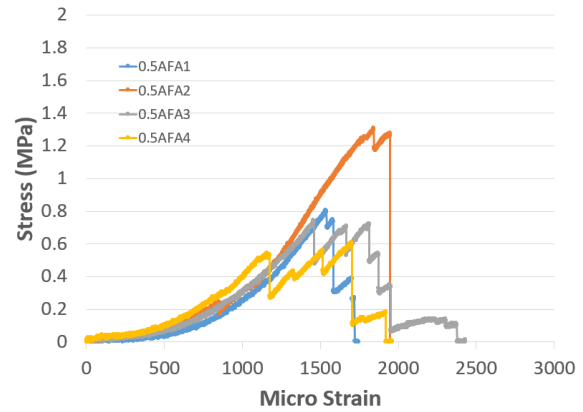


a)

b)



c)



d)

Figure 51(a) Stress vs strain graph of samples with neat epoxy in condition C (b, c) Stress vs strain graph of samples with GNP and NS mixed epoxy in Condition C (d) Stress vs Strain graph of samples with 0.5 wt.% GNP mixed epoxy in Condition C

#### 4.5. Summary of results

Based on the questions which were previously raised during the start of this study, the following objectives were met,

- The major reason for failure in CFRP strengthened concrete with neat epoxy in aggressive environment is due to moisture and elevated temperature and the failure mode is de-bonding most of the times.
- Even though there are so many methods attempted to improve the bond quality between CFRP and concrete substrate, modification with nano particles were seldom researched. GNP and NS have been proved to be two most suitable nanoparticles which has been used to provide very good results when experimented in other engineering industries.
- A novel approach used with 0.25 wt.%, 0.5 wt.% GNP and 0.25 wt.%, 0.5 wt.% NS to understand the effect of nanohybrid epoxy in concrete substrate exposed to aggressive environmental conditions has given promising results for future studies.



#### 4.6. Conclusion

According to the experimental data acquired from this series of tests, it has been discovered that:

- There was a significant drop in concrete compressive strength by 14.7% depicting the damage caused to the concrete substrate by moisture, salt, and high temperatures.
- Epoxy adhesive loses strength with aggressive ageing. A rapid drop of 73% in shear stress was observed when the CFRP retrofitted concrete cubes which went through aggressive environmental aging condition C were tested under double shear. The main failure mode observed was interfacial debonding, which was caused due to extensive moisture ingress into the epoxy polymer, weakening the crosslinks.
- Nanoparticles can be added to epoxy adhesives to increase their load bearing capacities. To fully profit from nanoparticles, the kind of dispersion technique employed is essential. Further to this, NS is also used in this experiment to avoid agglomeration and disperse GNP efficiently.
- According to this investigation, 0.25 wt.% GNP blended epoxy has significantly outperformed, with an overall improvement under harsh environmental conditions of 181%. Since the young's modulus is crucial for structural parts utilised in the building industry, it is important to take into account the 0.25 wt.% weight mixed epoxy's performance once again, since it still produces a better stiffness for the composite. With the introduction of nanoparticles the failure mode shifted from interfacial bonding to cohesive debonding in condition C when compared with neat epoxy in the same condition.
- The ultimate shear stress and stiffness of the composite incorporated with nanohybrid resins GNP and NS showed significant increase when compared to neat epoxy. 0.5 wt.% GNP and 0.5 wt.% NS mixed epoxy performed well in all three environmental conditions ( Condition A,B and C) with a considerable good stiffness even in condition C.
- Utilising GNP alone in the epoxy mix improves the adhesive's overall performance in terms of toxicological and cost.

#### 4.7. Future work

Many studies are being done on this specific topic, but in relation to what has been discussed here, the following areas should be of future research interest:

- Bond slip analysis of the experiment carried out- this is to analyse the effect of nano particles in the modified adhesive, the shear angle, and the shear modulus of the modified adhesive.
- The effectiveness of 0.25 wt.% GNP and 0.25 wt.%, 0.5 wt.% NS mix in harsh environmental conditions.
- The potential for the enhanced nano/nanohybrid adhesive mix to shorten the bond length needed to terminate CFRP on concrete. That is by testing the efficiency with 75 mm to 200 mm bond length keeping the type of concrete and surface preparation constant.
- Impact of concrete type and substrate surface area preparation on the effectiveness of nanohybrid adhesives in harsh settings. That is by changing the aggregate size used in the concrete, grades of concrete, etc.
- The ability of the modified adhesive to be transported in different transporting modes such as air lifting and sea voyage.
- How longer shelf life of nanomodified adhesive would affect the performance in aggressive environmental condition (rate of sedimentation of nanoparticles with time)
- This study is done only for a period of 56 ageing cycles. More data need to be collected for longer periods.
- How the nanomodified epoxy would react to other aggressive environments such as acidity, UV, fire etc.
- The effects of cyclic loading on the nano modified adhesive
- Cost analysis to find out the cheapest and effective nanomodified adhesive for aggressive environments.
- How does different dispersion methods and time duration of mixing affect the performance of the nanomodified adhesive and to find the most practical and cost-effective method that can be used in the industry.
- Finding alternative nano particles for the nano hybrid mixture.

## 5. Reference

1. Abbood, I. S., Odaa, S. A., Hasan, K. F., & Jasim, M. A. (2021). Properties evaluation of fiber reinforced polymers and their constituent materials used in structures - A review. *Materials Today: Proceedings*, 43. <https://doi.org/10.1016/j.matpr.2020.07.636>
2. Al-Khafaji, A., El-Zohairy, A., Mustafic, M., & Salim, H. (2022). Environmental Impact on the Behavior of CFRP Sheet Attached to Concrete. *Buildings*, 12(7). <https://doi.org/10.3390/buildings12070873>
3. Alkhrdaji, T. (2015). Strengthening of Concrete Structures Using FRP Composites. *STRUCTURE Magazine*.
4. Alnuaimi, N., Sohail, M., Hawileh, R., Abdalla, J., & Douier, K. (2021). Durability of Reinforced Concrete Beams Externally Strengthened with CFRP Laminates under Harsh Climatic Conditions. *Journal of Composites for Construction*, 25, 04021005 (1-17). [https://doi.org/10.1061/\(ASCE\)CC.1943-5614.0001113](https://doi.org/10.1061/(ASCE)CC.1943-5614.0001113)
5. Al-Rousan, R. Z., & Abu-Elhija, A. M. (2020). Predicting the bond-slip relationship between concrete and CFRP using anchoring holes technique. *Case Studies in Construction Materials*, 13. <https://doi.org/10.1016/j.cscm.2020.e00462>
6. Alwash, D., Kalfat, R., Du, H., & Al-Mahaidi, R. (2021). Development of a new nano modified cement-based adhesive for FRP strengthened RC members. *Construction and Building Materials*, 277. <https://doi.org/10.1016/j.conbuildmat.2021.122318>
7. Al-Zu'bi, M., Fan, M., & Anguilano, L. (2024). Near-surface mounted-FRP flexural retrofitting of concrete members using nanomaterial-modified epoxy adhesives. *Journal of Building Engineering*, 84. <https://doi.org/10.1016/j.jobe.2024.108549>
8. American Concrete Institute., & ACI Committee 440. (2017). *Guide for the design and construction of externally bonded FRP systems for strengthening concrete structures*. American Concrete Institute.
9. Benmokrane, B., Ali, A. H., Mohamed, H. M., ElSafty, A., & Manalo, A. (2017). Laboratory assessment and durability performance of vinyl-ester, polyester, and epoxy glass-FRP bars for concrete structures. *Composites Part B: Engineering*, 114. <https://doi.org/10.1016/j.compositesb.2017.02.002>
10. Blackman, B. R. K., & Teo, W. S. (2009). *The adhesive bonding of polymeric matrix composites*. <https://www.researchgate.net/publication/265922053>
11. Böer, P., Holliday, L., & Kang, T. (2013). Independent environmental effects on durability of fiber-reinforced polymer wraps in civil applications: A review. *Construction and Building Materials*, 48, 360–370. <https://doi.org/10.1016/j.conbuildmat.2013.06.077>
12. Choi, S., Gartner, A. L., Etten, N. Van, Hamilton, H. R., & Douglas, E. P. (2012). Durability of Concrete Beams Externally Reinforced with CFRP Composites Exposed to Various Environments. *Journal of Composites for Construction*, 16(1). [https://doi.org/10.1061/\(asce\)cc.1943-5614.0000233](https://doi.org/10.1061/(asce)cc.1943-5614.0000233)
13. Clemons, C. B., Roberts, M. W., Wilber, J. P., Young, G. W., Buldum, A., & Quinn, D. D. (2010). Continuum plate theory and atomistic modeling to find the flexural rigidity of a graphene sheet interacting with a substrate. *Journal of Nanotechnology*. <https://doi.org/10.1155/2010/868492>
14. Cui, E., Jiang, S., Wang, J., & Zeng, X. (2021). Bond behavior of CFRP-concrete bonding interface considering degradation of epoxy primer under wet-dry cycles. *Construction and Building Materials*, 292. <https://doi.org/10.1016/j.conbuildmat.2021.123286>

15. Dai, H., Wang, B., Zhang, J., Zhang, J., & Uji, K. (2021). Study of the interfacial bond behavior between cfrp grid–pcm reinforcing layer and concrete via a simplified mechanical model. *Materials*, 14(22). <https://doi.org/10.3390/ma14227053>
16. de Sousa, D. E. S., Scuracchio, C. H., de Oliveira Barra, G. M., & de Almeida Lucas, A. (2015). Expanded graphite as a multifunctional filler for polymer nanocomposites. In *Multifunctionality of Polymer Composites: Challenges and New Solutions* (pp. 245–261). Elsevier Inc. <https://doi.org/10.1016/B978-0-323-26434-1.00007-6>
17. Dolan, C. W., Tanner, J., Mukai, D., Hamilton, H. R., & Douglas, E. (n.d.). *Web-Only Document 155: Design Guidelines for Durability of Bonded CFRP Repair/ Strengthening of Concrete Beams National Cooperative Highway Research Program*.
18. Falahi, N., Abdul Halim, N. H. F., C. Alih, S., Vafaei, M., Baniahmadi, M., & Fallah, A. (2017). Durability of Fibre Reinforced Polymer under Aggressive Environment and Severe Loading: A Review. *International Journal of Applied Engineering Research*, 12, 12519–12533.
19. Fry-Taylor, R., Meng, M., & Wang, X. (2023). Marine environmental effects on a graphene reinforced epoxy adhered single lap joint between metals and CFRP. *International Journal of Adhesion and Adhesives*, 125. <https://doi.org/10.1016/j.ijadhadh.2023.103423>
20. Fu, G., Huo, D., Shyha, I., Pancholi, K., & Alzahrani, B. (2020). Experimental investigation on micromachining of epoxy/graphene nano platelet nanocomposites. *International Journal of Advanced Manufacturing Technology*, 107(7–8), 3169–3183. <https://doi.org/10.1007/s00170-020-05190-4>
21. Gamage, J. C. P. H., Wong, M. B., & Al-Mahaidi, R. (2005). *PERFORMANCE OF CFRP STRENGTHENED CONCRETE MEMBERS UNDER ELEVATED TEMPERATURES*.
22. Gao, S. L., & Mäder, E. (2015). Multifunctional interphases in polymer composites. In *Multifunctionality of Polymer Composites: Challenges and New Solutions* (pp. 338–362). Elsevier Inc. <https://doi.org/10.1016/B978-0-323-26434-1.00010-6>
23. Gharehbash, N., & Shakeri, A. (2015). Preparation and thermal and physical properties of nano-silica modified and unmodified. *Oriental Journal of Chemistry*, 31. <https://doi.org/10.13005/ojc/31.Special-Issue1.25>
24. *Guidelines and Recommended Practices for Fiber-Reinforced-Polymer (FRP) Architectural Products*. (2016). [www.acmanet.org](http://www.acmanet.org)
25. *guide-to-composites-1*. (n.d.).
26. Gunaslan, E., Karasin, A., Günaslan, E., Karaşin, A., & Öncü, M. E. (2014). Properties of FRP Materials for Strengthening. In *IJISSET-International Journal of Innovative Science, Engineering & Technology* (Vol. 1, Issue 9). [www.ijiset.com](http://www.ijiset.com)
27. Hadigheh, S. A., Gravina, R. J., & Smith, S. T. (2017). Effect of acid attack on FRP-to-concrete bonded interfaces. *Construction and Building Materials*, 152. <https://doi.org/10.1016/j.conbuildmat.2017.06.140>
28. Han, X., Yuan, B., Tan, B., Hu, X., & Chen, S. (2019). Repair of subsurface micro-cracks in rock using resin pre-coating technique. *Construction and Building Materials*, 196. <https://doi.org/10.1016/j.conbuildmat.2018.11.145>
29. Hashim, U. R., Jumahat, A., & Jawaid, M. (2021). Mechanical properties of hybrid graphene nanoplatelet-nanosilica filled unidirectional basalt fibre composites. *Nanomaterials*, 11(6). <https://doi.org/10.3390/nano11061468>
30. Hattori, A., Etoh, A., Ohnishi, Y., & Miyagawa, T. (2000). Evaluation of concrete with FRP sheet under accelerated degradation environments. In *Non-Destructive Testing in Civil Engineering 2000*. <https://doi.org/10.1016/b978-008043717-0/50048-9>
31. Hood, K. (n.d.). *INTRODUCTION 37.2 SOME COMMERCIALY IMPORTANT EPOXY RESINS 37.2.1 Glycidyl Resins 37.2.2 Ene-Oxide Resins*.

32. Huang, S., Fu, Q., Yan, L., & Kasal, B. (2021). Characterization of interfacial properties between fibre and polymer matrix in composite materials – A critical review. In *Journal of Materials Research and Technology* (Vol. 13, pp. 1441–1484). Elsevier Editora Ltda. <https://doi.org/10.1016/j.jmrt.2021.05.076>
33. Jack Weitsman, B. Y. (1995a). “Effects of Fluids on Polymeric Composites-A Review.”
34. Jack Weitsman, B. Y. (1995b). “Effects of Fluids on Polymeric Composites-A Review.”
35. Jia, Z., Feng, X., & Zou, Y. (2018). An investigation on mode II fracture toughness enhancement of epoxy adhesive using graphene nanoplatelets. *Composites Part B: Engineering*, 155, 452–456. <https://doi.org/10.1016/j.compositesb.2018.09.094>
36. Jiang, F., Han, X., Wang, Y., Wang, P., Zhao, T., & Zhang, K. (2022). Effect of freeze-thaw cycles on tensile properties of CFRP, bond behavior of CFRP-concrete, and flexural performance of CFRP-strengthened concrete beams. *Cold Regions Science and Technology*, 194. <https://doi.org/10.1016/j.coldregions.2021.103461>
37. Jojibabu, P., Ram, G. D. J., Deshpande, A. P., & Bakshi, S. R. (2017). Effect of carbon nano-filler addition on the degradation of epoxy adhesive joints subjected to hygrothermal aging. *Polymer Degradation and Stability*, 140. <https://doi.org/10.1016/j.polymdegradstab.2017.04.017>
38. K, A.-T. A., A, H. R., A, A. J., A, R. H., & Riadh, A.-M. (2015). Durability of the Bond between CFRP Plates and Concrete Exposed to Harsh Environments. *Journal of Materials in Civil Engineering*, 27(9), 04014252. [https://doi.org/10.1061/\(ASCE\)MT.1943-5533.0001226](https://doi.org/10.1061/(ASCE)MT.1943-5533.0001226)
39. Karbhari, V. M., Chin, J. W., Hunston, D., Benmokrane, B., Juska, T., Morgan, R., Lesko, J. J., Sorathia, U., & Reynaud, D. (2003). Durability Gap Analysis for Fiber-Reinforced Polymer Composites in Civil Infrastructure. *Journal of Composites for Construction*, 7(3). [https://doi.org/10.1061/\(asce\)1090-0268\(2003\)7:3\(238\)](https://doi.org/10.1061/(asce)1090-0268(2003)7:3(238))
40. Karbhari, V. M., & Ghosh, K. (2009). Comparative durability evaluation of ambient temperature cured externally bonded CFRP and GFRP composite systems for repair of bridges. *Composites Part A: Applied Science and Manufacturing*, 40(9). <https://doi.org/10.1016/j.compositesa.2009.01.011>
41. Keshavarz, R., Aghamohammadi, H., & Eslami-Farsani, R. (2020). The effect of graphene nanoplatelets on the flexural properties of fiber metal laminates under marine environmental conditions. *International Journal of Adhesion and Adhesives*, 103. <https://doi.org/10.1016/j.ijadhadh.2020.102709>
42. Keyte, J., Pancholi, K., & Njuguna, J. (2019a). Recent Developments in Graphene Oxide/Epoxy Carbon Fiber-Reinforced Composites. In *Frontiers in Materials* (Vol. 6). Frontiers Media S.A. <https://doi.org/10.3389/fmats.2019.00224>
43. Keyte, J., Pancholi, K., & Njuguna, J. (2019b). Recent Developments in Graphene Oxide/Epoxy Carbon Fiber-Reinforced Composites. In *Frontiers in Materials* (Vol. 6). Frontiers Media S.A. <https://doi.org/10.3389/fmats.2019.00224>
44. Khalid, M. Y., Kamal, A., Otabil, A., Mamoun, O., & Liao, K. (2023). Graphene/epoxy nanocomposites for improved fracture toughness: A focused review on toughening mechanism. In *Chemical Engineering Journal Advances* (Vol. 16). <https://doi.org/10.1016/j.ceja.2023.100537>
45. Khan, Z. U., Kausar, A., & Ullah, H. (2016). A Review on Composite Papers of Graphene Oxide, Carbon Nanotube, Polymer/GO, and Polymer/CNT: Processing Strategies, Properties, and Relevance. In *Polymer - Plastics Technology and Engineering* (Vol. 55, Issue 6). <https://doi.org/10.1080/03602559.2015.1098693>

46. Lalwani, G., D'Agati, M., Khan, A. M., & Sitharaman, B. (2016). Toxicology of graphene-based nanomaterials. In *Advanced Drug Delivery Reviews* (Vol. 105). <https://doi.org/10.1016/j.addr.2016.04.028>
47. Lee, J., Kim, J., Bakis, C. E., & Boothby, T. E. (2021). Durability assessment of FRP-concrete bond after sustained load for up to thirteen years. *Composites Part B: Engineering*, 224. <https://doi.org/10.1016/j.compositesb.2021.109180>
48. Li, K., Cao, S., Yang, Y., & Zhu, J. (2018). Bond-slip relationship for CFRP sheets externally bonded to concrete under cyclic loading. *Materials*, 9(3). <https://doi.org/10.3390/ma11030336>
49. Liu, J. Y., & Sayes, C. M. (2022). A toxicological profile of silica nanoparticles. In *Toxicology Research* (Vol. 11, Issue 4). <https://doi.org/10.1093/toxres/tfac038>
50. Loud, S. (1996). Three steps toward a composite's revolution in construction. *SAMPE Journal*, 32(1).
51. Lu, Z. (2021). Review on the precursor preparation and carbon fiber manufacturing. *Journal of Physics: Conference Series*, 1798(1). <https://doi.org/10.1088/1742-6596/1798/1/012003>
52. Marangu, J. M., Sharma, M., Scheinherrová, L., Kafodya, I., Mutai, V. K., Latif, E., Novelli, V. I., Ashish, D. K., & Maddalena, R. (2024). Durability of Ternary Blended Concrete Incorporating Rice Husk Ash and Calcined Clay. *Buildings*, 14(5), 1201. <https://doi.org/10.3390/buildings14051201>
53. Marom, G., & Broutman, L. J. (n.d.). *Location: LCD Call#: TA 418.9 .C6 P64 Journal Title: Polymer composites Article Title: Moisture penetration into composites under external stress Charges: No Charge Moisture Penetration into Composites under External Stress.*
54. *METHOD STATEMENT Substrate Preparation for Sika® Rigid Bonding and Structural Strengthening Systems.* (n.d.).
55. Minea, A. A. (2020). Barriers and challenges in hybrid nanofluids development and implementation. In *Hybrid Nanofluids for Convection Heat Transfer* (pp. 255–280). Elsevier. <https://doi.org/10.1016/B978-0-12-819280-1.00007-0>
56. Mohammadi Ghahsareh, F., & Mostofinejad, D. (2021). Groove classification in EBROG FRP-to-concrete joints. *Construction and Building Materials*, 275. <https://doi.org/10.1016/j.conbuildmat.2020.122169>
57. Mohammadi, M., & Mostofinejad, D. (2021). CFRP-to-concrete bond behavior under aggressive exposure of sewer chamber. *Journal of Composite Materials*, 55(24). <https://doi.org/10.1177/00219983211004699>
58. Mukhtar, F. M., & Arowajolu, O. (2020). Recent developments in experimental and computational studies of hygrothermal effects on the bond between FRP and concrete. *Journal of Reinforced Plastics and Composites*, 39(11–12). <https://doi.org/10.1177/0731684420912332>
59. Neto, A. S., Da Cruz, D. T. L., & Ávila, A. F. (2013). Nano-modified adhesive by graphene: The single lap-joint case. *Materials Research*, 16(3), 592–596. <https://doi.org/10.1590/S1516-14392013005000022>
60. Neto, A. S., Ferreira Ávila, A., & Meireles, M. M. (n.d.). *GRAPHENE-BASED NANO REINFORCEMENT OF ADHESIVES: THE SINGLE LAP JOINT STUDY.*
61. Qureshi, J. (2022). A Review of Fibre Reinforced Polymer Structures. In *Fibers* (Vol. 10, Issue 3). <https://doi.org/10.3390/fib10030027>
62. Ravindran, A. R., Feng, C., Huang, S., Wang, Y., Zhao, Z., & Yang, J. (2018). Effects of graphene nanoplatelet size and surface area on the AC electrical conductivity and dielectric constant of epoxy nanocomposites. *Polymers*, 10(5). <https://doi.org/10.3390/polym10050477>

63. Razavi, S. M. J., Ayatollahi, M. R., Nemati Giv, A., & Khoramishad, H. (2018). Single lap joints bonded with structural adhesives reinforced with a mixture of silica nanoparticles and multi walled carbon nanotubes. *International Journal of Adhesion and Adhesives*, 80, 76–86. <https://doi.org/10.1016/j.ijadhadh.2017.10.007>
64. *Resin choice*. (2024). Excel Composite.
65. *RESINS IN FRP*. (n.d.). Beetles Plastic.
66. Rifai, M. Al, El-Hassan, H., El-Maaddawy, T., & Abed, F. (2020). Durability of basalt FRP reinforcing bars in alkaline solution and moist concrete environments. *Construction and Building Materials*, 243. <https://doi.org/10.1016/j.conbuildmat.2020.118258>
67. Ruíz de Azúa, O., Agulló, N., Arbusà, J., & Borrós, S. (2023). Improving Glass Transition Temperature and Toughness of Epoxy Adhesives by a Complex Room-Temperature Curing System by Changing the Stoichiometry. *Polymers*, 15(2). <https://doi.org/10.3390/polym15020252>
68. Salimian, M. S., & Mostofinejad, D. (2019). Experimental Evaluation of CFRP-Concrete Bond Behavior under High Loading Rates Using Particle Image Velocimetry Method. *Journal of Composites for Construction*, 23(3). [https://doi.org/10.1061/\(asce\)cc.1943-5614.0000933](https://doi.org/10.1061/(asce)cc.1943-5614.0000933)
69. Shrestha, J., Ueda, T., & Zhang, D. (2015). Durability of FRP Concrete Bonds and Its Constituent Properties under the Influence of Moisture Conditions. *Journal of Materials in Civil Engineering*, 27(2). [https://doi.org/10.1061/\(asce\)mt.1943-5533.0001093](https://doi.org/10.1061/(asce)mt.1943-5533.0001093)
70. *Standard Test Method for Pull-Off Strength of Coatings on Concrete Using Portable Pull-Off Adhesion Testers 1*. (n.d.). <https://doi.org/10.1520/D7234-22>
71. Stelios Antoniou. (2022, January 20). *Fibre – Reinforced Polymers (FRPs)* Read more at: <https://seismosoft.com/fibre-reinforced-polymers-frps/>. Seismosoft.
72. Wang, F., Li, M., Qu, Z., Hu, S., & Wang, J. (2018). Improvement of the FRP sheet bonded to concrete substrate by silane coupling agent. *Journal Wuhan University of Technology, Materials Science Edition*, 33(1). <https://doi.org/10.1007/s11595-018-1795-y>
73. Wang, S., Cao, M., Wang, G., Cong, F., Xue, H., Meng, Q., Uddin, M., & Ma, J. (2022). Effect of graphene nanoplatelets on water absorption and impact resistance of fibre-metal laminates under varying environmental conditions. *Composite Structures*, 281. <https://doi.org/10.1016/j.compstruct.2021.114977>
74. Wang, Y. L., Guo, X. Y., Shu, S. Y. H., Guo, Y. C., & Qin, X. M. (2020). Effect of salt solution wet-dry cycling on the bond behavior of FRP-concrete interface. *Construction and Building Materials*, 254. <https://doi.org/10.1016/j.conbuildmat.2020.119317>
75. Wei, M. W., Xie, J. H., Zhang, H., & Li, J. L. (2019). Bond-slip behaviors of BFRP-to-concrete interfaces exposed to wet/dry cycles in chloride environment. *Composite Structures*, 219, 185–193. <https://doi.org/10.1016/j.compstruct.2019.03.049>
76. Worrall, C. (n.d.). *JOINING OF FIBRE-REINFORCED POLYMER COMPOSITES A Good Practice Guide 2 ACKNOWLEDGEMENTS*.
77. Wu, W., He, X., Ibrahim shah, Y., He, J., & Yang, W. (2022). Long-term bond degradation of GFRP-RC beams in the complex alkaline environment for eight years. *Composite Structures*, 299. <https://doi.org/10.1016/j.compstruct.2022.116093>
78. Yang, S., Liu, C., Sun, Z., Xu, M., & Feng, Y. (2022). *Effects of resin pre-coating treatment and fibre reinforcement on adhesive bonding between CFRP sheet and concrete*. <https://doi.org/10.1016/j.compstruct.2022.115610>
79. Yin, Y., Zhang, J., & Zhang, G. (2023). Effect of hygrothermal acid rain environment on the shear bonding performance of CFRP-concrete interface. *Construction and Building Materials*, 364. <https://doi.org/10.1016/j.conbuildmat.2022.130002>

80. Yuan, C. (2020). *School of Civil and Mechanical Engineering Interfacial Bond Behaviour between FRP Sheet and Concrete under Static and Dynamic Loads*.
81. Zafeiropoulou, K., Kostagiannakopoulou, C., Sotiriadis, G., & Kostopoulos, V. (2020). A preliminary study of the influence of graphene nanoplatelet specific surface area on the interlaminar fracture properties of carbon fiber/epoxy composites. *Polymers*, 12(12), 1–15. <https://doi.org/10.3390/polym12123060>
82. Zamani, P., Jaamialahmadi, A., & da Silva, L. F. M. (2021). The influence of GNP and nano-silica additives on fatigue life and crack initiation phase of Al-GFRP bonded lap joints subjected to four-point bending. *Composites Part B: Engineering*, 207. <https://doi.org/10.1016/j.compositesb.2020.108589>



## 6. Appendix

### Technical Data Sheet

BUILDING TRUST



## PRODUCT DATA SHEET

# SikaWrap®-231 C

WOVEN UNIDIRECTIONAL CARBON FIBRE FABRIC, DESIGNED FOR STRUCTURAL STRENGTHENING APPLICATIONS AS PART OF THE SIKA® STRENGTHENING SYSTEM.

### PRODUCT DESCRIPTION

SikaWrap®-231 C is a unidirectional woven carbon fibre fabric with high strength, designed for installation using the dry or wet application process.

### USES

SikaWrap®-231 C may only be used by experienced professionals.

Structural strengthening of reinforced concrete, masonry, brickwork and timber elements or structures, to increase flexural and shear loading capacity for:

- Improved seismic performance of masonry walls
- Replacing missing steel reinforcement
- Increasing the strength and ductility of columns
- Increasing the loading capacity of structural elements
- Enabling changes in use / alterations and refurbishment
- Correcting structural design and / or construction defects
- Increasing resistance to seismic movement
- Improving service life and durability
- Structural upgrading to comply with current standards

### CHARACTERISTICS / ADVANTAGES

- Manufactured with heat-set weft fibres to keep the fabric stable
- Multifunctional fabric for use in many different strengthening applications
- Flexible and accommodating to different surface planes and geometry (beams, columns, chimneys, piles, walls, soffits, silos etc.)
- Available in different widths for optimum utilisation
- Low density for minimal additional weight
- Extremely cost effective in comparison to traditional strengthening techniques

### APPROVALS / STANDARDS

- Poland: Technical Approval IBDiM Nr AT/2008-03-0336/1 „Płaskowniki, pręty, kształtki i maty kompozytowe do wzmacniania betonu o nazwie handlowej: Zestaw materiałów Sika CarboDur® do wzmacniania konstrukcji obiektów mostowych
- USA: ACI 440.2R-08, Guide for the Design and construction of Externally Bonded FRP Systems for strengthening concrete structures, July 2008
- UK: Concrete Society Technical Report No. 55, Design guidance for strengthening concrete structures using fibre composite material, 2012.

### PRODUCT INFORMATION

<b>Construction</b>	Fibre orientation	0° (unidirectional)	
	Warp	Black carbon fibres 99 %	
	Weft	White thermoplastic heat-set fibres 1 %	
<b>Fibre type</b>	Selected high strength carbon fibres		
<b>Packaging</b>		<b>Fabric length per roll</b>	<b>Fabric width</b>
	1 roll in cardboard box	≥ 50 m	600 mm

Product Data Sheet  
SikaWrap®-231 C  
February 2020, Version 02.02  
020206020010000010

<b>Shelf Life</b>	24 months from date of production	
<b>Storage Conditions</b>	Store in undamaged, original sealed packaging, in dry conditions at temperatures between +5 °C and +35 °C. Protect from direct sunlight.	
<b>Dry Fibre Density</b>	1.80 g/cm <sup>3</sup>	
<b>Dry Fibre Thickness</b>	0.129 mm (based on fibre content)	
<b>Area Density</b>	235 g/m <sup>2</sup> ±10 g/m <sup>2</sup> (carbon fibres only)	
<b>Dry Fibre Tensile Strength</b>	4 900 N/mm <sup>2</sup>	(ISO 10618)
<b>Dry Fibre Modulus of Elasticity in Tension</b>	230 000 N/mm <sup>2</sup>	(ISO 10618)
<b>Dry Fibre Elongation at Break</b>	1.7 %	(ISO 10618)

## TECHNICAL INFORMATION

<b>Laminate Nominal Thickness</b>	0.129 mm		
<b>Laminate Nominal Cross Section</b>	129 mm <sup>2</sup> per m width		
<b>Laminate Tensile Strength</b>	<b>Average</b>	<b>Characteristic</b>	(EN 2561*)
	4 300 N/mm <sup>2</sup>	3 850 N/mm <sup>2</sup>	
* modification: sample with 50 mm Values in the longitudinal direction of the fibres Single layer, minimum 27 samples per test series			
<b>Laminate Tensile Modulus of Elasticity</b>	<b>Average</b>	<b>Characteristic</b>	(EN 2561*)
	225 kN/mm <sup>2</sup>	210 kN/mm <sup>2</sup>	
* modification: sample with 50 mm Values in the longitudinal direction of the fibres Single layer, minimum 27 samples per test series			
<b>Laminate Elongation at Break</b>	1.91 %	(EN 2561)	
<b>Tensile Resistance</b>	<b>Average</b>	<b>Characteristic</b>	(EN 2561)
	555 N/mm	497 N/mm	
<b>Tensile Stiffness</b>	<b>Average</b>	<b>Characteristic</b>	(EN 2561)
	29.0 MN/m 29.0 kN/m per % elongation	27.1 MN/m 27.1 kN/m per % elongation	

## SYSTEM INFORMATION

<b>System Structure</b>	The system build-up and configuration as described must be fully complied with and may not be changed. Concrete substrate adhesive primer <u>Sikadur®-330</u> Impregnating / laminating resin <u>Sikadur®-330 or Sikadur®-300</u> Structural strengthening fabric <u>SikaWrap®-231 C</u>
	For detailed information on Sikadur®-330 or Sikadur®-300, together with the resin and fabric application details, refer to the Sikadur®-330 or Sikadur®-300 Product Data Sheet.

## APPLICATION INFORMATION

Consumption	Dry application with Sikadur®-330
	First layer including primer layer
	Following layers
	0.8–1.2 kg/m <sup>2</sup>
	0.7 kg/m <sup>2</sup>
	Wet application with Sikadur®-300, primer Sikadur®-330
	Primer layer
	Fabric layers
	0.4–0.6 kg/m <sup>2</sup>
	0.6 kg/m <sup>2</sup>

Refer to the relevant Technical Information Manual for further information.

## APPLICATION INSTRUCTIONS

### SUBSTRATE QUALITY

Minimum substrate tensile strength: 1.0 N/mm<sup>2</sup> or as specified in the strengthening design. Refer to the relevant Technical Information Manual for further information.

### SUBSTRATE PREPARATION

Concrete must be cleaned and prepared to achieve a laitance and contaminant free, open textured surface. Refer to the relevant Technical Information Manual for further information.

### APPLICATION METHOD / TOOLS

The fabric can be cut with special scissors or a Stanley knife (razor knife / box-cutter knife). Never fold the fabric.

SikaWrap®-231 C is applied using the dry or wet application process.

Refer to the relevant Technical Information Manual for details on the impregnating / laminating procedure.

## FURTHER DOCUMENTS

### Technical Information Manuals

Ref. 850 41 02: SikaWrap® manual dry application  
Ref. 850 41 03: SikaWrap® manual wet application  
Ref. 850 41 04: SikaWrap® machine wet application

## LIMITATIONS

- SikaWrap®-231 C shall only be applied by trained and experienced professionals.
- A specialist structural engineer must be consulted for any structural strengthening design calculation.
- SikaWrap®-231 C fabric is coated to ensure maximum bond and durability with the Sikadur® adhesives / impregnating / laminating resins. To maintain and ensure full system compatibility, do not interchange different system components.
- SikaWrap®-231 C can be over coated with a cementitious overlay or other coatings for aesthetic and / or protective purposes. The over coating system selection is dependent on the exposure and the project specific requirements. For additional UV light protection in exposed areas use Sikagard®-550 W Elastic, Sikagard® ElastoColor-675 W GB or Sikagard®-680 S.

- Refer to the Technical Information Manual for SikaWrap® manual dry application (Ref. 850 41 02), SikaWrap® manual wet application (Ref. 850 41 03) or SikaWrap® machine wet application (Ref. 850 41 04) for further information, guidelines and limitations.

## VALUE BASE

All technical data stated in this Product Data Sheet are based on laboratory tests. Actual measured data may vary due to circumstances beyond our control.

## LOCAL RESTRICTIONS

Please note that as a result of specific local regulations the performance of this product may vary from country to country. Please consult the local Product Data Sheet for the exact description of the application fields.

## ECOLOGY, HEALTH AND SAFETY

### REGULATION (EC) NO 1907/2006 - REACH

This product is an article as defined in article 3 of regulation (EC) No 1907/2006 (REACH). It contains no substances which are intended to be released from the article under normal or reasonably foreseeable conditions of use. A safety data sheet following article 31 of the same regulation is not needed to bring the product to the market, to transport or to use it. For safe use follow the instructions given in this product data sheet. Based on our current knowledge, this product does not contain SVHC (substances of very high concern) as listed in Annex XIV of the REACH regulation or on the candidate list published by the European Chemicals Agency in concentrations above 0.1 % (w/w)

## LEGAL NOTES

The information, and, in particular, the recommendations relating to the application and end-use of Sika products, are given in good faith based on Sika's current knowledge and experience of the products when properly stored, handled and applied under normal conditions in accordance with Sika's recommendations. In practice, the differences in materials, substrates and actual site conditions are such that no warranty in respect of merchantability or of fitness for a

Product Data Sheet  
SikaWrap®-231 C  
February 2020, Version 02.02  
020206020010000010



BUILDING TRUST



## PRODUCT DATA SHEET

# Sikadur<sup>®</sup>-300

Epoxy impregnating / laminating resin for SikaWrap<sup>®</sup> structural strengthening fabrics

### PRODUCT DESCRIPTION

Sikadur<sup>®</sup>-300 is a 2-part, epoxy based impregnating / laminating resin for SikaWrap<sup>®</sup> structural strengthening fabrics.

### USES

Sikadur<sup>®</sup>-300 may only be used by experienced professionals.

- As an impregnating / laminating resin for the SikaWrap<sup>®</sup> fabric reinforcement wet application method.
- As a substrate primer for the wet application method.

### CHARACTERISTICS / ADVANTAGES

- Easy to mix.
- Application by impregnation roller.
- Formulated for manual or mechanical saturation methods.
- Good adhesion to many substrates.
- High mechanical properties.
- Extra long pot-life.

### APPROVALS / STANDARDS

- Flat bars and composite mats PN-EN 196-1, DIN 53452, Sika CarboDur, IBDiM, Approval No. AT/2008-03-0336/1.
- CE Marking and Declaration of Performance to EN 1504-4: Structural bonding.

### PRODUCT INFORMATION

<b>Product Declaration</b>	EN 1504-4: Structural bonding	
<b>Chemical Base</b>	Epoxy resin	
<b>Packaging</b>	Part A	22,305 kg pre-batched unit
	Part B	7,695 kg pre-batched unit
	Bulk containers	Refer to current price list
	Refer to current price list for packaging variations	
<b>Shelf Life</b>	24 months from date of production	
<b>Storage Conditions</b>	The product must be stored in original, unopened and undamaged packaging in dry conditions at temperatures between +5 °C and +30 °C. Always refer to packaging.	
<b>Colour</b>	Part A	~amber liquid
	Part B	~pale yellow liquid
	Parts A + B mixed	~light-yellow liquid
<b>Density</b>	Mixed resin ~1,16 kg/l Value at +23 °C.	



---

3050 Spruce Street, Saint Louis, MO 63103, USA

Website: [www.sigmaaldrich.com](http://www.sigmaaldrich.com)Email USA: [techserv@sial.com](mailto:techserv@sial.com)Outside USA: [eurtechserv@sial.com](mailto:eurtechserv@sial.com)

## Product Specification

Product Name:  
Graphene nanoplatelets - surface area 500 m<sup>2</sup>/g

**Product Number:** 900439  
**CAS Number:** 7782-42-5

**Formula:** C  
**Formula Weight:** 12.01 g/mol

### TEST

### Specification

---

Appearance (Color)	Black
Appearance (Form)	Powder
Infrared Spectrum	Conforms to Structure
X-Ray Diffraction	Conforms to Structure
Surface Area	
Specification: Report Only	
Product of Supplier	Confirmed
XG Sciences; Inc.	
Registered Trademark	Note
xGnP® is a registered tradename of XG Sciences; Inc.	

Specification: PRD.0.ZQ5.10000104522

**SIGMA-ALDRICH®**[sigma-aldrich.com](http://sigma-aldrich.com)

3050 Spruce Street, Saint Louis, MO 63103, USA

Website: [www.sigmaaldrich.com](http://www.sigmaaldrich.com)Email USA: [techserv@sial.com](mailto:techserv@sial.com)Outside USA: [eurtechserv@sial.com](mailto:eurtechserv@sial.com)

## Product Specification

Product Name:  
Silica - 99.8%

**Product Number:** 381276  
**CAS Number:** 112945-52-5  
**MDL:** MFCD00011232  
**Formula:** O<sub>2</sub>Si  
**Formula Weight:** 60.08 g/mol

SiO<sub>2</sub>

TEST	Specification
Appearance (Color)	White
Appearance (Form)	Powder
Loss on Ignition Typically 2 - 10%	
Surface Area	175 - 225 m <sup>2</sup> /g
ICP Major Analysis Confirms Silicon Component	Conforms
Purity 99.8% Based on Trace Metals Analysis	Conforms
Trace Metal Analysis	≤ 2500.0 ppm

Specification: PRD.1.ZQ5.10000008023

assay	99.8%
form	powder
grade	standard
InChI key	VYPSYNLAJGMNEJ-UHFFFAOYSA-N
InChI	1S/O2Si/c1-3-2
matrix active group	silica
matrix	Silica
particle size	0.011 $\mu\text{m}$
pore size	60 Å mean pore size
Quality Level	100
separation technique	hydrophilic interaction (HILIC)
SMILES string	O=[Si]=O
surface area	175-225 $\text{m}^2/\text{g}$
technique(s)	LPLC: suitable



